Measurements and modelling of eutrophication processes in Lake Rotoiti, New Zealand

A thesis
submitted in partial fulfilment
of the requirements for the degree of

Doctor of Philosophy

at

The University of Waikato

by

Nina von Westernhagen

THE UNIVERSITY OF
WAIKATO
Te Whare Wānanga o Waikato

The University of Waikato

2010

For Luca and Alea

“Live as if you were to die tomorrow. Learn as if you were to live forever.”

[Mahatma Gandhi]

Abstract

Deterioration of water quality is a common problem for aquatic systems globally, which is accelerated by factors such as urban settlement, farming, forestry and recreation. Spatial variability of water quality in these systems hinders a more advanced understanding of their dynamics, to better enable strategies to be developed to combat their deterioration. Understanding the drivers for spatial variability is fundamentally important for predicting how lake ecosystems will respond to management scenarios and which management actions are most likely to be successful to improve lake health. Through a field study in a morphologically diverse lake in New Zealand, and the application of a lake ecosystem model, this study examined the spatial and temporal variability of phytoplankton biomass and made a detailed consideration of the performance of three–dimensional lake ecosystem models.

To gain insight in the spatial variability in phytoplankton productivity, surface phytoplankton productivity measurements were carried out at three stations in morphologically complex Lake Rotoiti, North Island, New Zealand, with the objective of defining variations between sites and seasons, and the dominant environmental drivers of these variations. There was no overarching statistical relationship between measured environmental variables and primary productivity or specific production. Inorganic nutrient concentrations at the surface of the shallow station were low throughout the whole year but at the other two stations they showed a typical pattern for monomictic lakes of higher levels during winter

mixing and declining concentrations during thermal stratification. The high variability between the three sites indicates that it is important to account for local differences in productivity in morphologically diverse lakes, and that whole–lake productivity estimates may vary greatly depending on the location and depth at which measurements are made.

To gain understanding of the spatial variability, a higher resolution three–dimensional (3D) model, ELCOM–CAEDYM, was used to simulate the time–varying horizontal and vertical variations in water quality over one year (May 2004–May 2005). The main inflow to Lake Rotoiti arises via the Ohau Channel from adjacent eutrophic Lake Rotorua. Highly spatially resolved field data were collected monthly to validate the model performance for simulations of temperature, dissolved oxygen and chlorophyll *a*. The model was configured to simulate a geothermal heat source in the deepest part of the main lake basin. Model simulations of temperature, dissolved oxygen and chlorophyll *a* were highly correlated with measurements of these variables but simulations of spatial variations in nutrient concentration showed relatively low correlation coefficient values, in particular at a station located in a shallow embayment. An examination of the behaviour of a conservative tracer introduced into the major inflow of Lake Rotoiti, the Ohau Channel, confirmed previous findings that this inflow could enter the lake as a surface inflow, interflow or underflow, depending on temperature gradients between the inflow and the lake water column. The results showed that ELCOM–CAEDYM is capable of reproducing highly spatially resolved field data in a complex, geothermally–influenced lake, and can provide important insights into the fate of heat and constituents in major inflows.

A wall to divert Ohau Channel water directly towards the outflow of Lake Rotoiti was implemented in August 2008. Based on parameter values calibrated for the time period before the inflow diversion (May 2004–May 2005), ELCOM–CAEDYM was applied to the post–diversion wall period of August 2008–August 2009. The model showed good fit with observed data for temperature, dissolved oxygen and chlorophyll *a*, but the model showed a poor fit when simulations were

compared with in situ nutrient concentrations at all stations. Simulations with ELCOM–CAEDYM suggest that model accuracy may be improved when a simplified dynamic sediment diagenesis model is available. This could provide for less sensitivity to sediment nutrient release rates of the model and better model fit to in situ data. Ecosystem modelling is likely to play an increasingly important role in lake management and scientific understanding of lake processes as computer speed increases and models undergo further refinements. The model development is in a phase of relative maturity in which water quality simulations provide an efficient and rational tool to compare water quality outcomes and cost effectiveness of lake improvement techniques, to provide for preservation and improvement in water quality in the future.

Table of Contents

List of Figures ix
List of Tables xiii
Acknowledgments xv
Preface xvii

1. General Introduction 18
1.1 Motivation 18
1.2 Main objectives 19
1.3 Field studies 20
1.4 Model applications 21
1.5 Thesis overview 22
1.6 References 24

2. Temporal and spatial variations in phytoplankton productivity in surface waters of a warm–temperate, monomictic lake in New Zealand 29
Abstract 29
2.1 Introduction 30
2.2 Site description 31
2.3 Material and methods 33
2.3.1 Environmental data collection 33
2.3.2 Primary productivity 35
2.4 Results 38

2.4.1 Environmental data 38
2.4.2 Productivity and light 43
2.5 Discussion 47
2.6 Conclusions 51
2.7 References 53

3. The impact of a large river inflow and complex morphometry on hydrodynamics of a temperate lake: A three–dimensional modelling study. 61
Abstract 61
3.1 Introduction 63
3.2 Methods 67
3.2.1 Site description 67
3.2.1 Field data 69
3.2.1 Data analysis 70
3.2.2 Model description and set–up 72
3.2.3 Model calibration and sensitivity analysis 78
3.3 Results 80
3.3.1 Water temperature comparisons 81
3.3.2 Dissolved oxygen comparisons 85
3.3.3 Biogeochemical variable comparisons 85
Nurients 85
Chlorophyll *a* 88
3.3.4 Comparison across a fixed transect 88
Ohau Channel tracer concentration 97
3.4 Discussion 99
3.4.1 Model limitations 99
3.4.2 Geothermal influence and temperature validation 101
3.4.1 Phytoplankton, chlorophyll *a* and zooplankton 104
3.4.2 Inflow analysis 106
3.5 Conclusions 108
3.6 References 110

4. Modelling the impact of the Ohau Channel diversion wall on water quality of Lake Rotoiti, New Zealand 120
Abstract 120
4.1 Introduction 121
4.2 Study Site 124
4.3 Materials and methods 127
4.4 Results 130
4.4.1 Water temperature simulations 130
4.4.2 Dissolved oxygen simulations 132
4.4.3 Chlorophyll *a* simulations 134
4.4.4 Nutrient simulations 136
4.4.5 Ohau Channel and Okawa Bay tracer 139
4.5 Discussion 142
4.5.1 Water quality in Lake Rotoiti after the inflow diversion 142
4.5.2 Change in tracer post diversion 144
4.5.3 Model comparison and performance 145
Model uncertainties and limitations 146
Geothermal heat source 148
Model calibration process 149
4.6 Conclusions 151
4.7 References 153

5. General Conclusions 161
5.1 Research summary 161
5.2 Future work 163
5.3 References 167

List of Figures

Figure 2.1: Location map of Lake Rotoiti, North Island, New Zealand with depth contours 5, 10, 20, 30, 40, 50, 60, 70, 80 , 90 m and the location of sampling Stations 1–3. 34
Figure 2.2: Contour plot of temperature (°C) for (A) Station 1, (B) Station 2 and (C) Station 3 from June 2004 to June 2005. (A) and (B) are from thermistor chain records at 15 minute intervals and (C) from monthly CTD profiles. Field sampling dates are marked with x. 39
Figure 2.3: Surface concentrations ammonium (NH_4–N) and nitrate (NO_3–N) (left–hand vertical axis) and phosphate (SRP) (right–hand vertical axis) in Lake Rotoiti at (A) Station 1, (B) Station 2 and (C) Station 3 from June 2004 to May 2005. 41
Figure 2.4: Chlorophyll *a* concentrations at Station 1, Station 2 and Station 3 sampled from June 2004 to May 2005. 42
Figure 2.5: Photosynthetically active radiation (PAR) at Stations 1–3 and at depths of 0 and 5 m from June 2004 to May 2005. 43
Figure 2.6: Primary productivity at (A) 0 m and (B) 5 m from June 2004 to May 2005, at the three sampling stations. Error bars indicate standard deviation ($n \leq 3$). Asterisks denote significant differences ($p<0.05$) in primary productivity between the stations, analysed with one–way analysis of variance followed by Student Newman–Keul test. See Table 2.2 for results of the post–hoc test. 44
Figure 2.7: Rates of phytoplankton chlorophyll *a* specific production at (A) 0 m and (B) 5 m from June 2004 to May 2005. Error bars describe standard deviation

(n≤3). Asterisks denote significant differences ($p<0.05$) in specific production between the stations, analysed with one–way ANOVA followed by Student Newman–Keul test. See Table 2.2 for results of the post–hoc test. 46
Figure 3.1: Locations of sampling Stations 1, 2 and 3 on Lake Rotoiti. Black line shows the Biofish transect path 68
Figure 3.2: Conceptual diagram of the (A) underflow, (B) interflow and (C) overflow condition of Ohau Channel inflow. 69
Figure 3.3: Conceptual diagram of (A) nitrogen and (B) phosphorus dynamics. POP(N)L and DOP(N)L represent particulate and dissolve labile organic phosphorus (nitrogen), respectively (after Hipsey et al. 2007). 76
Figure 3.4: Simulated (–) and observed (○) values for (A) temperature (ºC), (B) dissolved oxygen (mg L^{-1}) and (C) total chlorophyll *a* (µg L^{-1}) at Stations 1(I), 2 (II) and 3 (III) from June 2004 to April 2005. 82
Figure 3.5: Temperature (ºC) measurements from thermistor chain at (A) Station 1 and (B) Station 2 compared with corresponding simulated ELCOM output in the main basin from 22 May 2004 to 16 May 2005. 84
Figure 3.6: Simulated (–) and observed values (●) for nutrients TP, PO_4–P, TN, NH_4–N and NO_3–N at (A) Stations 1, (B) Station 2 and (C) Station 3 at the surface over the simulated period (May 2004 – May 2005). 87
Figure 3.7: Comparison between simulated (coloured background) and measured (○) values of temperature (ºC) from June 2004 to April 2005. Measured values were derived from Biofish transect measurements, displaying every second measured value. 89
Figure 3.8: Comparison between simulated (coloured background) and measured (○) values dissolve oxygen (DO) (mg L^{-1}) from June 2004 to April 2005. Measured values were derived from Biofish transect measurements displaying every second measured value. 91
Figure 3.9: Comparison between simulated (coloured background) and measured (○) values of chlorophyll *a* (µg L^{-1}) calibrated to surface chlorophyll measurements from June 2004 to April 2005. Measured values were derived from Biofish fluorescence transect measurements displaying every second measured value. 93

Figure 3.10: Simulated for chlorophyll *a* concentrations (µg L^{-1}) (combined value for the two groups of phytoplankton; diatoms and cyanobacteria) at (A) Station 1, (B) Station 2 and (C) Station 3. Line plot in B shows chlorophyll *a* concentration in Ohau Channel inflow. 95
Figure 3.11: Simulated chlorophyll *a* concentration (µg L^{-1}) partitioned into the two modelled phytoplankton groups, cyanobacteria (black line) and diatoms (grey line) at (A) Station 1, (B) Station 2 and (C) Station 3 at the surface over the simulated period (May 2004– May 2005)..... 96
Figure 3.12: Rate of change of tracer concentration as % per month relative to the assigned tracer concentration (100%) in the Ohau Channel at (A) Station 1, (B) Station 2 and (C) Station 3. 98
Figure 4.1: Bathymetric map of Lake Rotoiti. Monthly Biofish transect (black line) for sampling August 2008 – July 2009. The area within the dashed line is shown in greater detail in Figure 4.2. 125
Figure 4.2: Bathymetric map of the western basin of Lake Rotoiti. Ohau Channel diversion wall is represented by the bold black line. 126
Figure 4.3: Comparison of simulated water temperature (coloured background, ºC) and measurements (○) taken at monthly intervals fr om August 2008 to June 2009. 131
Figure 4.4: Comparison of simulated dissolved oxygen (coloured background, mg L^{-1}) and measurements (○) taken at monthly intervals from August 2008 to June 2009. 133
Figure 4.5: Comparison of simulated chlorophyll *a* (coloured background, µg L^{-1}) and measurements (○) taken at monthly intervals from August 2008 to June 2009. 135
Figure 4.6: Simulated (line) and observed (○) values for total nutrients TP and TN and dissolved inorganic nutrients PO_4–P, NH_4–N and NO_3–N at (A) Station 1, (B) Station 2 and (C) Station 3 at the surface over the simulated period of August 2008 until August 2009. 138
Figure 4.7: Rate of change of tracer concentration as % per month relative to the assigned tracer concentration (100%) in the Ohau Channel at (A) Station 1, (B) Station 2 and (C) Station 3. 139

Figure 4.8: Rate of change of Okawa Bay tracer concentration as % per month relative to the assigned tracer concentration (100%) in the Okawa Bay at (A) Station 1 and (B) Station 2 pre– (left) and post–diversion wall (right). 141
Figure 4.9: Wind rose of speed and direction for the period of the model simulations from (A) May 2004 to May 2005 and (B) August 2008 to August 2009; (C) western basin of Lake Rotoiti and Okawa Bay. 142

List of Tables

Table 2.1: Pearson correlation coefficients (R) for surface nutrient concentrations as a function of sampling station. 40
Table 2.2: Results of post–hoc Student Newman–Keul test to determine significant differences ($p<0.05$) of primary productivity and specific production among stations within sampling months. 47
Table 3.1: Parameter values used in CAEDYM v3.3 application to Lake Rotoiti. Individually assigned parameter for cyanobacteria (Cyano) and diatoms (Diat) when applicable. 79
Table 3.2: Monthly mean, standard deviation of mean, minimum and maximum values of the coefficient of variation of temperature ($C_{vTemperature}$) and chlorophyll *a* ($C_{vChlorophyll\ a}$). C_v was calculated for Biofish transect measurements corresponding to each model cell in Lake Rotoiti. 80
Table 3.3: Root–mean–square–error (RMSE) and Pearson correlation coefficient (R) values for Stations 1, 2 and 3 for comparisons of model simulations and measurements of temperature and concentrations of dissolved oxygen (DO) and chlorophyll *a*. 81
Table 3.4: Root–mean–square–error (RMSE) and Pearson correlation coefficient (R) values for Stations 1, 2 and 3 for total phosphorus (TP), phosphate (PO_4–P), total nitrogen (TN), ammonium (NH_4–N) and nitrate (NO_3–N). 86

Table 3.5: Values of Root–Mean–Square–Error (RMSE) and Pearson correlation coefficient (R) for comparison of model simulation values against corresponding Biofish measurements averaged for each model grid cell of the transect over a one year simulation period commencing 17 May 2004 compared with the model simulations of temperature (n=5250), dissolved oxygen (n=3972) and total chlorophyll *a* (n=5250). 90
Table 4.1: Values of Root–Mean–Square–Error (RMSE) and Pearson correlation coefficient (R) for comparison of model simulation values against corresponding Biofish measurements averaged for each model grid cell of the transect over a one year simulation period commencing 19 August 2008 compared with the model simulations of temperature (n=8527), dissolved oxygen (n=6986) and total chlorophyll *a* (n=8527). 132
Table 4.2: Root–mean–square–error (RMSE) and Pearson correlation coefficient (R) values for Stations 1, 2 and 3 for total phosphorus (TP), phosphate (PO_4–P), total nitrogen (TN), ammonium (NH_4–N) and nitrate (NO_3–N)..... 137

Acknowledgments

First and foremost I would like to thank my chief supervisor Professor David Hamilton for his ideas, in particular writing lessons, and for his motivation. I also greatly appreciate the support from my secondary supervisor Dr. Conrad Pilditch and his valuable input and discussions. I thank both of you for believing in me.

Throughout this study, I was supported financially by a post–graduate scholarship granted from Environment Bay of Plenty. Thank you to the employees of EBoP who supported me throughout my field work.

A big thanks goes to overseas supporters, Dr. Ben Hodges, Dr. Matt Hipsey and Dr. Liancong Luo who gave me valuable input for, and suggestions regarding the model application. Dr. Robert Spigel shared his long experience and research on Lake Rotoiti.

I have always been greatly supported by a lot of people at Waikato University. Thank you to everybody who was there when I needed help. I thank associate Professor Chris Hendy for valuable discussions and input. Special thanks to Lee Laboyrie, Dr. Deniz Özkundakci, Mat Allan, Chris McBride, Kohji Muraoka and Lisa Pearson for valuable input and support. I would like to thank especially Hilke and Tony Giles and Amanda Baldwin for helping out in several aspects of life over the last few years, including a lot of chocolate, pumpkin soup and laughs and even providing a home, when necessary.

Eternal gratitude goes to my mother, for your endless love and support and believing in me. Thank you to my father, for planting the seed of scientific enthusiasm. Thank you to my brother and everybody from my home country who came to visit, sent letters, photographs, presents and brought a part of home to this side of the world. Thank you for always supporting me.

A very special thanks goes to my friend Sabine Deckers; you have been the most amazing friend throughout the last years and helped me in every possible way. No words could possibly describe what you have done for me.

Last but not least, thank you to my wonderful children Luca and Alea. You certainly kept me going and put my Ph.D into perspective. You are definitely right that rainbows, caterpillars, ants, bikes, surf boards and race cars are more exciting than scientific papers without colourful pictures. Thank you for your patience. I am sure one day you will understand.

"Anyone can give up, it's the easiest thing in the world to do. But to hold it together when everyone else would understand if you fell apart, that is true strength."

[Dr. George Sheehan]

Preface

The main body of this thesis comprises three Chapters (Chapters 2–4) which have been prepared in a paper format to assist with submission for publication in peer reviewed scientific journals. I was responsible and am accountable for the field work programme, laboratory and data analysis, and for writing this thesis. Except when referenced, the material in this thesis was produced from my own ideas and work undertaken under the supervision of Prof. David Hamilton and Dr. Conrad Pilditch (The University of Waikato, New Zealand). These co–authors of the published paper constituting Chapter 2 (below) have contributed with discussions and revisions to the manuscript prior to submission.

Chapter 2 has been published as: von Westernhagen, N., Hamilton, D. P. and Pilditch, C. A. (2010): Temporal and spatial variations in phytoplankton productivity in surface waters of a warm–temperate, monomictic lake in New Zealand. *Hydrobiologia* 652: 57–70.

Chapter 3 has been prepared to be submitted to *Ecological Modelling*. The title is "The impact of a large river inflow and complex morphometry on hydrodynamics of a temperate lake: A three–dimensional modelling study".

Chapter 4 has been prepared to be submitted to a peer reviewed scientific journal. The title is "Modelling the impact of the Ohau Channel diversion wall on water quality of Lake Rotoiti, New Zealand".

Chapter 1

General Introduction

1.1 Motivation

Attention has been focussed globally on the deterioration of freshwaters due to human activities. Restoration programmes have therefore been implemented to restore and to protect the world's freshwaters (Jeppesen et al. 2005). Only 1% of the world's freshwater is accessible for human use, of which c. 85% is contained within lakes. Highly eutrophic and productive lakes are influenced by interactions amongst light, nutrients, mixing depth and phytoplankton biomass and composition (Schindler 1978; Urabe et al. 1999; McIntire et al. 2007). Morphological characteristics may affect algae blooms and cause variations in response within and amongst lakes (Sakamoto 1966; Håkanson 2005). Due to the increasing interest in lake restoration, there is a need to understand sources of nutrient loading, their influence on productivity and the temporal and spatial scale on which lakes respond (Descy et al. 2005; Çelik 2006; Qu et al. 2007). A lack of attention to spatial variations in some lake studies may be partly due to the time and expense required for intensive field studies. To overcome this, three dimensional (3D) models have been used to analyse spatial varying conditions in multi–basin lakes (Rueda et al. 2008; Missaghi & Hondzo 2010). To capture heterogeneity of water quality, different and evolving techniques have been applied to improve model simulations. For example, Spillmann et al. (2007) used remote sensing to compare observed chlorophyll *a* distributions with model

predictions for the Po River discharge into the Northern Adriatic Sea in Italy. Furthermore, extensive arrays of thermistors and three discrete stations for dissolved oxygen measurements were used in Lake Erie to initialise ELCOM/CAEDYM for analyses of the magnitude of oxygen depletion in bottom waters of the lake (León et al. 2006).

Lake Rotoiti is a large morphologically complex, geothermally–influenced lake with one main inflow. The lake is located in the Central Volcanic Plateau (CVP), North Island, New Zealand, and is a popular holiday and fishing destination. Lake Rotoiti has undergone long–term deterioration in water quality associated with excess nutrients loadings and eutrophication (Vincent et al. 1984; Rutherford et al. 1996; Hamilton 2003; Rutherford 2003) mainly attributed to the main inflow entering Lake Rotoiti via the Ohau Channel from adjacent Lake Rotorua. This inflow may plunge into the main basin of Lake Rotoiti as an underflow depending on density differences from temperature gradients between the inflow and through the water column (Gibbs 1983).

This thesis examines spatial variability of water quality and productivity in Lake Rotoiti and the effect of the Ohau Channel inflow on Lake Rotoiti's water quality. This work also includes analyses on the effect of a newly built structure to divert the Ohau Channel inflow directly towards the main outflow of Kaituna River. Highly spatially resolved field measurements are used to validate 3D modelling predictions. This unique field data set was used to test the model performance and assess its accuracy and capability for prediction of the Ohau Channel diversion case.

1.2 Main objectives

The overall objective of this thesis was to analyse spatial variability of phytoplankton productivity and water quality in morphologically complex, deep Lake Rotoiti and to assess the impact of Ohau Channel inflow on the spatial variability of water quality within the lake. The spatial performance of the 3D water quality model was tested with highly spatially resolved field data. A geothermal heat source which was required to match changes in hypolimnion

temperature added an interesting and unusual aspect to the modelling component of the study. The last objective was to assess model performance when the Ohau channel inflow diversion in form of a diversion wall was used as a means to reduce the nutrient load and improve water quality. This change provided an opportunity to qualitatively assess whether the model was sufficiently robust to simulate the resulting changes in water quality.

The principal work conducted for this study included a comprehensive nutrient and productivity field study, high frequency spatial data collection and a computer–based modelling study.

1.3 Field studies

Historically, lakes were perceived to be relatively homogeneous horizontally and even today there is a lack of attention given to spatial variations in large lakes and numerous previous studies have focused on temporal variations within a lake (Vincent et al. 1984; Carrick et al. 1993; Berman et al. 1995). However morphologically complex lakes, especially those with nutrient–enriched inflows can show high spatial variability. Small lakes may have large variations in phytoplankton biomass (Sayg–Basbug & Demirkalp 2004) and spatial variation of phytoplankton production may have an important influence on ecological assessments of trophic status and whole–lake productivity. For this study productivity measurements were undertaken to analyse the variability at three morphologically diverse stations. To calibrate the model these stations were additionally profiled for temperature, chlorophyll *a* and dissolved oxygen concentrations. To complement this sampling regime and to validate the model on a spatial basis, vertical and horizontal high frequency field measurements of temperature, chlorophyll *a* and dissolved oxygen, were undertaken following a fixed transect which included the three selected stations. Monthly sampling was undertaken for one year from May 2004 to May 2005.

To be able to assess the influence of the main inflow on water quality of Lake Rotoiti, and to test the ability of the model to use a fixed parameter approach for management predictions, a fixed transect was sampled after the construction of

the Ohau Channel diversion wall (August 2008 to June 2009). Data collected following the wall construction were used to test model performance and evaluate the effect of the inflow diversion and the benthic geothermal source.

1.4 Model applications

Part of the reason for the 3D model application to Lake Rotoiti was to simulate the effect of the main inflow (Ohau Channel) on the lake's water quality. A 3D model was considered necessary (as opposed to a model of lower spatial resolution) to encompass two distinct basins connected via a narrow constriction, as well as several bays. This morphological variability provides an excellent opportunity to evaluate variations in phytoplankton across the basin and to assess other influences such as geothermal heat sources.

The 3D lake ecosystem model ELCOM–CAEDYM, developed by the Centre for Water Research, University of Western Australia has been applied to several lakes (e.g., León et al. 2006; Njuguna et al. 2006; Burger et al. 2008; Trolle et al. 2008a; 2008b; Chung et al. 2009; Gal et al. 2009; Missaghi & Hondzo 2010), estuaries (e.g., Dallimore et al. 2003; Robson & Hamilton 2004; Loveless 2009) and coastal ocean (Okely et al. 2006; Spillman et al. 2007). Various attempts have been made to improve the performance of ELCOM and ELCOM–CAEDYM. For example Laval et al. (2003) used a spatially varying wind field to improve the seiche amplitude and simulate mean surface circulation; León et al. (2005) used thermistor data at three stations in the eastern basin of Lake Erie to understand the flushing of the deep basin and circulation dynamics as drivers for future studies of fate and transport of nutrients. Hillmer et al. (2008) used 33 stations in Lake Kinneret to simulate phytoplankton patchiness in terms of concentration and composition. Most studies have used spatial field data for initialisation. None of these studies has used highly resolved spatial field data and an array of statistical measures of goodness–of–fit to compare model output and to assess the temporal and spatial complexity of both field data and model simulations.

1.5 Thesis overview

This thesis is based on three main research Chapters (Chapter 2–4) which have been prepared for, or published in, peer–reviewed scientific journals. Chapter 2 examines the spatial variability of phytoplankton productivity in Lake Rotoiti. Previous assessments of lake productivity have generally one centrally located station (Berman & Pollingher 1974; Lehmann et al. 2004; Arst et al. 2008). This work of productivity gives new insights into the potential for high spatial variability within one water body. It also pointed to the importance of site selection when productivity studies are undertaken in lakes.

The main focus of Chapter 3 relates to outcomes from a 3D model application to Lake Rotoiti. A geothermal energy input of 165 MW was added to the hypolimnion of Lake Rotoiti via an inflow in order to best match the temperature increase of the hypolimnion over the 8 to 9–month period of stratification. Monthly temperature, chlorophyll *a* and dissolved oxygen measurements were used to calibrate the model for the period May 2004–May 2005. Validation was undertaken within the same year but using highly resolved spatial (horizontal and vertical) field data. The model was used to analyse the intrusion of the Ohau Channel inflow into Lake Rotoiti and the resulting spatial variability of temperature, dissolved oxygen and chlorophyll *a* within the lake.

In Chapter 4 I analysed the performance of ELCOM–CAEDYM under a changed set of environmental conditions in relation to the inflow diversion while using a fixed parameter approach. The diversion wall was completed at the beginning of August 2008 and simulations commenced from 19 August 2008 for a period of one year, based on the identical model parameters calibrated for Chapter 3. Forcing data was adjusted according to the simulation period. The effect of the implementation of the wall was analysed by assessing the monthly change in inflow tracer concentration. To test the model accuracy, calculations of Root–Mean–Square–Error and Pearson correlation coefficient between averaged values of highly resolved field data relating to one model cell and model simulation, were undertaken

This Ph.D. study provides a fundamental understanding of the spatial variability of physical and biochemical variables in a complex waterbody with heterogeneous morphology and geothermal inflows and contributes to the knowledge on how well a ‘state of the art’ 3D model can simulate these variables and predict future scenarios.

1.6 References

Arst, H., T. Nõges, P. Nõges & B. Paavel (2008): Relations of phytoplankton in situ primary production, chlorophyll concentration and underwater irradiance in turbid lakes. *Hydrobiologia* 599: 169-176.

Berman, T. & U. Pollingher (1974): Annual and seasonal variations of phytoplankton, chlorophyll, and photosynthesis in Lake Kinneret. *Limnology and Oceanography* 19: 31-54.

Berman, T., L. Stone, Y. Z. Yacobi, B. Kaplan, M. Schlichter, A. Nishri & U. Pollingher, 1995. Primary production and phytoplankton in Lake Kinneret: A long-term record (1972-1993). *Limnology and Oceanography* 40: 1064-1076.

Burger, D. F., Hamilton, D. P. and Pilditch, C. A. (2008): Modelling the relative importance of internal and external nutrient loads on water column nutrient concentrations and phytoplankton biomass in a shallow polymictic lake. *Ecological Modelling* 211(3–4): 411–423.

Carrick, H. J., F. J. Aldridge & C. L. Schelske (1993): Wind influences phytoplankton biomass and composition in a shallow, productive lake. *Limnology and Oceanography* 38: 1179-119.

Çelik, K. (2006): Spatial and seasonal variations in chlorophyll–nutrient relationship in the shallow hypertrophic Lake Manyas, Turkey. *Environmental Monitoring and Assessment* 117: 261–269.

Chung, S. W., Hipsey, M. R. and Imberger, J. (2009): Modelling the propagation of turbid density inflows into a stratified lake: Daecheong Reservoir, Korea. *Environmental Modelling & Software* 24(12): 1467–1482.

Dallimore, C. J., Hodges, B. R. and Imberger, J. (2003): Coupling an underflow model to a three–dimensional hydrodynamic model. *Journal of Hydraulic Engineering* 129(10): 748.

Descy, J.–P., Hardy, M.–A., Sténuite, S., Pirlot, S., Leporcq, B., Kimirei, I., Sekadende, B., Mwaitega, S. R. and Sinyenza, D. (2005): Phytoplankton pigments and community composition in Lake Tanganyika. *Freshwater Biology* 50: 668–684.

Gal, G., Hipsey, M. R., Parparov, A., Wagner, U., Makler, V. and Zohary, T. (2009): Implementation of ecological modeling as an effective management and investigation tool: Lake Kinneret as a case study. *Ecological Modelling* 220(13–14): 1697–1718.

Gibbs, M. M. (1983): Penetration of Ohau Channel water into Lake Rotoiti. Taupo Research Laboratory, Department of Scientific and Industrial Research. File report 63. 9 pp.

Håkanson, L. (2005): The importance of lake morphometry for the structure and function of lakes. *International Review of Hydrobiology* 90: 433–461.

Hamilton, B. (2003): A review of short–term management options for lakes Rotorua and Rotoiti. A report for the New Zealand Ministry for the Environment. Hamilton Integrated Management. December 2003. 68 pp.

Hillmer, I., van Reenen, P., Imberger, J. and Zohary, T. (2008): Phytoplankton patchiness and their role in the modelled productivity of a large, seasonally stratified lake. *Ecological Modelling* 218(1–2): 49–59.

Jeppesen, E., Søndergaard, M., Jensen, J. P., Havens, K. E., Anneville, O., Carvalho, L., Coveney, M. F., Deneke, R., Dokulil, M. T., Foy, B., Gerdeaux, D., Hampton, S., Hilt, S., Kangur, K., Köhler, J., Lammens, E. H. H. R., Lauridsen, T. L., Manca, M., Miracle, M. R., Moss, B., Nõges, P., Persson, G., Phillips, G., Portielje, R., Romo, S., Schleske, C. L., Straille, D., Tatrai, I., Willén, E. and Winder, M. (2005): Lake response to reduced

nutrient loading – an analysis of contemporary long–term data from 35 case studies. *Freshwater Biology* 50: 1747–1771.

Laval, B., Jörg Imberger, J., Hodges, B.R. and Stocker, R. (2003): Modeling Circulation in Lakes: Spatial and Temporal Variations. *Limnology and Oceanography* 48(3): pp. 983–994

Lehmann, M. F., S. M. Bernasconi, J. A. McKenzie, A. Barbieri, M. Simona & M. Veronesi (2004): Seasonal variation of the d13C and d15N of particulate and dissolved carbon and nitrogen in Lake Lugano: Constraints on biogeochemical cycling in a eutrophic lake. *Limnology and Oceanography* 49: 415-429.

León, L. F., Imberger, J. Smith, R. E. H., Hecky, R. E., Lam,, D. C. L. and Schertzer, W. M., (2005): Modeling as a tool for nutrient management in Lake Erie: a hydrodynamic study. *Journal Great Lakes Research* 31: 309–318.

León, L. F., Smith, R. E. H., Romero, J. R. and Hecky, R. E. (2006): Lake Erie hypoxia simulations with ELCOM–CAEDYM. 3rd Biennial meeting of the International Environmental Modelling and Software Society. 6 pp.

Loveless, A. M. (2009). A multi–dimensional receiving water quality model for Botany Bay (Sydney, Australia). 18th World IMACS / MODSIM Congress. Cairns, Australia.

McIntire, C. D., Larson, G. L. and Truitt, R. E. (2007): Seasonal and interannual variability in the taxonomic composition and production dynamics of phytoplankton assemblages in Crater Lake, Oregon. *Hydrobiologia* 574: 179–204.

Missaghi, S. and Hondzo, M. (2010): Evaluation and application of a three–dimensional water quality model in a shallow lake with complex morphometry. *Ecological Modelling* 221: 1512–1525.

Njuguna, H., Romero, J. R., Khisa, P., Ewing, P., Antenucci, J. P., Imberger, J. and Okungu, J. (2006): The effect of turbid inflows into Winam Gulf, Lake Victoria: a 3D modeling study with ELCOM–CAEDYM. Lake Victoria Environmental Management Program. 5 pp.

Okely, P., Yeates, P. S., Antenucci, J. P., Imberger, J. and Hipsey, M. R. (2006): Modelling of the impact of the Perth Seawater Desalination Plant discharge on dissolved oxygen in Cockburn Sound. Centre of Water Research, University of Western Australia. Final Report: WP2136PO.

Qu, W., Morrison, R. J., West, R. J. and Su, C. (2007): Spatial and temporal variability in dissolved inorganic nitrogen fluxes at the sediment–water interface in Lake Illawarra, Australia. *Water, Air & Soil Pollution* 186: 15–28.

Robson, B. J. and Hamilton, D. P. (2004): Three–dimensional modelling of a Microcystis bloom event in the Swan River estuary, Western Australia *Ecological Modelling* 174(1–2): 203–222.

Rueda, F. J., Schladow, S. G. and Clark, J. F. (2008): Mechanisms of contaminant transport in a multi–basin lake. *Ecological Applications* 18(8): 72–87.

Rutherford, J. C., Dumnov, S. M. and Ross, A. H. (1996): Predictions of phosphorus in Lake Rotorua following load reductions. *New Zealand Journal of Marine and Freshwater Research.* 30: 383–396.

Rutherford, K. (2003): Lake Rotorua Nutrient Load Targets. National Institute of Water & Atmospheric Research Ltd, Hamilton, New Zealand (NIWA) – Client Report: HAM2003–155. 64 pp.

Sakamoto, M. (1966): Primary productivity by phytoplankton community in some Japanese lakes and its dependence on lake depth. *Archiv für Hydrobiologie* 62: 1–28.

Sayg–Basbug, Y. and Demirkalp, F. Y. (2004): Primary production in shallow eutrophic Yenicaga Lake (Bolu, Turkey). *Fresenius Environmental Bulletin* 13: 98–104.

Schindler, D. W. (1978): Factors regulating phytoplankton production and standing crop in the world's freshwaters. *Limnology and Oceanography* 23: 478–486.

Spillman, C. M., Imberger, J., Hamilton, D. P., Hipsey, M. R. and Romero, J. R. (2007): Modelling the effects of Po River discharge, internal nutrient cycling and hydrodynamics on biogeochemistry of the Northern Adriatic Sea. *Journal of Marine Systems* 68(1–2): 167–200.

Trolle, D., Jørgensen, T. B. and Jeppesen, E. (2008a): Predicting the effects of reduced external nitrogen loading on the nitrogen dynamics and ecological state of deep Lake Ravn, Denmark, using the DYRESM–CAEDYM model. *Limnologica* 38: 220–232.

Trolle, D., Skovgaard, H. and Jeppesen, E. (2008b): The Water Framework Directive: Setting the phosphorus loading target for a deep lake in Denmark using the 1D lake ecosystem model DYRESM–CAEDYM. *Ecological Modelling* 219(1–2): 138–152.

Urabe, J., Sekino, T., Nozaki, K., Tsuji, A., Yoshimizu, C., Kagami, M., Koitabashi, T., Miyazaki, T. and Nakanishi, M. (1999): Light, nutrients and primary productivity in Lake Biwa: An evaluation of the current ecosystem situation. *Ecological Research* 14(3): 233–242.

Vincent, W. F., Gibbs, M. M. and Dryden, S. J. (1984): Accelerated eutrophication in a New Zealand lake: Lake Rotoiti, Central North Island. *New Zealand Journal of Marine and Freshwater Research.* 18: 431–440.

Chapter 2

Temporal and spatial variations in phytoplankton productivity in surface waters of a warm–temperate, monomictic lake in New Zealand

Abstract

Surface phytoplankton productivity measurements were carried out in morphologically complex Lake Rotoiti with the objective of defining variations between sites and seasons, and the dominant environmental drivers of these variations. Measurements were carried out monthly at two depths at each of three morphologically diverse stations for one year in the lake. Productivity at the surface of the shallow embayment was significantly higher in most months of the year compared with the surface of the other two stations but there were no significant differences from September–December 2004. There were no relationships between measured environmental variables and primary productivity or specific production. Inorganic nutrient concentrations at the surface of the shallow station were low throughout the whole year but at the other two stations they showed a typical pattern for monomictic lakes of higher levels during winter mixing and declining concentrations during thermal stratification. The high variability between sites found in this study indicates that it is important to account for local differences in productivity in morphologically diverse lakes, and that whole lake productivity estimates may vary greatly depending on the location and depth of productivity measurements.

2.1 Introduction

Seasonal patterns of phytoplankton primary productivity are influenced by interactions amongst temperature, light, nutrients, mixing depth and phytoplankton biomass and composition (Schindler 1978; Urabe et al. 1999; McIntire et al. 2007), as well as lake morphological characteristics (Sakamoto 1966; Håkanson 2005). Production in the surface mixed layer of temperate lakes may be highly seasonal, often restricted by availability of nutrients as particulate material is lost from the trophogenic zone over the stratified period, and by seasonal variations in light (Vanni & Temte 1990). A common pattern of phytoplankton productivity in dimictic lakes of the Northern Hemisphere is low to moderate rates during winter stratification and during spring circulation, an increase associated with the rapid increase in diatom biomass, and a peak later in spring–summer before a decline in autumn (Wetzel 2001). By contrast, in tropical lakes productivity and biomass maxima may occur at any time of the year in response to upwelling of nutrient–rich water from the breakdown of stratification, internal seiches or often related to seasonal cooling or storm–induced circulation (Coulter 1963; Descy et al. 2005; Naithani et al. 2007).

Numerous previous studies of phytoplankton productivity have focused on temporal variations within a lake (Vincent et al. 1984; Carrick et al. 1993; Berman et al. 1995), generally at seasonal time scales and using only one sampling station (Berman & Pollingher 1974; Lehmann et al. 2004; Arst et al. 2008). Recently there has been increased interest in horizontal variations in phytoplankton productivity within lakes (Descy et al. 2005; Çelik 2006; Qu et al. 2007). Large horizontal variations in primary production are characteristic of estuaries and coastal areas (Gong et al. 2003; Glé et al. 2008), but many lakes are perceived to be relatively homogeneous horizontally, partly because of their small size compared with coastal or open waters and the reduced influence of inflows compared with estuaries. A lack of attention to spatial variations in lake productivity may also be partly attributed to difficulties in performing simultaneous measurements of productivity across a number of stations, a problem somewhat circumvented by on–boat or laboratory incubations (Satoh et

al. 2006), but with inherent issues of extrapolation to in situ conditions. Studies which have focussed on spatial distributions of phytoplankton have found large variations in biomass (Fietz et al. 2005; Wondie et al. 2007), even in small, shallow lakes (Sayg–Basbug & Demirkalp 2004). Spatial heterogeneity of phytoplankton production may play an important role in ecological assessments of whole–lake trophic status and productivity, which do not adequately reflect localised variations in growth rates. This heterogeneity has been examined with mathematical models (Naithani et al. 2007; Hillmer et al. 2008) but there are few in situ studies.

The objective of this study was to quantify the relative importance of spatial and seasonal variations in phytoplankton productivity in surface or near–surface waters in a morphologically complex, deep lake. Spatial variations in phytoplankton productivity can be caused by physical, chemical, biological processes and their interactions. For example, shallow areas of a lake tend to have higher mean water column irradiance or may be proximal to localised nutrient sources such as inflows (Qin et al. 2007; Zhang et al. 2007) or resuspended sediments (Schallenberg & Burns 2004).

I chose to study spatial variations in surface primary production in Lake Rotoiti because of its basin morphology, which is highly complex, with shallow embayments connected to a large central basin. In addition a major inflow enters the shallow western basin. Vincent et al. (1984b) previously described the seasonal pattern of productivity in the main basin of Lake Rotoiti, and provide data which can be used to make historical comparisons against my results. I hypothesised that categorisations of lake productivity into seasonal patterns may be too simplistic and could be biased by site specificity related to lake morphology as well as heterogeneity of the key driving variables.

2.2 Site description

Lake Rotoiti (38º 02’ 39.5 S, 176º 25’ 30.0 E) is a deep (max. depth 124 m), warm monomictic, eutrophic lake in North Island, New Zealand (Figure 2.1). It is located 278 m a.s.l. and has a surface area of 34.6 km^2. The lake is relatively long

and narrow but with two distinct basins; a deep eastern basin and a shallower western basin (max depth 25 m), separated by a narrow constriction. Lake Rotoiti has several bays, notably Okawa Bay, which connects to the south–west end of the western basin via a shallow constriction of c. 1.5 m depth. Adjacent to Okawa Bay is the Ohau Channel inflow to Lake Rotoiti, which arises from eutrophic Lake Rotorua (Burger et al. 2008). Despite waste water diversion in 1991 from Lake Rotorua the water quality has not improved (Burger et al. 2008) recent research suggests further deterioration (Hamilton et al. 2010). The only surface outflow from Lake Rotoiti is Kaituna River (mean discharge 2004/2005: 22.5 m^3 s^{-1}) at the northern end of the western basin. Ohau Channel inflow (mean discharge 2004/2005: 18.9 m^3 s^{-1}) can intrude into Lake Rotoiti as an underflow, interflow or overflow, depending on the temperature of the Channel relative to the thermal structure of Lake Rotoiti (Vincent et al. 1986; 1991). There are seven smaller surface inflows arising from nearby groundwater springs (discharges of 0.0048 to 0.472 m^3 s^{-1}; mean temperature c. 13 °C) and three geothermal springs (discharges of 0.0018 to 0.0157 m^3 s^{-1} mean temperature c. 26 °C).

Phytoplankton biomass in Lake Rotoiti is highest in winter (Cassie 1978) and primary productivity in the main basin of Lake Rotoiti generally exceeds summer productivity rates by a factor of 2.5 to 3.5 (Burnet & Davis 1980; Vincent et al. 1984). The lake underwent a relatively rapid process of eutrophication between the first limnological investigation by Jolly (1968) and a subsequent study by Vincent et al. (1986). The main reason for this rapid deterioration was considered to be the nutrient–enriched status of the Ohau Channel inflow arising from Lake Rotorua (Vincent et al. 1984; 1991). This inflow is commonly present as an underflow in autumn (March/April) through to spring (September), though the lake is normally well mixed vertically through winter (June–August). The underflow condition was considered to have some benefit in reducing deoxygenation of bottom waters when Lake Rotoiti is stratified (Gibbs 1992).

Early limnological studies of other warm monomictic lakes of the Central Volcanic Plateau (CVP) of North Island, New Zealand, showed that there is peak phytoplankton production and biomass during seasonal mixing in winter, not only

in Lake Rotoiti (Vincent et al. 1984), but also in oligotrophic Lake Taupo (mean depth, $\bar{z}$ = 97 m) where levels were found to be around ten–fold higher in winter than in summer (Vincent 1983). By contrast, in Lake Waikaremoana, another deep ($\bar{z}$ = 93 m), oligotrophic lake of the CVP, the annual maximum of phytoplankton productivity occurred in summer at a time that coincided with formation of a deep chlorophyll maximum (Howard–Williams et al. 1986). In mesotrophic Lake Rotorua ($\bar{z}$ = 11 m), immediately upstream of Lake Rotoiti, the seasonal productivity maximum occurred during summer or early autumn (Burnet & Davis 1980).

2.3 Material and methods

2.3.1 Environmental data collection

Sampling stations were established at a deep (c. 100 m) site in the main (eastern) basin (Station 1), a 25 m site in the narrow region that delineates the eastern and western basins and is approximately 2 km from the Ohau Channel entrance (Station 2), and a semi–enclosed, shallow (< 5 m) embayment, Okawa Bay (Station 3; Figure 2.1) c. 600 m south of Ohau Channel. Mid–lake sites (close to my Station 1) have a long observation history and are considered to be representative of the main lake basin (Jolly 1968; Fish 1975; Burnet & Davis 1980; Vincent et al. 1984). Station 2 has been used previously to examine underflows arising from the Ohau Channel (Vincent et al. 1991) while Station 3 was chosen because of frequently reported algal blooms in this embayment. Temperature at Stations 1 and 2 was measured at 15 minute intervals with thermistor chains. Tidbit Underwater Data Loggers (resolution <0.3 °C; accuracy +/- 0.2 °C) were used to record temperature profiles. At Station 1 the thermistors were placed at depths of 0, 2.5, 5, 7.5, 10, 12.5, 15, 20, 25, 30, 35, 40, 45, 50, 55, 60, 65, 70, 75 and 80 m and at Station 2 at depths of 0, 2.5, 5, 7.5, 10, 12.5, 15, 17.5, 20 and 25 m.

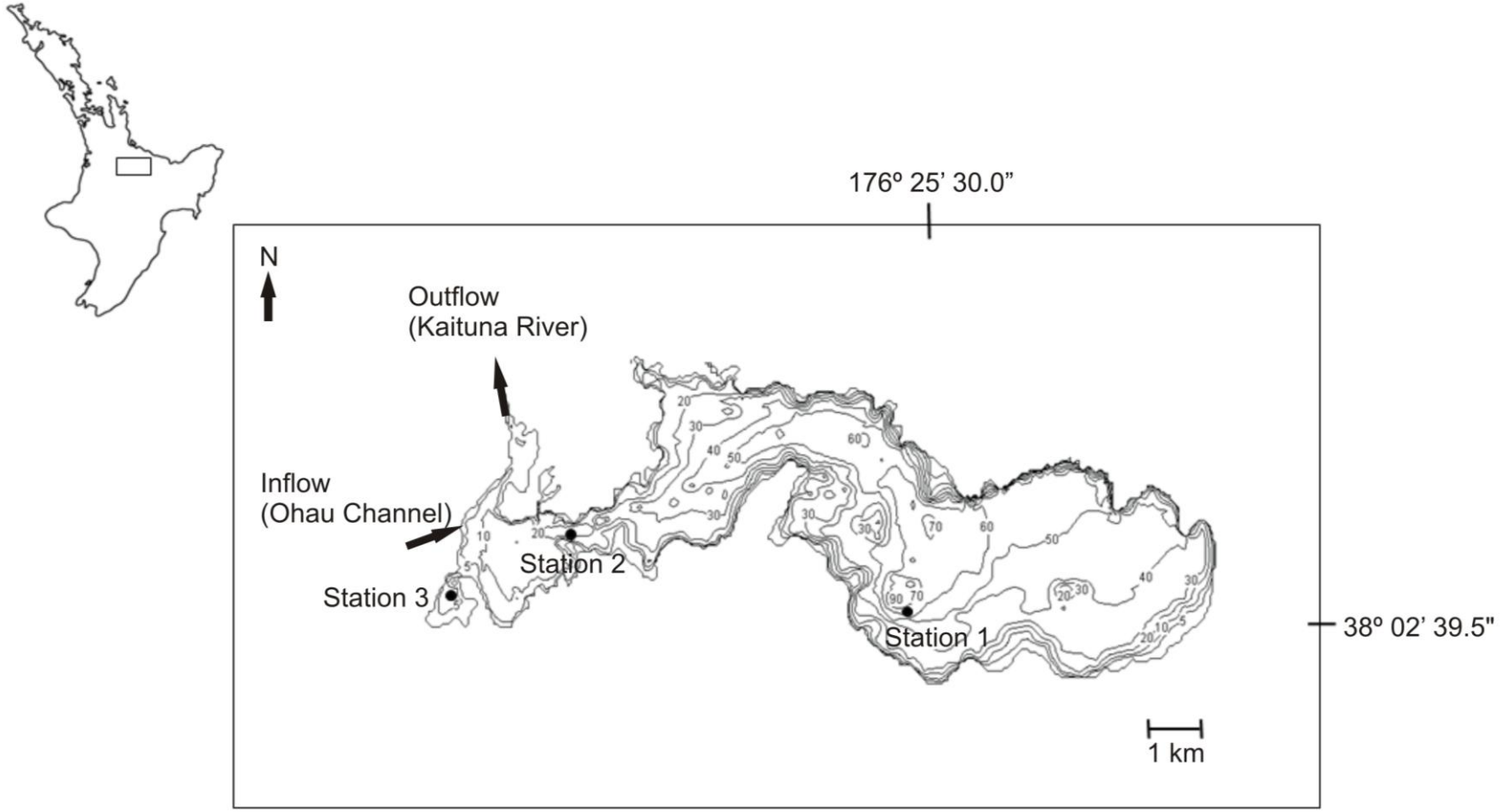

Figure 2.1: Location map of Lake Rotoiti, North Island, New Zealand with depth contours 5, 10, 20, 30, 40, 50, 60, 70, 80 , 90 m and the location of sampling Stations 1–3.

Stations were sampled monthly from June 2004 to May 2005. Temperature profiles (resolved at c. 0.1 m) were taken with a Seabird Electronics (SBE) 19plus Seacat CTD profiler fitted with an additional sensor for photosynthetically available radiation (PAR, Licor Inc.). Discrete water samples for dissolved nutrient analysis were collected with a Schindler–Patalas trap immediately below the water surface (denoted as 0 m). These samples were filtered on the boat, immediately after collection, through a Whatman GF/C filter with nominal pore size of 1.2 µm, and the filtrate was stored on ice for transportation to the laboratory, where samples were deep–frozen before analysis for ammonium (denoted as NH_4–N), oxidised nitrogen species (denoted as NO_3–N + NO_2–N; NO_2–N) and soluble reactive phosphorus (denoted as SRP) by flow injection analysis on a Lachat CQ8000 FIA system employing standard methods (Zellweger Analytics 2000, Diamond 2000). Priscu et al. (1986) showed no distinct seasonal trend in DON concentration in Lake Rotoiti. During the time of this study (1981-1982) N limitation experiments were undertaken (White 1985), when it was found that Lake Rotoiti is N limited, which suggests that DON is not available for phytoplankton uptake. Central North Island lakes are rich in reactive silicon due to high levels of pumice and ignimbrite from successive volcanic eruptions (Viner & White 1987). Silica was therefore not expected to be a limiting nutrient in my study.

Concentrations of NO_3–N were determined by subtraction of NO_2–N from NO_3–N + NO_2–N. Discrete water samples for chlorophyll analysis were taken at depth of 0, 20, 40, 60, 80 m at Station 1, 0, 15, 25 m at Station 2, and 0 and 5 m at Station 3. Filters were immediately shock–frozen in liquid nitrogen and transported to the laboratory. Chlorophyll *a* concentrations were determined using 90% acetone extraction and fluorometric assay (Turner Design 10–AU Fluorometer) with an acidification step to correct for phaeophytin (Axler & Owen 1994).

2.3.2 Primary productivity

Water samples for measurements of primary production were collected with a Schindler–Patalas trap from immediately below the water surface (denoted as 0

m) and from a depth of 5 m. The vertical data collection was restricted according to the shallow nature of Station 3, to allow direct depth comparisons between stations and also because of the time involved to be able to perform simultaneous productivity incubations at three stations. Sample water from the respective depths was used to rinse and then fill one dark and four transparent 280 mL glass bottles. A fixed amount of labelled carbon–13 ($NaH^{13}CO_3$) was added to four bottles (one dark, three light) to achieve a ^{13}C concentration between 5–15 % of the expected dissolved inorganic carbon (DIC) concentration in the water samples (Hama et al. 1983). Bottles were then incubated in situ at 0 m and 5 m for 4 h centred approximately around the solar zenith.

The dark bottle from each depth was used to correct for non–photosynthetic carbon uptake and an un–incubated bottle without added ^{13}C was used to correct for natural abundance of ^{13}C in the water sample. After incubation the bottles were stored on ice in the dark for transportation to the laboratory, where each sample was immediately filtered under a light vacuum onto a pre–combusted Whatman glass–fibre filter (1.2 µm GF/C) and dried in a vacuum desiccator prior to analysis.

Water samples for analysis of dissolved inorganic carbon (DIC) were taken at arm's length under the surface using an airtight syringe. Samples were stored at 4 °C during transport to the laboratory where they were placed in a 100 mL beaker and brought to 25 °C. An automated titration procedure (Metrohm 702SM Titrino with pH glass electrode) with 0.1 N HCl was used to determine DIC concentrations from titration curves (Marchetto et al. 1997). This concentration was used to correct for total carbon in the sample bottles based on the amount of ^{13}C added.

The concentration of particulate organic carbon (POC) as well as the atom % of ^{13}C in the natural and incubated samples were determined on the vacuum–dried filters by mass spectrometry (Dumas Elemental Analyser; Europa Scientific ANCA–SL) interfaced with an isotope mass spectrometer (Europa Scientific 20–20 Stable Isotope Analyser). The atom percent of the inorganic carbon (A_{ic}) was

calculated by the amount of ^{13}C added to the 280 mL bottle and later corrected for the amount of DIC in the water samples. Productivity (P) was determined using the average value for the triplicate light bottles corrected for the dark bottle carbon uptake and for natural ^{13}C abundance (Hama et al. 1983):

$$P = POC \frac{(A_{is} - A_{ns})}{t\,(A_{ic} - A_{is})}$$

where A_{ns} is the atom % of the natural (unincubated) sample, A_{is} is the atom % of the incubated sample, POC is the concentration of particulate organic carbon (mg m^{-3}) and P is the productivity (mg C m^{-3} h^{-1}) and t duration of incubation (h). Chlorophyll–specific productivity was determined by dividing P by chlorophyll *a* concentrations from 0 m samples for the purpose of comparisons over time and amongst sites.

Hourly shortwave radiation data were obtained from Rotorua Airport meteorological station on the southern shore of Lake Rotorua, 7 km from Lake Rotoiti. Photosynthetically available radiation (PAR) was taken to be 45% of the shortwave radiation (Papaioannou et al. 1993). The vertical diffuse attenuation coefficient (K_d(PAR)) for downward irradiance was determined from the slope of the linear regression of the natural logarithm of downwelling irradiance (ln(E_d(PAR)) versus depth, where PAR(z) is the photosynthetically active radiation at depth z derived from the CTD profiles.

Pearson's correlation analysis was used to examine relationships among dissolved nutrient concentrations, both within and among sites, and potential relationships between surface (upper 5 m) primary production and environmental variables (light, nutrients, surface mixed layered depth). Variations in primary productivity among the sampling stations within each sample date or depth were evaluated with a one–way analysis of variance (ANOVA). For significant ($p < 0.05$) test results a Student–Newmann–Keul (SNK) test was then used to identify which sampling stations differed from one another. Data were tested for normal distribution and homogeneity of variance by visual inspection of the residuals.

2.4 Results

2.4.1 Environmental data

Results of temperature profiles from Stations 1 and 2 indicate that Lake Rotoiti is a monomictic lake, but at Station 3, in the shallow bay, the water column was generally well mixed throughout the year, as denoted by the vertical isotherms (Figure 2.2). At comparable depths, temperatures were very similar across the three stations. The thermocline at Station 1 and Station 2, which initially formed in November 2004, was at least partially disrupted in December 2004, but re–established later in the same month, progressively deepening for the remainder of the stratified period until the water column was fully mixed again in June 2005. Water temperature at the surface at Stations 1 and 2 was at its minimum of 10.1 °C in July 2004 and at its maximum of 22 °C in mid–February 2005. Minimum measured water temperature was slightly lower at Station 3 at 9.8 °C in August 2004, while the maximum measured temperature for Station 3 (February 2005) was the same as for the other stations.

Surface concentrations of NH_4–N, NO_3–N and PO_4–P varied widely in Lake Rotoiti among stations and with time of year (Figure 2.3). Nutrient concentrations were low (NH_4–N < 38.3 mg m^{-3}, NO_3–N < 33.6 mg m^{-3}, SRP < 12.1 mg m^{-3}) at all three stations when the main body of the lake was stratified. In winter 2004 nutrient concentrations were comparably high at Stations 1 and 2 (NH_4–N > 111.5 mg m^{-3} in July 2004, NO_3–N > 166.6 mg m^{-3} in August 2004, SRP > 42.7 mg m^{-3} in July 2004) following the breakdown of stratification. Concentrations of NO_3–N and SRP gradually declined towards detection limits (c. 1 mg m^{-3}) by December 2004 when the thermocline had re–established. Concentrations of NH_4–N at Stations 1 and 2 showed only a brief winter peak (112 and 115 mg m^{-3}, respectively) during July 2004 and remained at relatively low levels throughout the remainder of the year. A slight increase in all nutrient species coincided with the mixing event in December 2004 at Station 2. While NH_4–N and SRP concentrations at Stations 1 and 2 were similar, NO_3–N at Station 1 exceeded values at Station 2 by 1.5–fold. Station 3 showed relatively low nutrient

concentrations for all species throughout the year compared to Station 1 and 2, with maximum concentrations of 10.7 mg m^{-3} for NH_4–N, 28.1 mg m^{-3} for NO_3–N and 12.4 mg m^{-3} for SRP.

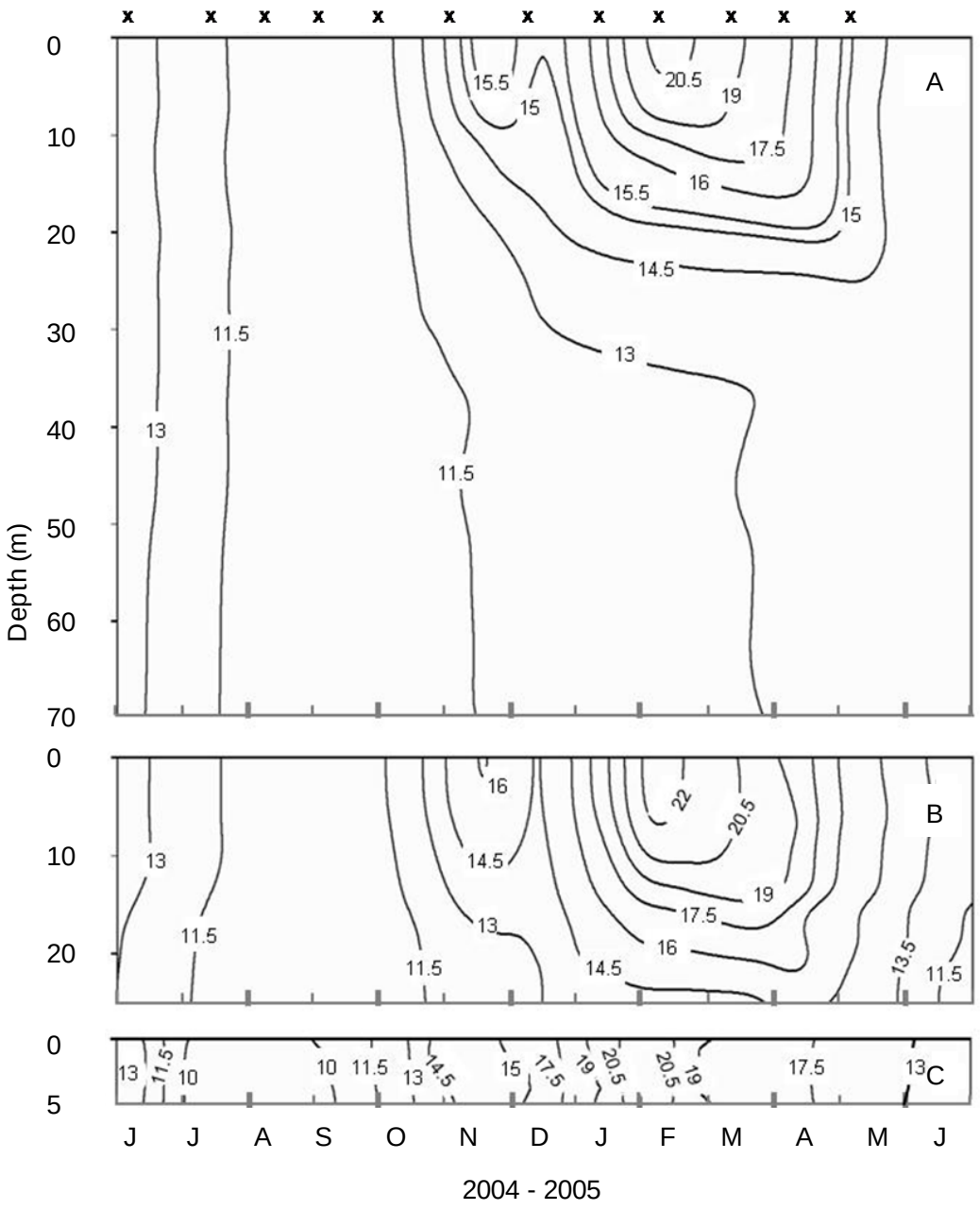

Figure 2.2: Contour plot of temperature (°C) for (A) Station 1, (B) Station 2 and (C) Station 3 from June 2004 to June 2005. (A) and (B) are from thermistor chain records at 15 minute intervals and (C) from monthly CTD profiles. Field sampling dates are marked with x.

Table 2.1: Pearson correlation coefficients (R) for surface nutrient concentrations as a function of sampling station.

* p<0.05	Station 1			Station 2			Station 3		
** p<0.01	NH_4-N	SRP	NO_3-N	NH_4-N	SRP	NO_3-N	NH_4-N	SRP	NO_3-N
Station 1									
NH_4-N	-								
SRP	0.55	-							
NO_3-N	0.12	0.81 *	-						
Station 2									
NH_4-N	0.92 **	0.44	-0.04	-					
SRP	0.73 **	0.88 **	0.61 *	0.71 **	-				
NO_3-N	0.22	0.84 **	0.98 **	0.09	0.65 *	-			
Station 3									
NH_4-N	-0.06	-0.12	0.01	-0.08	-0.25	0.12	-		
SRP	-0.33	-0.06	0.1	-0.3	-0.29	0.18	0.69 *	-	
NO_3-N	-0.23	0.19	0.19	-0.18	-0.14	0.27	0.24	0.63 *	-

Table 2.1 shows Pearson correlation coefficients for surface nutrient concentrations between nutrient species and sites. There were significant correlations between Station 1 and Station 2 for PO_4–P, NH_4–N and NO_3–N but at Station 3 nutrient concentrations were not significantly correlated ($p > 0.05$) with the other two stations.

Chlorophyll *a* fluctuated differently with time at each Station (Figure 2.4). Station 3 consistently showed the highest concentrations and variations over the year, followed by Station 2 and Station 1. Chlorophyll *a* at Stations 1 and 2 remained below 20 mg m^{-3} while at Station 3 it was generally higher and showed distinct peaks in the months of August 2004 and April 2005; values were 10– and 11–fold higher than at Station 1 and 8– and 4–fold higher than at Station 2 in those months. From June 2004 to November 2004 contrary to previous finding (Vincent 1983), Stations 1 and 2 showed a similar trend in surface chlorophyll *a*, with low concentrations in winter, an increase at the end of winter and a relatively stable period during spring. Over the summer months (December 2005 to February 2006) surface chlorophyll *a* at Station 2 followed a similar trend to Station 3, with increasing values in December 2004 and January 2005 followed by a sudden drop in February 2005. By contrast surface chlorophyll *a* at Station 1 decreased continuously over summer. All stations showed a trend of a rapid increase in chlorophyll *a* in April, which was greatest at Station 3.

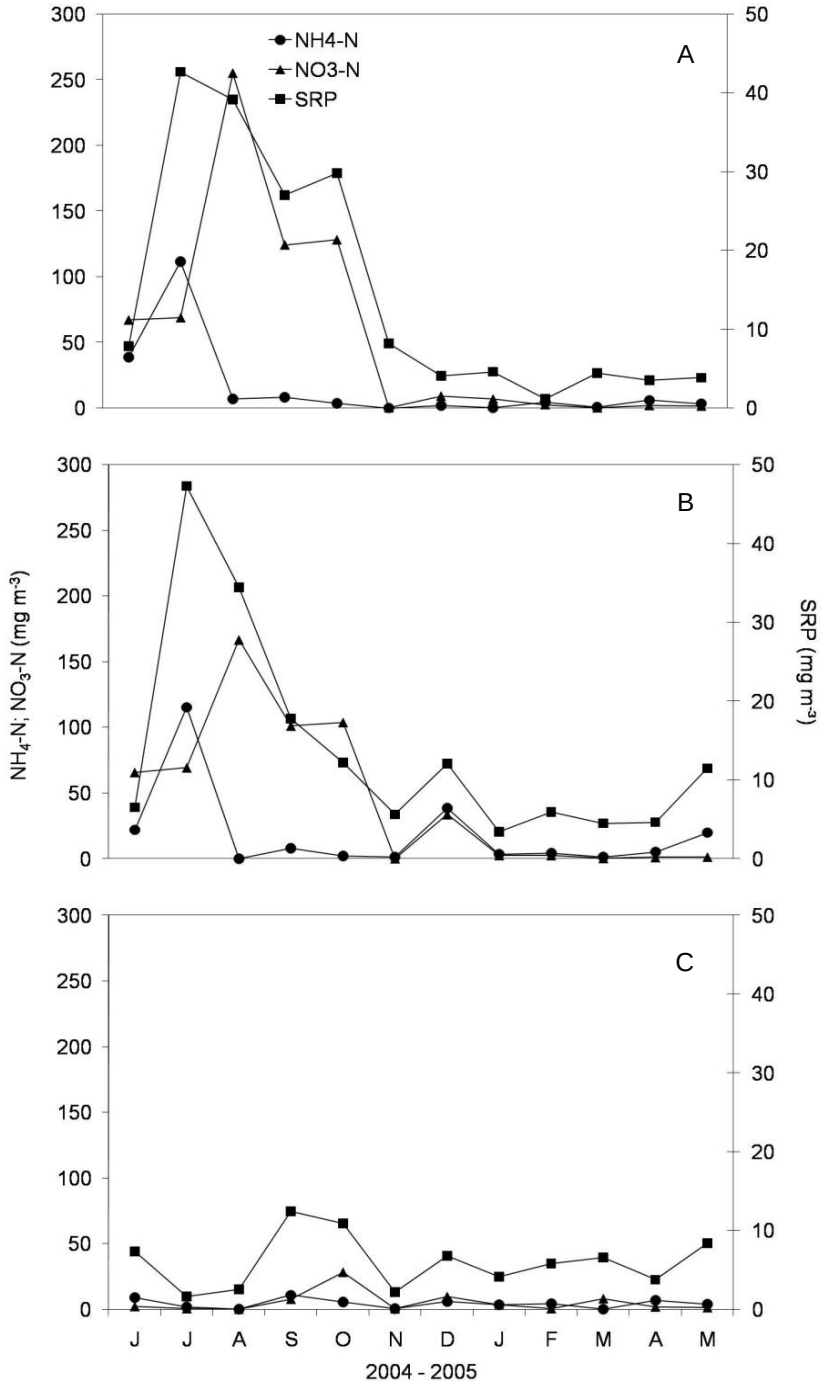

Figure 2.3: Surface concentrations ammonium (NH_4–N) and nitrate (NO_3–N) (left–hand vertical axis) and phosphate (SRP) (right–hand vertical axis) in Lake Rotoiti at (A) Station 1, (B) Station 2 and (C) Station 3 from June 2004 to May 2005.

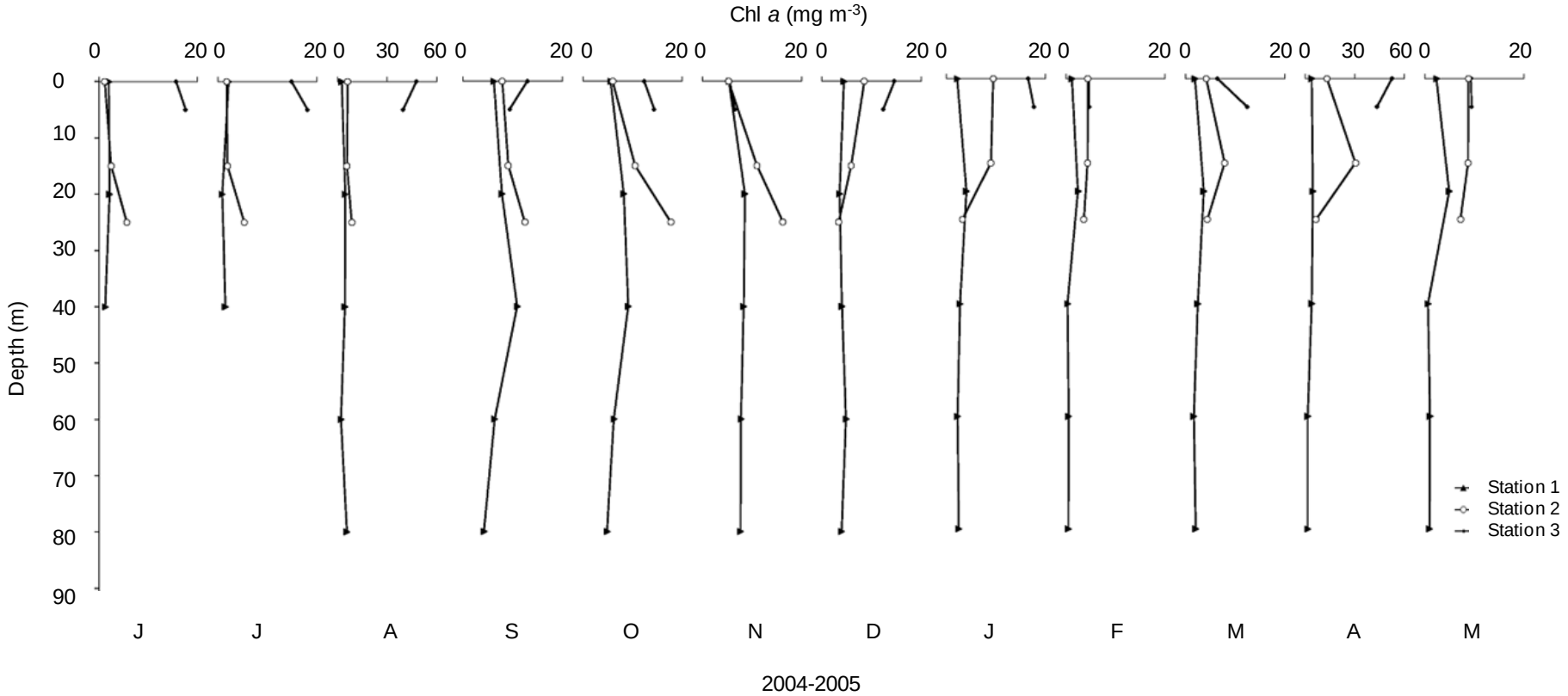

Figure 2.4: Chlorophyll *a* concentrations at Station 1, Station 2 and Station 3 sampled from June 2004 to May 2005.

2.4.2 Productivity and light

The average photosynthetically active radiation (PAR) at 0 and 5 m for the 4–hour period of productivity incubations was quite variable, driven by variations in surface irradiance and by K_d values specific to each station (Figure 2.5). Low surface PAR values in October 2004 were followed by a 17–fold increase at the surface in November 2004 (Figure 2.5). The decrease of PAR at the surface in December coincided with the seasonally unexpected weakening of temperature stratification (Figure 2.2). Levels of PAR at 5 m at Station 3 were substantially reduced compared with Stations 1 and 2. Levels of PAR at 5 m were above 1% of surface values with the exception of Station 3 in April 2005 and Stations 1 and 2 in March 2004. Secchi depths measured through an independent program (Scholes 2009) varied between 3.2 and 7.1 m in the main basin, 1.3 and 7.2 m at Station 1 and 0.7 to 4.6 m at Station 3 during the time of my sampling in 2004–2005.

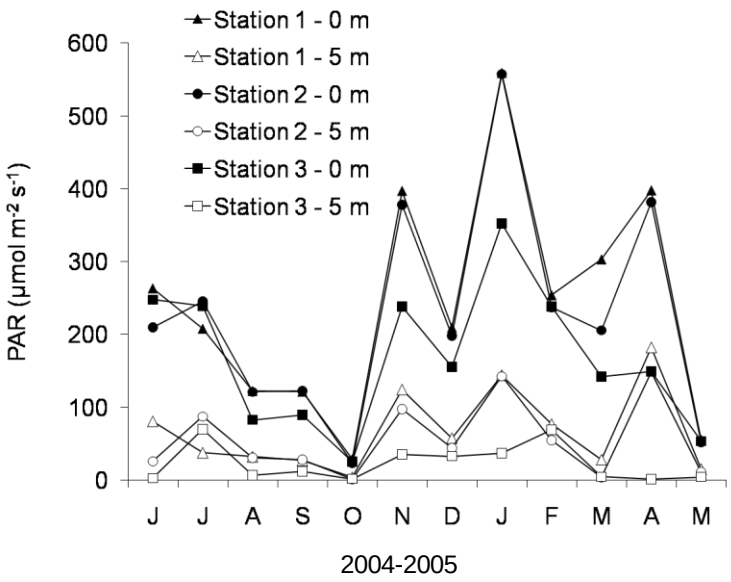

Figure 2.5: Photosynthetically active radiation (PAR) at Stations 1–3 and at depths of 0 and 5 m from June 2004 to May 2005.

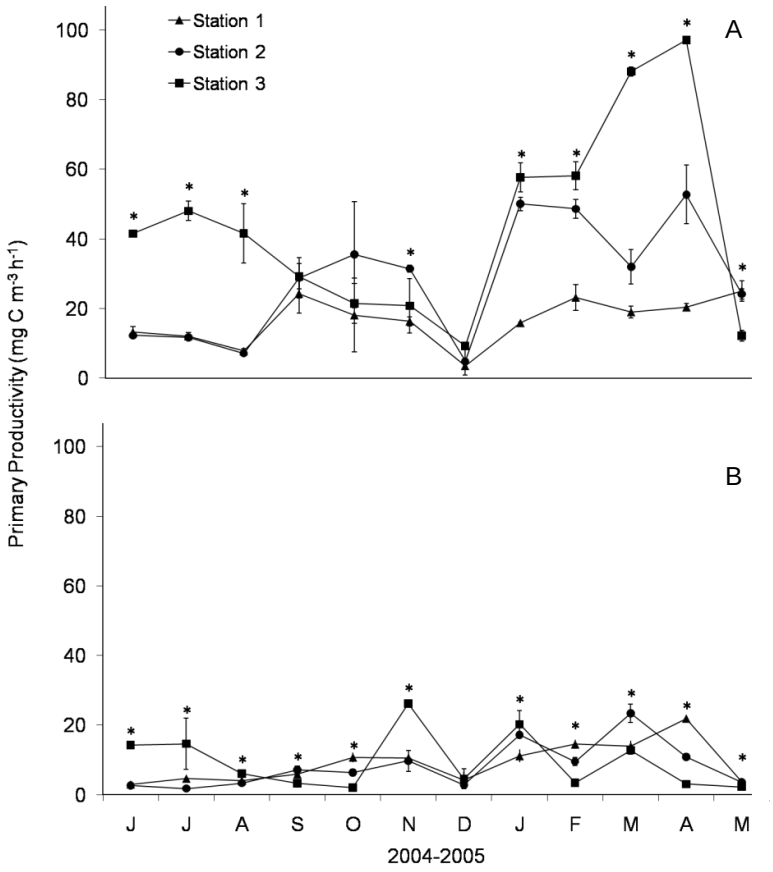

Figure 2.6: Primary productivity at (A) 0 m and (B) 5 m from June 2004 to May 2005, at the three sampling stations. Error bars indicate standard deviation ($n \leq 3$). Asterisks denote significant differences ($p<0.05$) in primary productivity between the stations, analysed with one–way analysis of variance followed by Student Newman–Keul test. See Table 2.2 for results of the post–hoc test.

There were large variations in phytoplankton productivity at the surface through time and among stations (Figure 2.6). Values at 5 m were very similar across the three stations and were considerably lower than at depths of 0 m, e.g., 6.6– and 6.7–fold lower at Stations 1 and 2, respectively, in May 2005. At Station 3 differences with depth were highest in April 2005 when productivity at the surface exceeded the bottom by a factor of 32 and productivity was the highest across all stations and sampling months.The range of surface productivity at Station 1 was small, with values < 25.1 mg C m^{-3} h^{-1}, while Station 2 had a greater range, with values < 52.8 mg C m^{-3} h^{-1}. Station 3 had the widest range, between 9.2 and 97.1 mg C m^{-3} h^{-1}. Maximum productivity at the surface at Station 1 occurred in late autumn (May 2005, 25.1 mg C m^{-3} h^{-1}), but was comparable with September

2004 (24.3 mg C m^{-3} h^{-1}) the other sites showed their maximum in April 2005. For all three sites lowest surface productivity occurred in December 2004 (< 9.2 mg C m^{-3} h^{-1}). The annual minimum in December coincided with a decrease in PAR compared with the previous month, as well as a deep, weak thermocline at Station 1 and a completely mixed water column at Station 2. Lowest and highest differences in monthly productivity between 0 and 5 m coincided with the months of minimum and maximum productivity at each station. During spring and early summer (September–December 2004) when surface waters were heating rapidly, spatial differences in productivity between stations were smallest and mostly not statistically significant ($p > 0.05$). With the transition from winter to spring, productivity at Stations 1 and 2 increased rapidly but decreased at Station 3, resulting in little difference between stations at this time. Only spring productivity results at Station 2 were higher than at Station 3. Generally productivity at Station 3 was considerably higher than at Station 1 and 2.

While phytoplankton productivity was generally highest at Station 3, this was not the case for chlorophyll *a* specific production (dark corrected production/chlorophyll *a*) (Figure 2.7). Specific production was generally highest at station1 throughout the year. Only during spring specific production at the surface of Station 2 exceeded the results at Station 1. Specific production at the surface ranged from 0.8 to 19.4, 0.6 to 11.0 and 0.6 to 13.6 mg C (mg chl *a*)$^{-1}$ h^{-1} at Stations 1, 2 and 3, respectively. The range of the results at 5 m was smaller than at the surface. The minimum measured value for specific production at all stations and depths occurred in December 2004. Only in April 2005 results for depth 5 m at Station 3 showed slightly lower values compared with December. Maximum values occurred in February/March 2005 with the exception of a peak at 5 m at Station 3 in November 2004. The general trend of specific production at Stations 1 and 2 was for higher values in mid–winter (June–July 2004) and in late summer (January–March 2005), while higher values at Station 3 occurred during late summer at the surface.

During most of the year phytoplankton productivity was statistically significantly different between stations (Student–Newman–Keul test; $p < 0.05$; Table 2.2).

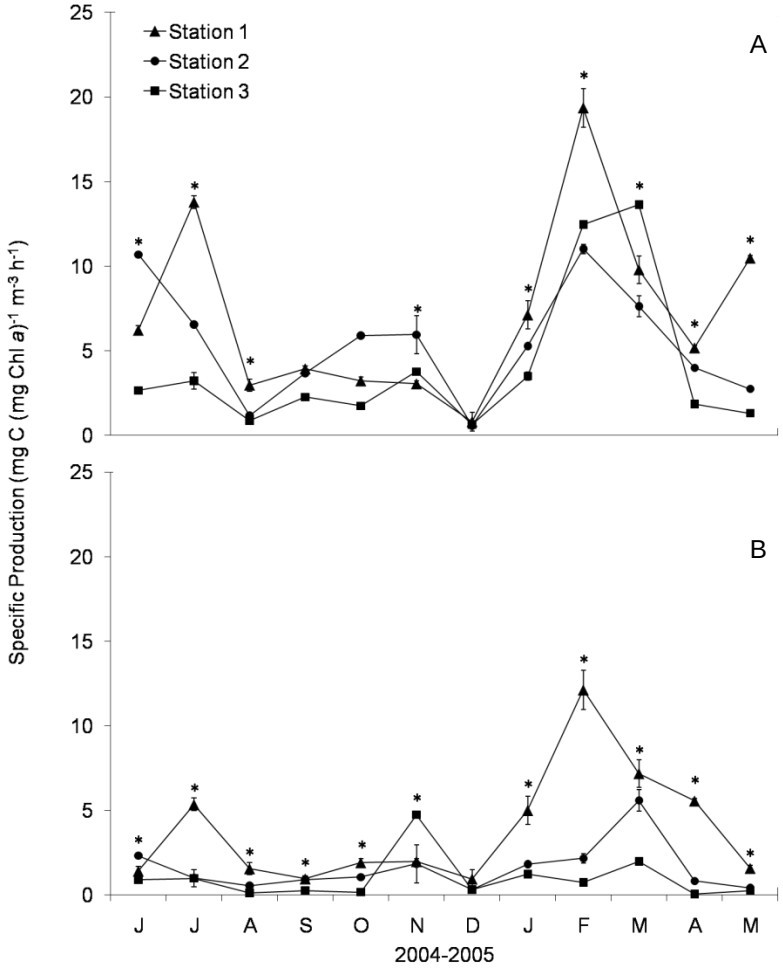

Figure 2.7: Rates of phytoplankton chlorophyll *a* specific production at (A) 0 m and (B) 5 m from June 2004 to May 2005. Error bars describe standard deviation (n≤3). Asterisks denote significant differences ($p<0.05$) in specific production between the stations, analysed with one–way ANOVA followed by Student Newman–Keul test. See Table 2.2 for results of the post–hoc test.

Only in September, October and December 2004 surface productivity showed no significant difference between stations and in December 2004 no significant difference between stations was found at 5 m (Table 2.2, Figure 2.6A). Between June 2004 and August 2004, and January 2005 and May 2005, productivity at Station 3 was significantly higher than at the other stations. Surface productivity at Stations 1 and 2 did not differ significantly from June 2004 to October 2004, December 2004 and May 2005. At 5 m depth there were significant differences among stations throughout the whole year with the exception of December 2004 (Table 2.2). This difference was mostly due to Station 3, while Stations 1 and 2 did not show significant differences from June–September 2004, November–

December 2004 and May 2005. Chlorophyll *a* specific production was generally highest at Station 1 and lowest at Station 3 ($p < 0.05$; Table 2.2), which differs from the results for primary productivity. However the months in which the results showed no significant differences in chlorophyll *a* specific production between stations were identical with the months when primary productivity showed no significant differences between stations.

I tested for correlations of all nutrient species, PAR, chlorophyll a and mixing depth with primary production at both depths at the three stations and surface chlorophyll a with surface nutrient species. The only significant correlation was between PAR and primary production at depth 5 m at Station 2 ($r = 0.74$, $p< 0.05$).

Table 2.2: Results of post–hoc Student Newman–Keul test to determine significant differences ($p<0.05$) of primary productivity and specific production among stations within sampling months.

	Primary Productivity		Specific Production	
	0 m	5 m	0 m	5 m
Jun-04	S3>(S1=S2)	S3>(S1=S2)	S2>S1>S3	(S2=S1)>S3
Jul-04	S3>(S1=S2)	S3>(S1=S2)	S1>S2>S3	S1>(S2=S3)
Aug-04	S3>(S1=S2)	S3>(S1=S2)	S2>S1>S3	(S2=S1)>S3
Sep-04	NS	(S2=S1)>S3	NS	(S1=S2)>S3
Oct-04	NS	S1>S2>S3	NS	S1>S2>S3
Nov-04	(S2>S1)=S3	S3>(S1=S2)	S2>(S1=S3)	S3>S1>S2
Dec-04	NS	NS	NS	NS
Jan-05	S3>S2>S1	(S3=S2)>S1	S1>S2>S3	S1>S2>S3
Feb-05	S3>S2>S1	S1>S2>S3	S1>(S3=S2)	S1>S2>S3
Mar-05	S3>S2>S1	S2>(S1=S3)	S3>S1>S2	S1>S2>S3
Apr-05	S3>S2>S1	S1>S2>S3	S1>S2>S3	S1>S2>S3
May-05	(S1=S2)>S3	(S1=S2)>S3	S1>S2>S3	S1>S2>S3

2.5 Discussion

Studies of phytoplankton productivity in lakes have commonly extrapolated results from a single station to estimate whole–lake productivity (Larson 1972; Tadonléké et al. 2009). This approach may be appropriate for smaller stratified lakes when seasonal variations dominate over spatial variations (Staehr & Sand–Jensen 2006) but even in larger lakes measurements at more than one station are not commonplace. In coastal marine systems, it has been shown that despite high rates of horizontal dispersion, there may be high spatial variability in productivity,

particularly in bays where dispersion can be restricted (Glé et al. 2008). While Lake Rotoiti is considerably smaller than the domain encompassed within most coastal productivity studies, there was up to 10–fold variation in chlorophyll *a* and 5–fold variation in productivity across my three sites on any given sampling day.

Annual productivity in Lake Rotoiti, based on my three stations, was lower at 5 m depth than at the surface. Vincent et al. (1984) took measurements corresponding to my Station 1 at seven depths to a maximum depth of 20 m. They found that P_{max} was confined to waters from the surface to 5 m depth. During one year of sampling they measured two distinct peaks (August 1981, April 1982) in productivity. They also found that productivity increased rapidly from low values in January to an April peak (1982), similar to my findings of increasing productivity from a minimum in December 2004 to high values in April 2005 (Station 2 and 3) and May 2005 (Station 1). My December sampling coincided with coldest recorded air temperatures for this month since 1945. Cold temperatures and strong winds interfered with the establishment of the thermocline in Lake Rotoiti in December 2004; creating a deep mixed layer that would be likely to hinder phytoplankton growth (Kim et al. 2007).

My historical comparison of productivity is restricted to the main lake station used by Vincent et al. (1984). Similar to the historic study I observed highest values of similar magnitude, in September 2004 (24.3 mg C m^{-3} h^{-1}) and May 2005 (25.1 mg C m^{-3} h^{-1}) in the main lake, but compared with the remaining year and the historic study these values did not occur as distinct peaks at this station. Vincent (1983) hypothesised that Lake Taupo, where there is a winter maximum of productivity, may be considered to be a hybrid temperate–tropical system, with characteristics intermediate between the classic winter minimum typical of many temperate lakes and the maximum during the circulation period, which is characteristic of tropical lakes. Similarly, my observations indicate that the timing of the monthly productivity peaks was outside of the summer period of intense seasonal stratification and warm temperatures, but not sufficiently synchronous with winter to be linked with the water column overturn at this time.

My volumetric measurements of productivity at the surface in the main basin of Lake Rotoiti are around one–half of those measured by Vincent et al. (1984). Part of this variation may be attributed to a restriction of measurements to only two depths used in my study, compared with seven depths used by Vincent et al. (1984). It is also possible that other methodological variations contributed to the differences, notably the use of ^{14}C by Vincent et al. (1984) and ^{13}C in my study, though differences between the two isotopic methods have been shown to be small (Mateo et al. 2001). My results support the recent synopsis of Hamilton et al. (2004) that trophic status of Lake Rotoiti may have remained relatively stable, in the meso– to eutrophic range since the 1980s and that there was a period of rapid eutrophication of the lake in the 1960s and 70s.

Productivity at Station 2 and 3 in particular was usually higher than in the main lake basin represented by Station 1. MacIntyre et al. (2002) found in Lake Victoria that temperature differences between shallow constricted bays can generate significant water exchange due to density interflows. I found little difference in temperature at corresponding depths at Stations 2 and 3. It should be noted, however, that temperature measurements in the shallow bay represented by Station 3 were based on monthly profiles which would not reflect diurnal variations in temperature with solar heating. Station 3 is also in close proximity (c. 600 m) to the Ohau Channel inflow while Station 2 is about 2 km east of the Ohau Channel inflow in the direction of the main lake basin (Figure 2.1). High frequency measurements of water temperature in the Ohau Channel inflow show large diurnal fluctuations (Gibbs 1983; Vincent et al. 1991), which would likely drive intrusions of the inflow at different water column depths over the course of a day.

Further to this the shallow Okawa Bay with relatively high sediment surface: water column ratio would be likely to have enhanced nutrient supply arising from mineralisation processes in the bottom sediments (Søndergaard et al. 1996). Levels of inorganic nutrients within the bay (Station 3) remained consistently low over time, however, the high productivity relative to other stations may simply be related to the higher efficiency of converting the available phosphorus into

phytoplankton biomass of shallow systems compared with deep ones (Nixdorf & Deneke 1997). However, the relatively shallow, productive Okawa Bay represents only 1.3 % of the surface area of Lake Rotoiti, so its direct impact on whole lake productivity may be small. Nevertheless there are additional shallow areas in Lake Rotoiti that may collectively contribute phytoplankton biomass while at the same time acting as nutrient sinks.

Vincent et al. (1991) found 10–fold higher nitrate concentrations in the shallow western end of Lake Rototi close to the Ohau Channel inflow compared with the open water area in the main basin. During summer, when the mixing depth in the western basin and the open lake is comparable, Ohau Channel inflow enters Lake Rotoiti as an overflow or interflow, dependent on the temperature gradient between the inflow and the water column of Lake Rotoiti (Vincent et al. 1991; Gibbs 1992). This inflow has the potential to increase primary production in the western basin of Lake Rotoiti by two mechanisms; first by introducing nutrients which can enhance phytoplankton growth and second by increasing phytoplankton biomass which arises from the source water of eutrophic Lake Rotorua (Vincent et al. 1991; Burger et al. 2008). There was no obvious increase in inorganic nutrient concentrations in surface waters of Lake Rotoiti in summer; however, this may have reflected high rates of uptake associated with elevated phytoplankton biomass at this site compared with the main basin. For example, in the Swan River estuary in Western Australia, there was an inverse correlation between inorganic nutrients and biomass, reflecting strong depletion of nutrients when phytoplankton biomass was elevated (Chan et al. 2002).

Spatial comparisons of specific production revealed that the highest rates occur in the main basin. The unusually high rates of specific production at Station 1 in February 2005 (19.4 mg C (mg Chl a)$^{-1}$ h^{-1}) found in my study are close to a light–saturated theoretical maximum (Falkowski 1981). Studies in the marine environment, where chlorophyll *a* may regularly be close to detection limits, have reported values exceeding the theoretical maximum of 25 mg C (mg Chl a)$^{-1}$ h^{-1} (Lohrenz et al. 1994). Surface chlorophyll *a* values in February 2005 at the surface of Station 1 were relatively low (<1.3 μg L^{-1}), which could potentially

lead to large variability in calculations of specific production. Nevertheless specific production values derived from Vincent et al. (1984) were similarly high in February 1982 and suggest that phytoplankton are indeed highly productive at this time of year.

My study did not establish any simple statistical relationships between productivity and nutrient species, PAR, chlorophyll *a* or mixing depth. This reaffirms the complex interactions amongst factors that influence productivity through time and space, and that these factors are not easily able to be separated as to their relative effects of phytoplankton biomass and productivity. My study supports the research of Dabrowski & Berry (2009) who suggest a methodology to identify the best sites for water quality monitoring in complex water bodies, based on flushing rates. I suggest that measurements of water currents in areas where there are constrictions in the lake would be valuable to estimate residence time where there are bays that have the potential to lead to differences in productivity compared with the main basin.

2.6 Conclusions

Estimates of whole lake productivity are inherently difficult to make but for morphologically complex basins it is clear that estimates may be highly biased by the location of the sampling station. The high spatial and temporal variability of productivity observed in Lake Rotoiti points to the difficulty of extrapolating measurements from a single sampling station to a whole lake basin, and highlights the importance of site choice for studies of productivity. Large seasonal variations in productivity observed in my temperate system also suggest that sampling frequency could have an important influence on annual estimates of productivity. While a single sampling station may be suitable for long–term productivity studies involving inter–annual changes in productivity, a more detailed analysis involving several stations may be required to understand the interactions of basin morphology, horizontal and vertical dispersion, and productivity in morphologically complex basins. My findings indicate the potential for different dominant environmental drivers to be acting in association with morphological

effects such as bays or proximity to inflows, which generally complicate the ability to develop simply empirical functions to relate productivity to environmental drivers such as light and temperature.

2.7 References

Arst, H., Nõges, T., Nõges, P. and Paavel, B. (2008): Relations of phytoplankton in situ primary production, chlorophyll concentration and underwater irradiance in turbid lakes. *Hydrobiologia* 599: 169–176.

Axler, R. P. and Owen, C. J. (1994): Measuring chlorophyll and phaeophytin: Whom should you believe? *Lake and Reservoir Management* 8(2): 143–151.

Berman, T. and Pollingher, U. (1974): Annual and seasonal variations of phytoplankton, chlorophyll, and photosynthesis in Lake Kinneret. *Limnology and Oceanography* 19: 31–54.

Berman, T., Stone, L., Yacobi, Y. Z., Kaplan, B., Schlichter, M., Nishri, A. and Pollingher, U. (1995): Primary production and phytoplankton in Lake Kinneret: A long–term record (1972–1993). *Limnology and Oceanography* 40: 1064–1076.

Burger, D. F., Hamilton, D. P. and Pilditch, C. A. (2008): Modelling the relative importance of internal and external nutrient loads on water column nutrient concentrations and phytoplankton biomass in a shallow polymictic lake. *Ecological Modelling* 211(3–4): 411–423.

Burnet, A. M. R. and Davis, J. M. (1980): Primary production in Lakes Rotorua, Rerewhakaaitu and Rotoiti, North Island, New Zealand, 1973–78. *New Zealand Journal of Marine and Freshwater Research.* 14: 229–236.

Cassie, V. (1978): Seasonal changes in phytoplankton densities in four North Island lakes, 1973–74. *New Zealand Journal of Marine and Freshwater Research* 12(2): 153 – 166

Carrick, H. J., Aldridge, F. J. and Schelske, C. L. (1993): Wind influences phytoplankton biomass and composition in a shallow, productive lake. *Limnology and Oceanography* 38: 1179–119.

Çelik, K., 2006 (2006): Spatial and seasonal variations in chlorophyll–nutrient relationship in the shallow hypertrophic Lake Manyas, Turkey. *Environmental Monitoring and Assessment* 117: 261–269.

Chan, T., Hamilton, D. P., Robson, B., Hodges, B. and Dallimore, C. (2002): Impacts of hydrological changes on phytoplankton succession in the Swan River, Western Australia. *Estuaries and Coasts* 25(6): 1406–1415.

Coulter, G. W. (1963): Hydrological changes in relation to biological production in southern Lake Tanganyika. *Limnology and Oceanography* 8: 463–477.

Dabrowski, T. and Berry, A. (2009): Use of numerical models for determination of best sampling locations for monitoring of large lakes. *Science of the Total Environment* 407: 4207–4219.

Descy, J.–P., Hardy, M. A., Stenuite, S., Pirlot, S., Leporcq, S., Kimirei, I., Sekadende, B., S.R., M. and Sinyenza, D. (2005): Phytoplankton pigments and community composition in Lake Tanganyika. *Freshwater Biology* 50: 668–684.

Falkowski, P. G. (1981): Light–shade adaptation and assimilation numbers. *Journal of Plankton Research* 3(2): 203–216.

Fietz, S., Kobanova, G., Izmesteva, L. and Nicklisch, A. (2005): Regional, vertical and seasonal distribution of phytoplankton and photosynthetic pigments in Lake Baikal. *Journal of Plankton Research* 27: 793–810.

Fish, G. R. (1975): Lakes Rotorua and Rotoiti, North Island, New Zealand: Their trophic status and studies for a nutrient budget. New Zealand Ministry of Agriculture and Fisheries. Fisheries Research Bulletin. 8: 70 pp.

Gibbs, M. M. (1983): Penetration of Ohau Channel water into Lake Rotoiti. Taupo Research Laboratory, Department of Scientific and Industrial Research. File report 63: 9pp.

Gibbs, M. M. (1992): Influence of hypolimnetic stirring and underflow on the limnology of Lake Rotoiti, New Zealand. *New Zealand Journal of Marine and Freshwater Research.* 26: 453–463.

Glé, C., Del Amo, Y., Sautour, B., Laborde, P. and Chardy, P. (2008): Variability of nutrients and phytoplankton primary production in a shallow macrotidal coastal ecosystem (Arcachon Bay, France). *Estuarine, Coastal and Shelf Science* 76: 642–656.

Gong, G. C., Wen, Y. H., Wang, B. W. and Liu, G. J. (2003): Seasonal variation of chlorophyll *a* concentration, primary production and environmental conditions in the subtropical East China Sea. *Deep–Sea Research (Part II)* 50: 1219–1236.

Håkanson, L. (2005): The importance of lake morphometry for the structure and function of lakes. *International Review of Hydrobiology* 90: 433–461.

Hama, T., Miyazaki, T., Ogawa, Y., Iwakuma, T., Takahashi, M., Otsuki, A. and Ichimura, S. (1983): Measurements of photosynthetic production of a marine phytoplankton population using a stable ^{13}C isotope. *Marine Biology* 73: 31–36.

Hamilton, D. P., Hawes, I. and Gibbs, M. M. (2004): Climatic shifts and water quality response in North Island lakes, New Zealand. *Internationale Vereinigung für theoretische und angewandte Limnologie* 29(4): 1821–1824.

Hamilton, D. P., O'Brien, K. R., Burford, M. A.,Brookes, J. D. and McBride, C. G. (2010): Vertical distributions of chlorophyll in deep, warm monomictic lakes. *Acquatic Sciences* 72(3): 295–307.

Hillmer, I., van Reenen, P., Imberger, J. and Zohary, T. (2008): Phytoplankton patchiness and their role in the modelled productivity of a large, seasonally stratified lake. *Ecological Modelling* 218(1–2): 49–59.

Howard–Williams, C., Law, K., Vincent, C. L., da Vies, J. and Vincent, W. F. (1986): Limnology of Lake Waikaremoana with special reference to littoral and pelagic primary producers. *New Zealand Journal of Marine and Freshwater Research.* 20: 583–597.

Jolly, V. H. (1968): The comparative limnology of some New Zealand lakes. I. Physical and chemical. *New Zealand Journal of Marine and Freshwater Research.* 2: 214–259.

Kim, H., Yoo, S. and Oh, I. S. (2007): Relationship between phytoplankton bloom and wind stress in the sub–polar frontal area of the Japan/East Sea. *Journal of Marine Systems* 67: 205–216.

Larson, D. W. (1972): Temperature, transparency, and phytoplankton productivity in Crater Lake. *Limnology and Oceanography* 17: 410–417.

Lehmann, M. F., Bernasconi, S. M., McKenzie, J. A., Barbieri, A., Simona, M. and Veronesi, M. (2004): Seasonal variation of the $\delta^{13}C$ and $\delta^{15}N$ of particulate and dissolved carbon and nitrogen in Lake Lugano: Constraints on biogeochemical cycling in a eutrophic lake. *Limnology and Oceanography* 49: 415–429.

Lohrenz, S. E., Fahnenstiel, G. L. and Redalje, D. G. (1994): Spatial and temporal variations of photosynthetic parameters in relation to environmental conditions on coastal waters of the northern Gulf of Mexico. *Estuaries* 17(4): 779–795.

MacIntyre, S., Romero, J. R. and Kling, G. W. (2002): Spatial–temporal variability in surface layer deepening and lateral advection in an embayment of Lake Victoria, East Africa. *Limnology and Oceanography* 47: 656–671.

Marchetto, A., Bianchi, M., Geiss, H., Muntau, H., Serrini, G., Serrini–Lanza, G., Tartari, G. A. and Mosello, R. (1997): Performances of analytical methods for freshwater analysis assessed through intercomparison exercises. I. Total alkalinity. *Memorie dell'Istituto Italiano di Idrobiologia* 56: 1–13.

Mateo, M. A., Pere Renom, P., Hemminga, M. A. and Peene, J. (2001): Measurement of seagrass production using the ^{13}C stable isotope compared with classical O_2 and ^{14}C methods. *Marine Ecology Progress Series* 223: 157–165.

McIntire, C. D., Larson, G. L. and Truitt, R. E. (2007): Seasonal and interannual variability in the taxonomic composition and production dynamics of phytoplankton assemblages in Crater Lake, Oregon. *Hydrobiologia* 574: 179–204.

Naithani, J., Plisnier, P. D. and Deleersnijder, E. (2007): A simple model of the eco–hydrodynamics of the epilimnion of Lake Tanganyika. *Freshwater Biology* 52: 2087–2100.

Nixdorf, B. and Deneke, R. (1997): Why 'very shallow' lakes are more successful opposing reduced nutrient loads. *Hydrobiologia* 342/343: 269–284.

Papaioannou, G., Papanikolaou, N. and Retalis, D. (1993): Relationships of photosynthetically active radiation and shortwave irradiance. *Earth and Environmental Science* 48: 23–27.

Qin, B., Xu, P., Wu, Q., Luo., L. and Zhang, Y. (2007): Environmental issues of Lake Taihu, China. *Hydrobiologia* 581: 3–14.

Qu, W., Morrison, R. J., West, R. J. and Su, C. (2007): Spatial and temporal variability in dissolved inorganic nitrogen fluxes at the sediment–water interface in Lake Illawarra, Australia. *Water, Air & Soil Pollution* 186: 15–28.

Sakamoto, M., (1966): Primary productivity by phytoplankton community in some Japanese lakes and its dependence on lake depth. *Archiv für Hydrobiologie* 62: 1–28.

Satoh, Y., Katano, T., Satoh, T., Mitamura, O., Ambutsu, K., Nakano, S., Ueno, H., Kihira, M., Drucker, V., Tanaka, Y., Mimura, T., Watanabe, Y. and Sugiyama, M. (2006): Nutrient limitation in the primary production of phytoplankton in Lake Baikal. *The Japanese Society of Limnology* 7: 225–229.

Sayg–Basbug, Y. and Demirkalp, F. Y. (2004): Primary production in shallow eutrophic Yenicaga Lake (Bolu, Turkey). *Fresenius Environmental Bulletin* 13: 98–104.

Schallenberg, M. and Burns, C. W. (2004): Effects of sediment resuspension on phytoplankton production: teasing apart the influences of light, nutrients and algal entrainment. *Freshwater Biology* 49: 143–159.

Schindler, D. W. (1978): Factors regulating phytoplankton production and standing crop in the world's freshwaters. *Limnology and Oceanography* 23: 478–486.

Scholes, P. (2009): Rotorua Lakes Water Quality Report. Environment Bay of Plenty. Environmental Publication 12: 81 pp.

Søndergaard, M., Windolf, J. and Jeppesen, E. (1996): Phosphorus fractions and profiles in the sediment of shallow Danish lakes as related to phosphorus load, sediment composition and lake chemistry. *Water Research* 30: 992–1002.

Staehr, P. A. and Sand–Jensen, K. (2006): Seasonal changes in temperature and nutrient control of photosynthesis, respiration and growth of natural phytoplankton communities. *Freshwater Biology* 51: 248–262.

Tadonléké, R. D., Melazzarotto, J., Anneville, O. and Druart, J.–C. (2009): Phytoplankton productivity increased in Lake Geneva despite phosphorus loading reduction. *Journal of Plankton Research* 31: 1–16.

Urabe, J., Sekino, T., Nozaki, K., Tsuji, A., Yoshimizu, C., Kagami, M., Koitabashi, T., Miyazaki, T. and Nakanishi, M. (1999): Light, nutrients and primary productivity in Lake Biwa: An evaluation of the current ecosystem situation. *Ecological Research* 14(3): 233–242.

Vanni, M. J. and Temte, J. (1990): Seasonal patterns of gazing and nutrient limitation of phytoplankton in a eutrophic lake. *Limnology and Oceanography* 35: 697–709.

Vincent, W. F. (1983): Phytoplankton production and winter mixing: Contrasting effects in two oligotrophic lakes. *Journal of Ecology* 71: 1–20.

Vincent, W. F., Gibbs, M. M. and Dryden, S. J. (1984): Accelerated eutrophication in a New Zealand lake: Lake Rotoiti, Central North Island. *New Zealand Journal of Marine and Freshwater Research.* 18: 431–440.

Vincent, W. F., Gibbs, M. M. and Spigel, R. H. (1991): Eutrophication processes regulated by a plunging river inflow. *Hydrobiologia.* 226: 51–63.

Vincent, W. F., Spigel, R. H., Gibbs, M. M., Payne, G. W., Dryden, S. J., May, L. M., Woods, P., Pickmere, S., Davies, J. and Shakespeare, B. (1986): The impact of Ohau Channel outflow from Lake Rotorua on Lake Rotoiti. Taupo Research Laboratory, Division of Marine and Freshwater Science, DSIR 92: 46 pp.

Viner, A. B. and White, E. (1987). Phytoplankton growth. Inland Waters of New Zealand. A. B. Viner, DSIR Science Information Publishing Centre: 191–223.

Wetzel, R. G. (2001). Limnology – Lake and River Ecosystems, Academic Press. 1006 pp.

Wondie, A., Mengtistu, S., Vijverberg, J. and Dejen, E. (2007): Seasonal variation in primary productivity of a large high altitude tropical lake (Lake Tana, Ethiopia): Effects of nutrient availability and water transparency. *Aquatic Ecology* 41: 195–207.

Zhang, Y. L., Qin, B. Q. and Liu, M. L. (2007): Temporal–spatial variations of chlorophyll *a* and primary production in Meiliang Bay, Lake Taihu, China from 1995 to 2003. *Journal of Plankton Research* 29: 707–719.

Chapter 3

The impact of a large river inflow and complex morphometry on hydrodynamics of a temperate lake: A three–dimensional modelling study

Abstract

A three–dimensional (3D) model, ELCOM–CAEDYM, was used to analyse temporal and spatial variations (horizontal and vertical) in water quality in Lake Rotoiti, North Island, New Zealand. Lake Rotoiti has a complex morphometry and high horizontal variability in nutrient concentrations and productivity. The main inflow to the lake arises from adjacent eutrophic Lake Rotorua but Lake Rotoiti also receives water from smaller coldwater spring inflows and surface and sub–surface geothermal inflows that enter the lake. Highly spatially resolved field data was collected monthly to validate the model performance for predictions of temperature, dissolved oxygen and chlorophyll *a*. The heat input from a sub–surface geothermal spring was determined by heat flux simulations on either side of 140 MW, which was estimated based on former heat budget calculations (Calhaem 1973). To match measured temperature increases in the hypolimnion over the period of stratification an energy input around 165 MW was required. Data and model limitations do not provide for certainty regarding the actual magnitude and nature of the heat flux in Lake Rotoiti. The model simulations of temperature, dissolved oxygen and chlorophyll *a* were highly correlated with

measurements of these variables but simulations of spatial surface nutrient concentrations showed relatively low correlation coefficient values at the shallow station. A sensitivity analysis involving examination of sediment nutrient release parameters showed that the inability to accurately reproduce nutrient concentrations may be related to the inability of the model to dynamically adjust the composition and thus nutrient release rates of the bottom sediments. Adjustments were made to meet individual site differences in maximal sediment nutrient release which improved the accuracy of model simulations at local stations, but increased the error of chlorophyll *a* when the whole lake was taken into account. An examination of the behaviour of a conservative tracer set up in the major inflow to Lake Rotoiti, the Ohau Channel, confirmed previous findings that the tracer could enter the lake as a surface inflow, interflow or underflow, depending on temperature gradients between the inflow and lake water. This study highlights that the 3D model ELCOM–CAEDYM is capable of reproducing highly spatially resolved field data in a complex geothermally influenced lake, but spatial simulations of nutrient concentrations were relatively poor unless site–specific calibration was undertaken. Complex 3D models are likely to require greater process representation of bottom sediments in order to begin to accurately simulate the complex sediment–water interactions that occur in a morphometrically complex, eutrophic lake.

3.1 Introduction

Both large lakes (Tilzer 1990) and small lakes (Saygi–Babug 2004) can show marked horizontal variations in water quality. These variations arise to varying degrees from external factors at lake boundaries (e.g., inflows and climate) and internal processes (e.g., mixing and circulation patterns), which are in turn regulated by lake basin morphological characteristics (Robertson & Ragotzkie 1990; Mazumder & Taylor 1994). For example, nutrients are considered to be used more efficiently in shallow regions of a lake in association with higher mean light levels and more intense benthic pelagic coupling, thereby supporting greater phytoplankton biomass (Nixdorf & Deneke 1997; Søndergaard et al. 2005). Horizontal gradients in phytoplankton biomass and nutrients in lakes may be caused by mechanisms such as large river inflows (Vincent et al. 1991) or sediment resuspension (Hamilton & Mitchell 1996), that are not sufficiently rapidly removed by lake processes.

The complexity of spatial (horizontal and vertical) and temporal variations in lake water quality has led to an emphasis on applications of ecosystem models to improve understanding of the physical and biogeochemical interactions within lakes (e.g. Penny et al. 1996; Huang & Xia 2001). These models can be used in assessments of natural and human induced impacts on lake ecosystems, and to support management decisions, for example, by using simulation scenarios involving different management regimes. Several studies have used a one–dimensional (1D) approach to model vertical variations in water quality as stratified lakes were perceived to exhibit limited horizontal variations in water quality compared with vertical variations (Arhonditsis & Brett 2005a; Trolle et al. 2008a). However, in systems where there are large horizontal variations, a three–dimensional (3D) approach may be required, not only to capture the spatial complexity, but also to better represent temporal trends (Eder et al. 2008). For example, in large (area ~2,400 km^2) Lake Taihu, China, a 3D approach was necessary to capture the spatial–temporal variations in water temperature and concentrations of phosphorus, which were strongly influenced by wind–induced circulation (Mao et al. 2008). Despite the capacity of 3D models to capture the

horizontal heterogeneity not represented by 1D models, there have been only a small number of cases where direct comparisons have been made of output from 1D and 3D models (Romero et al. 2004; Kamarainen et al. 2009).

A series of ecological models have been developed over the past decades. Many different approaches have been recently published in two overviews by Jørgensen (2008, 2010) and a wider perspective revealing opportunities for the approaches has been addressed by Mooij et al. (2010). For large lakes in particular the Princeton Ocean Model (Blumberg & Mellor 1987) has been applied to simulate hydrodynamics and water quality (e.g. Schwab & Bedford 1994) or modified to be coupled with climate models (Song et al. 2004). However not often is the model complexity and runtime comparable with the model presented in this study.

Arhonditsis and Brett (2004) found a small but negative correlation between spatial complexity of models and their performance in predicting state variables. Different approaches have been used to improve the performance of complex 3D model ELCOM used for this study and to validate their output. For example, Spillman et al. (2007) used a combination of field data and remote sensing to obtain adequate spatial resolution to validate temperature and chlorophyll distributions from 3D numerical model simulations of the Northern Adriatic Sea. Other validation approaches have used high frequency measurements such as from thermistor chains (León et al. 2005). León et al. (2005) suggested that the ELCOM model could be more fully verified if high–resolution meteorological forcing data were collected and temperature profiles and current velocities were available in the central lake basin, though no comparison of horizontal variability was undertaken. Laval et al. (2003) used spatially resolved wind data to improve the accuracy of simulations with the 3D hydrodynamic model ELCOM. Routine monitoring data from 10 stations were used to model a bloom of the blue–green algae *Microcystis aeruginosa* in a Western Australian estuary (Robson & Hamilton 2004). The low temporal resolution of the sampling regime was found to make it difficult to fully validate the temporal dynamics of the bloom. Hillmer et al. (2008) compared results from a 3D numerical model (ELCOM) with routine measurements of nutrients and chlorophyll *a* at up to 33 stations throughout Lake

Kinneret, but in general it is difficult to obtain both the spatial and temporal resolution necessary for comprehensive validation of 3D models.

Lake Rotoiti shows considerable horizontal variability in phytoplankton assemblages and biomass (Vincent 1983) as well as productivity (Chapter 2). Part of this variability is due to the influence of the Ohau Channel inflow into the shallower western basin (Hamilton et al. 2010), but there are also several partially enclosed bays that have localised variations in phytoplankton biomass and productivity (Chapter 2). Capturing the scale of this variability and its significance to whole lake productivity in an ecosystem model is a major challenge for large lakes such as Rotoiti.

Intensive analysis has previously been undertaken on the impact of the Ohau Channel inflow on water quality of Lake Rotoiti, a meso– to eutrophic lake in North Island, New Zealand (Vincent et al. 1986; Vincent et al. 1991; Gibbs 1992). This inflow arises as an outflow from adjacent eutrophic Lake Rotorua (Burger et al. 2007a; 2008) and enters the western basin of Lake Rotoiti. Blooms of cyanobacteria have occurred with increasing frequency and more regularly in Lake Rotoiti over the past 2–3 decades (Vincent et al. 1984; Hamilton 2004). Progressively increasing nutrient concentrations in the Ohau Channel inflow to Lake Rotoiti are considered to be the main reason for this deterioration of water quality (Vincent et al. 1984; 1991). The Ohau Channel inflow enters Lake Rotoiti as an underflow, interflow or overflow, depending largely on the temperature of the Ohau Channel inflow relative to the vertical structure of temperature in the water column of Lake Rotoiti (Gibbs 1983; Vincent et al. 1991). During winter the cooler incoming water follows the deepest path into the main basin (Vincent et al. 1986). During summer, however, water from Ohau Channel enters as a plunging inflow in the morning, but with daytime solar heating it may become buoyant, increasing the probability that it will be rapidly short–circuited to the Kaituna River (Figure 3.1), the only surface outflow from Lake Rotoiti, which is also located in the western basin of the lake (Vincent et al. 1991).

The western basin of Lake Rotoiti is readily delineated from the deeper eastern basin by a narrow constriction. In most respects the deeper eastern basin behaves like a typical monomictic lake and is stratified for around nine months each year – from spring through autumn (Hamilton et al. 2010). However, there are geothermally heated groundwater inflows associated with the location of the lake in a major geothermal field within the larger, volcanically active Taupo Volcanic Zone. Large–scale models of water flow and heat transfer in this region indicate that water entering the lake may have a temperature of 200–230 ºC (Kissling & Weir 2005). The geothermal heat input to Lake Rotoiti raises the temperature of the hypolimnion by ~2–3 ºC over each period of stratification. The area of heat input into the hypolimnion is confined mostly to two small areas in the eastern basin of the lake where water depth exceeds 70 m (Calhaem 1973).

Geothermal heating affects water temperature in the hypolimnion of Lake Rotoiti through both conductive exchange with geothermally heated sediments and direct inputs of geothermal waters at different water depths (Calhaem 1973; Priscu et al. 1986; Viner & White 1987). Other lakes models have been applied to account for the influence of sediment heating, but these applications are confined mostly to systems where sediments are not especially strongly heated like Lake Rotoiti. These models have been used to analyse the heat budget of geothermally influenced lakes (Hurst et al. 1991; Taran & Rouwet 2008) and sub–glacial lakes such as Lake Vostok (Thoma et al. 2007) and Lake Concordia (Thoma et al. 2009) where ice cover increases the relative importance of sediment heating to the heat budget. There are several examples of water quality and nutrient analysis for geothermal lakes (Pedrozo et al. 2008; Beamud et al. 2009), however model applications for geothermal lakes focus mostly on energy exchanges and not on water quality (Hurst et al. 1991; Taran & Rouwet 2008).

In this study the primary objective was to model spatial and temporal variability of temperature and water quality in Lake Rotoiti and to quantify the spatial accuracy of simulations of water temperature, dissolved oxygen and chlorophyll *a*. A 3D numerical model, ELCOM–CAEDYM (Hodges & Dallimore 2007), was calibrated with data derived from three diverse stations. The ideal calibration–

validation process (Jørgensen 2002) was not followed for different time periods. Model validity was tested with highly spatially resolved field measured in year 2004–2005 and further validated in Chapter 4 using data obtained in year 2008-2009. I sought to evaluate model performance using an array of statistical measures of goodness–of–fit, by comparing a highly spatially resolved data set for temperature, dissolved oxygen and chlorophyll fluorescence, and to a lower–resolution nutrient data set.

3.2 Methods

3.2.1 Site description

Lake Rotoiti is a warm monomictic lake located 278 m a.s.l. (main basin located at 38º 02’ 39.5 S, 176º 25’ 30.0 E) in the Central Volcanic Plateau region of New Zealand (Figure 3.1). The large (34.6 km^2), deep (max. depth 124 m) lake is relatively long and narrow but with two distinct basins: a deep eastern basin and a shallow western basin, separated by a narrow constriction. The only outflow from Lake Rotoiti is into Kaituna River at the northern end of the western basin, in which c. 2 km south of the outflow the main inflow, Ohau Channel, enters. High variability of chlorophyll in Lake Rotoiti relates to this large, nutrient–rich inflow whose origin is from Lake Rotorua (Hamilton et al. 2010) as well as highly productive bays, notably Okawa Bay (Chapter 2) which connects to the south–west end of the western basin via a shallow constriction of c. 2 m depth. The Ohau Channel inflow can intrude into Lake Rotoiti as an underflow, interflow or overflow (see Figure 3.2 for a general conceptualisation), depending on the temperature difference between the Channel and the thermal structure of Lake Rotoiti (Vincent et al. 1986, 1991). There are seven smaller surface inflows arising mostly from groundwater springs entering the lake, with discharges of 4.8 to 472 L s^{-1} and three geothermally–influenced spring inflows (mean temperature c. 26 °C) with discharges of 1.8 to 15.7 L s^{-1}.

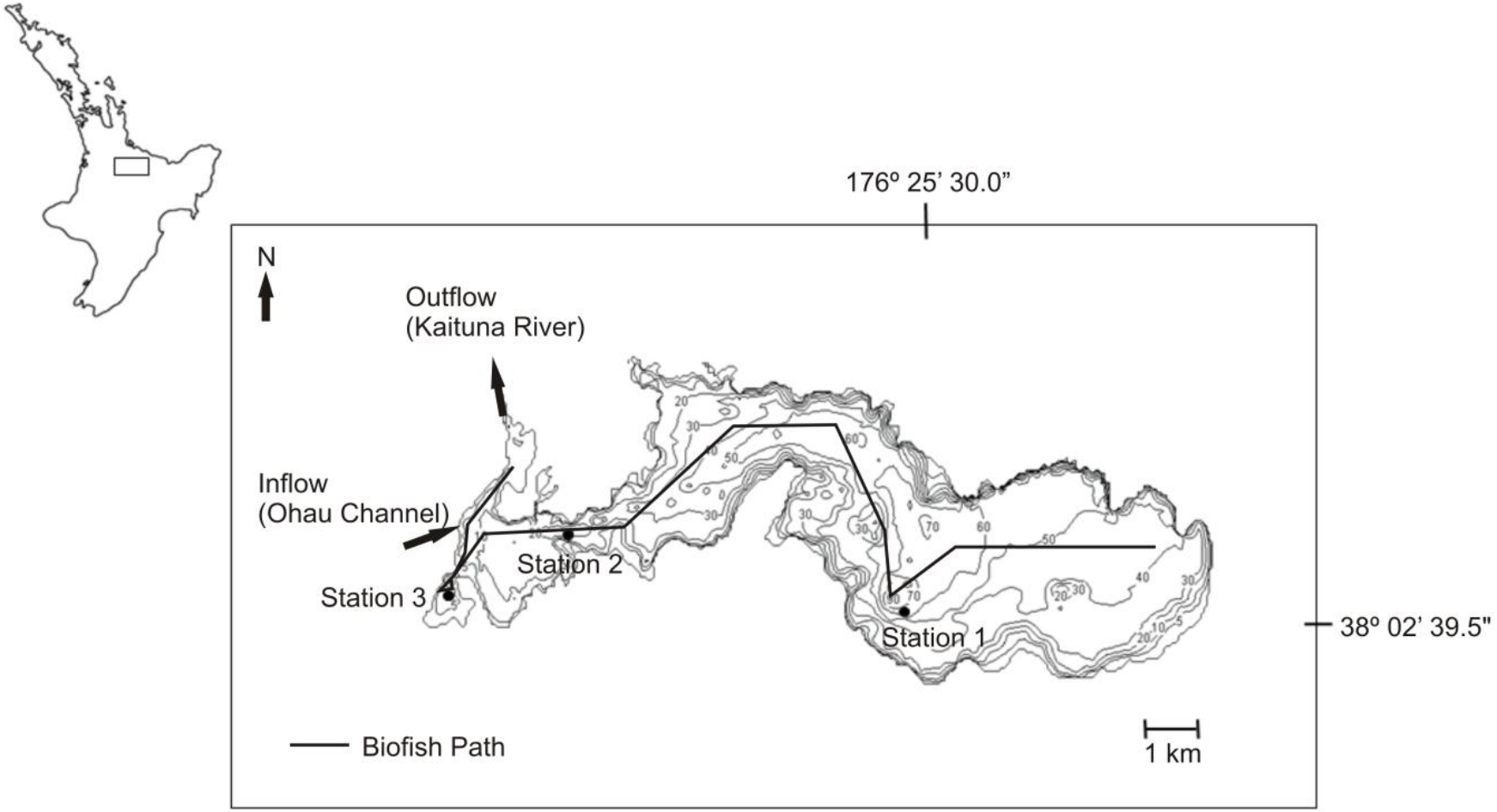

Figure 3.1: Locations of sampling Stations 1, 2 and 3 on Lake Rotoiti. Black line shows the Biofish transect path

The lake suffered a rapid process of eutrophication between the first limnological investigation by Jolly (1959) and a study by Vincent et al. (1984). The main cause of this deterioration was identified to be from changes in Lake Rotorua, which has a single outflow to the Ohau Channel inflow of Lake Rotoiti (Vincent et al. 1984, 1986, 1991; Gibbs 1992). This inflow has a detrimental effect in introducing nutrient–enriched water with elevated phytoplankton biomass from Lake Rotorua, but is also considered to have a beneficial effect in reducing deoxygenation of bottom waters when the inflow intrudes into stratified Lake Rotoiti as an underflow (Gibbs 1992). An underflow commonly starts in autumn and ends in spring, though the lake is mostly well mixed vertically through winter. An interflow or overflow may occur during summer when there is a strong diurnal temperature oscillation in the shallow Ohau Channel and Lake Rotorua (Vincent et al. 1991).

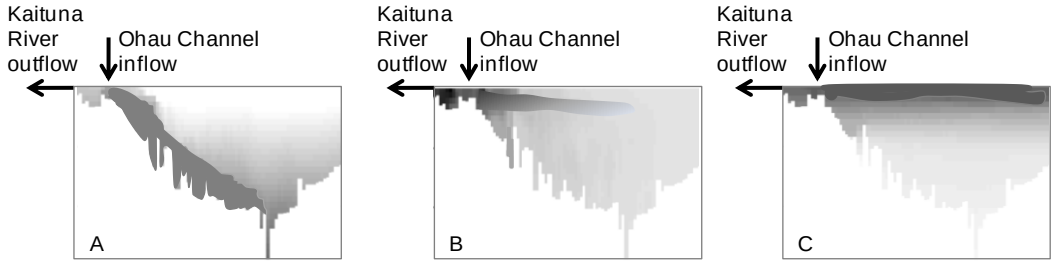

Figure 3.2: Conceptual diagram of the (A) underflow, (B) interflow and (C) overflow condition of Ohau Channel inflow.

3.2.1 Field data

Between May 2004 and May 2005 sampling was conducted at monthly intervals. Temperature, dissolved oxygen and fluorescence depth profiles (resolved at c. 0.1 m) were performed with a Seabird Electronics (SBE) 19plus Seacat CTD profiler at three stations (Figure 3.1). To complement CTD profiles, depth–undulating transects of chlorophyll fluorescence and dissolved oxygen were undertaken periodically with a Biofish (ADM–Elektronik, Germany) along the paths shown in Figure 3.1. The Biofish temperature sensor (ADM–Elektronik, Germany), fluorescence sensor (Dr. Haardt Optik Mikroelektronik miniBackScat I) and

oxygen sensor (Galvanic oxygen micro–sensor) took measurements at 4 Hz, together with a Global Positioning System reference and water depth (Garmin GPSMAP 168 Sounding). An average of 3500 discrete points was measured each month following a fixed path of 21 km along the lake.

Water temperature was measured at Stations 1 and 2 and in the Ohau Channel inflow (Figure 3.1) at 15 minute intervals with Tidbit Underwater Data Loggers which have a resolution of <0.3 °C and an accuracy of +/- 0.2 °C. The thermistors were placed at depths of 0, 2.5, 5, 7.5, 10, 12.5, 15 and then 5 m increments to 80 m for Station 1 and at 2.5 m increments between 0 and 25 m for Station 2.

The Biofish chlorophyll–fluorescence measurements and CTD fluorescence profiles were calibrated against chlorophyll *a* in water samples collected simultaneously, which were analysed by acetone extraction and corrected for phaeophytin (Axler & Owen 1994). Due to technical difficulties dissolved oxygen data from the Biofish were not available for some months of the study.

An independent programme undertaken by the Regional Council, Environmental Bay of Plenty, generally sampled the same three stations two weeks prior to the Biofish measurements, and provided monthly results of surface concentrations of TP, TN, PO_4, NH_4 and NO_3. All nutrient concentrations presented here are as the elemental form of the nutrient, i.e., PO_4–P, NH_4–N and NO_3–N. Model output was compared with surface concentrations of the specified nutrient species at the related station.

3.2.1 Data analysis

For vertical comparisons between model output and field data, the CTD profiles were compared with corresponding model profiles using error calculations (Root–Mean–Square–Error (RMSE) and Pearson correlation coefficient values). Pearson correlation coefficient and RMSE values were determined for water temperature, dissolved oxygen and chlorophyll fluorescence (calibrated to chlorophyll *a*) for Stations 1, 2 and 3, as well as for inorganic nutrient concentrations at these stations.

A monthly average coefficient of variation (C_v) was calculated for temperature and chlorophyll *a* as:

$$C_v = \frac{б}{\mu}$$

where б is the standard deviation for all measurements of a variable taken within the space represented by one model grid cell and μ is the mean of all measurements within this cell. Calculations of this coefficient for dissolved oxygen were not undertaken due to several gaps in the sampling regime. A monthly average, minimum and maximum, and standard error of the mean C_v were then calculated for all model cells where field data were available.

After calibration of chlorophyll fluorescence measurements of the Biofish with field measurements of chlorophyll *a* the monthly Biofish measurements of temperature, dissolved oxygen (not all months) and chlorophyll *a* were compared to values for the corresponding date and location in the model. Biofish measurements corresponding to one cell of the model bathymetry were averaged and Root–Mean–Square–Error (RMSE) and Pearson correlation coefficients were calculated for each variable (temperature, dissolved oxygen and chlorophyll *a*) to validate the spatial performance of the model output against the measurements at a higher resolution. Biofish data were processed with Matlab, filtered to every second measurement and projected onto the modeling results for visual comparisons of spatial accuracy on a monthly basis.

The path of Ohau Channel inflow was monitored by introducing a tracer of a constant daily value 1 in Ohau Channel. A tracer concentration of zero was allocated for the initial lake condition. The rate of change of Ohau Channel water tracer concentration was calculated on a monthly basis after allowing for a 14–days ‘spin up’ period as well as ten days after the tracer first reached Station 1 in the main basin at 21 m depth.

3.2.2 Model description and set–up

The Estuary, Lake and Coastal Ocean Computer Model (ELCOM) is a 3D hydrodynamic model used to simulate water temperature and salinity spatially and temporally (Hodges et al. 2000; Hodges & Dallimore 2007). It is driven by external environmental forcings, including wind stress, surface heating/cooling and inflows and outflows. The hydrodynamics of the model are based on the Euler–Lagrange method for advection of momentum (Casulli & Cheng 1992) with a conjugate–gradient solution for the free–surface height. ELCOM is based on the unsteady Reynolds–averaged, hydrostatic, Boussinesq, scalar transport and Navier–Stokes equation (Hodges et al. 2000) for incompressible flow using the hydrostatic assumption for pressure. This limits the model in terms of accurately predicting the geothermal energy as physical interactions in particular with an inflowing heat source at the bottom of the lake are not accurately represented. Koçyigit and Falconer (2004) showed in a shallow homogeneous lake that the hydrostatic pressure assumption made little difference to the modelled results when analysing wind–driven circulation, but in case of Lake Rotoiti vertical velocity is unlikely to be negligible and the effects of momentum cannot be ignored if sound assessment of the heat source is required. For the purpose of this model however in predicting spatial variability of phytoplankton the hydrostatic assumption is suitable.

In this study ELCOM was coupled to the Computational Aquatic Ecosystem Dynamics Model (CAEDYM), to simulate interactions between hydrodynamics and biogeochemical processes. CAEDYM consists of process–based differential equations that simulate concentrations of biogeochemical variables dynamically (see Figure 3.4 for a general conceptualisation). Ecological variables are updated by CAEDYM each timestep after transport processes and external forcings have been carried out by ELCOM (Romero et al. 2004). The model calibration was conducted in two phases: The ELCOM calibration, which only required minor adjustments due to small number of parameters, was followed by the CAEDYM calibration. In the present ELCOM–CAEDYM set–up, focus was placed on calibration of the key processes affecting transformation rates of phosphorus and

nitrogen, including mineralisation of organic matter, sediment–water exchanges and phytoplankton nutrient uptake. No data was available to simulate dynamic sediments fluxes in Lake Rotoiti. The sediment release was simulated using the static model employed with CAEDYM, which determines the flux with a function of overlying water temperature and dissolved oxygen concentration.

Salinity for the ELCOM application to Lake Rotoiti was set to zero so that density differences were generated entirely by temperature gradients. CAEDYM was set up with two dominant representative phytoplankton groups: cyanobacteria and diatoms the dominant species in Lake Rotoiti (Hamilton et al. 2010). Total chlorophyll *a* was partitioned amongst these two phytoplankton groups. No field data was available for zooplankton during the simulated period. An approach without zooplankton as a state variable was chosen, replicating the configuration used by Burger et al. (2008) for adjacent Lake Rotorua. Arhonditsis and Brett (2004) studied 153 mechanistic aquatic biochemical models and analysed the most appropriate level of model complexity. Significant negative correlation was found between r^2 of zooplankton simulations and model dimension and length of simulation. The relative error of zooplankton simulations was further significantly correlated with model complexity (measured in numbers of state variables). The complexity of my simulation setup places the here described model at the higher end at all three tested factors. The increased uncertainty and field data limitations supported the decision to exclude zooplankton simulations.

A hydrographic survey of the bathymetry of Lake Rotoiti was undertaken with accuracy specifications of 20 cm in the vertical and about 10 cm in the horizontal (Hamilton et al. 2005). Average values of the hydrographic survey were calculated to match a horizontal model dimension of 200 m x 200 m to balance model run times with required spatial resolution. The inflow boundary conditions for the model consisted of one major inflow (Ohau Channel) that enters Lake Rotoiti in the western basin, twelve smaller inflows at their locations around the main basin of the lake and two additional underwater geothermal springs which are assumed to intrude in the deepest part of the lake (Station 1) (Calhaem 1973) and were assigned to model grid cells where the depth exceeded 70 m.

Recent research in Lake Rotoiti has found the bubbles rising from the bottom of Lake Rotoiti to be collapsing, which lead the researchers to believe that heat is generated by a fluid flux (Lisa Pearson and Prof. Chris Hendy, Waikato University, personal comments). Cody (2007) describes in a report the geothermal features of the crater of Lake Rotoiti as a large hot alkaline-neutral spring. Calhaem (1973) also sets out reasons for hot water inflow in the crater of Lake Rotoiti, yet sound scientific proof is sparse.

The uncertain volume of the inflow was set as the residual of water balance calculations. Energy input from this source determined by heat flux simulations on either side of 140 MW, which was estimated based on former heat budget calculations (Calhaem 1973). A total geothermal energy of 165 MW was necessary to increase the hypolimnion temperature to the measured data. Two thirds were applied to the geothermal inflow at the deepest point (the crater) at a volume of 0.25 $m^3 s^{-1}$ and a temperature of 120 ºC. The remaining one–third was assigned to a flow of 0.58 $m^3 s^{-1}$ at 35 ºC, in the region north of the crater, a ratio congruent with the heat flow contours of Calheam (1973). Calculations from model output developed by Kissling and Weir (2005) suggest a total geothermal energy of 406 MW for region 8 (116km^2) around Lake Rotoiti. Based on the surface area of Lake Rotoiti they suggest a total energy input of c. 122 MW, assuming that the heat transfer is uniform throughout this region. An unknown fraction of geothermal heating occurs directly through conduction from the geothermally–heated bottom sediments, which were not represented explicitly in the model and were instead encompassed within the submerged geothermal inflows.

The temperature and volume of smaller, mostly groundwater–fed streams, were kept constant based on field measurements. The volume of the main inflow (Ohau Channel) and main outflow (Kaituna River) (Figure 3.1) were entered as daily averages calculated from continuously measured flow data (provided by the regional council, measured at two control gates). Over the model runtime an average total inflow of 19.52 $m^3 s^{-1}$ and average outflow of 22.35 $m^3 s^{-1}$ were entered, based on continuous flow measurements and an additional total of 0.61

m^3 s^{-1} was entered for the remaining surface spring inflows. Field data were unavailable for the nutrient concentrations of the geothermal inflows. The model was therefore setup with concentrations typical for geothermal springs in this region, which have elevated concentrations of NH_4–N and PO_4–P (Associate Professor Chris Hendy, pers. comm.). Nutrient concentrations of the minor, spring–fed inflows were based on snap shot measurements in these springs and kept constant over the simulation period based on averages from field measurements. The nutrient and phytoplankton (separated by diatom and cyanobacteria chlorophyll *a*) concentrations of the Ohau Channel inflow were interpolated to daily values based on monthly measurements.

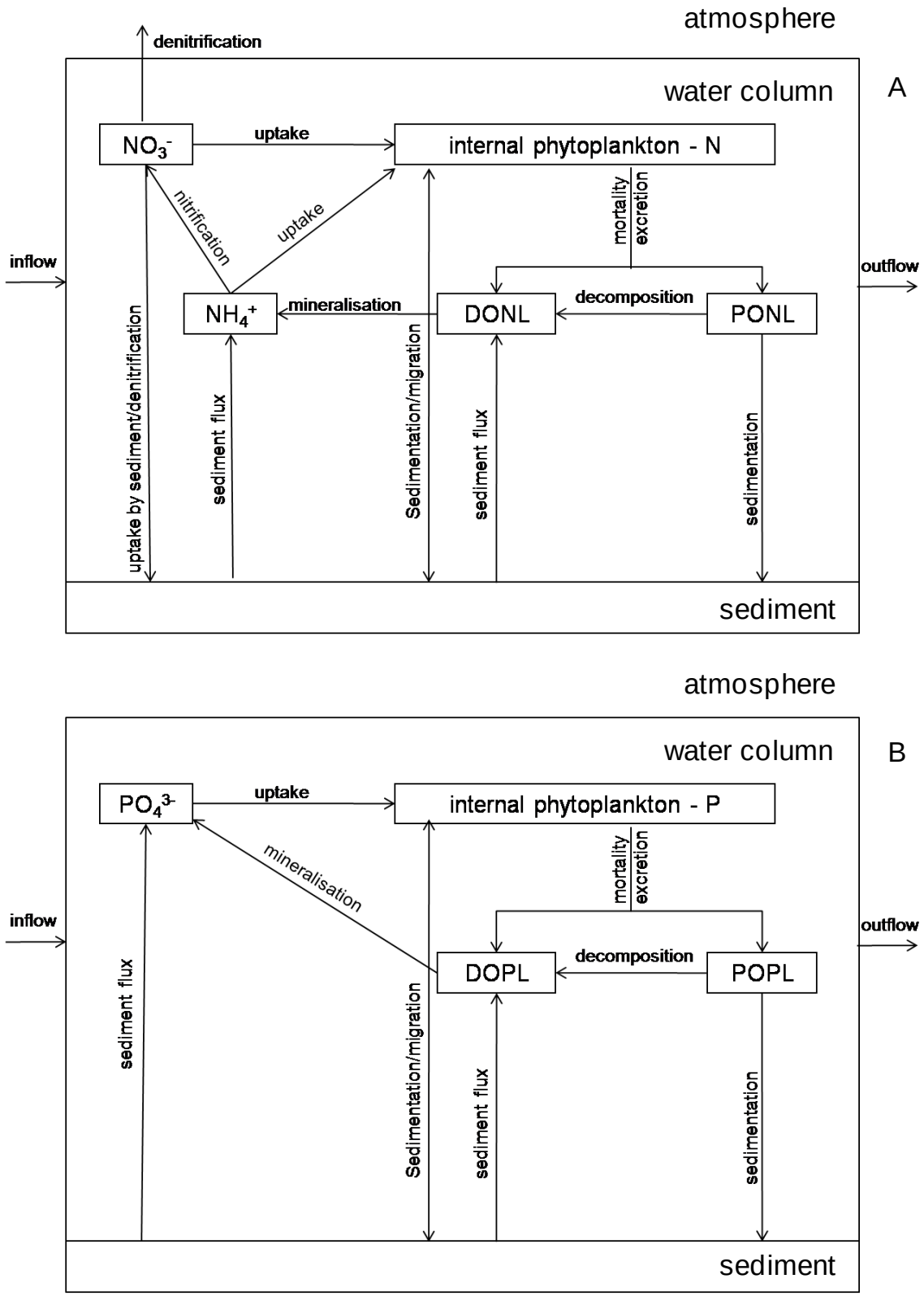

Figure 3.3: Conceptual diagram of (A) nitrogen and (B) phosphorus dynamics. POP(N)L and DOP(N)L represent particulate and dissolve labile organic phosphorus (nitrogen), respectively (after Hipsey et al. 2007).

The initial calibration of the water quality data (CAEDYM) was carried out in the 1D DYRESM–CAEDYM model for Lake Rotoiti (Hamilton et al. 2005). The calibrated parameters from this model were entered into ELCOM–CAEDYM and manual adjustments of parameters were made with a series of model runs using parameter ranges derived from literature (Schladow & Hamilton 1997; Gal et al. 2009; Table 3.1) to improve the calculated error derived from comparison of surface nutrient concentration (TN, TP, NH_4–N, NO_3, –N PO_4–P) and dissolved oxygen outputs against field data. Model runs were undertaken repeatedly to reduce the statistical error (RMSE, Pearson correlation coefficient) of the model against discrete field measurements of nutrient and chlorophyll *a* concentrations at the three stations.

The model was run for one year from 17 May 2004, which aligned with the first day of the monthly field measurements for the purpose of initialisation of the model run. Meteorological forcing data included daily averages of air temperature, solar radiation, atmospheric pressure, relative humidity, cloud cover to determine long wave radiation, and wind speed, and total daily rainfall. Climate data were retrieved from the weather station at Rotorua airport, 8 km from Lake Rotoiti. Daily averages were supplied by the CLIFLO institute of NIWA (National Institute of Water and Atmospheric Research 2005). The large horizontal cell length to vertical cell length required the model to be run with a short time-step of 120 seconds in order to keep the Courant-Friedrichs-Lewy (CFL) constant low to provide for model stability (Hodges 2000).

The initial conditions for the simulations were represented from temperature, dissolved oxygen and total chlorophyll fluorescence profiles from the three sampling stations and nutrient concentrations at 0 m, 50 m and near–bottom at Station 1, 0 m, 20 m and near–bottom at Station 2, and 0 m, 3 m and near–bottom at Station 3 (Figure 3.1). Linear interpolation between stations was applied in the ELCOM–CAEDYM model to derive initial conditions over the entire lake.

3.2.3 Model calibration and sensitivity analysis

Sensitivity analysis of the grid spacing (from 0.25 m up to 10 m vertically) and time steps (adjusted for model stability) was carried out to examine changes in the vertical distribution of temperature and thermocline position. A vertical resolution of 3 m in the vertical was chosen based on statistical error calculations for modelled temperature compared with field measurements. The results for smaller dz showed a narrower and shallower thermocline and indicated a smaller thermal diffusion than found in the field. The 3 m spacing in vertical direction compensated for the lack of vertical thermal diffusion compared with smaller grids. Sensitivity analysis was also carried out to understand the sensitivity to the geothermal energy inputs in the main basin of Lake Rotoiti.

The model was calibrated for the entire simulation period from May 2004 to May 2005. Model results of temperature, dissolved oxygen and total chlorophyll *a* (the sum of the assigned diatom and cyanobacteria groups) were compared against corresponding values derived from monthly CTD casts. Discrete nutrient measurements were compared spatially (horizontally) and temporally with the model results on the corresponding sampling days at all three stations (Figure 3.1).

I used an initial set of parameter values from a 1D model approach for Lake Rotoiti using DYRESM–CAEDYM (Hamilton et al. 2005), many of which were derived from literature values (e.g., Schladow & Hamilton 1997). A manual calibration followed using ranges within literature values and undertaking a stepwise approach to improve the statistical error between measurements and model simulations. Sensitivity analyses were undertaken for several model parameters. The parameter I_k (the initial slope of the productivity–irradiance curve), derived from the 1D approach, appeared to be unusually high (370 $\mu molm^{-2}s^{-1}$) and several runs were undertaken to test this parameter over a wide range (60 $\mu molm^{-2}s^{-1} < I_k < 370\ \mu molm^{-2}s^{-1}$), but there was no improvement in model fit compared with the value of 370 $\mu molm^{-2}s^{-1}$. The assigned value of the 1D approach best matched the field data.

Table 3.1: Parameter values used in CAEDYM v3.3 application to Lake Rotoiti. Individually assigned parameter for cyanobacteria (Cyano) and diatoms (Diat) when applicable.

Symbol	Description	Unit	Assigned value		Literature values/remarks
Phytoplankton parameters			**Cyano**	**Diat**	
P_{max}	Max. potential growth rate (20 ^{o}C)	day^{-1}	0.5	1.3	Robson and Hamilton (2004)
I_k	Initial slope of the I-P curve	$\mu mol\ m^{-2} \cdot s^{-1}$	370	48	Hamilton et al. (2005)
vT	Temperature multiplier for growth	dimensionless	1.09	1.06	Robson and Hamilton (2004)
KN	Half-saturation constant for N uptake	$mg\ L^{-1}$	0.012	0.011	Hamilton and Schladow (1997)
IN_{min}	Min. internal N concentration	mg N (mg chl *a*)$^{-1}$	0.9	5	Robson and Hamilton (2004)
IN_{max}	Max. internal N concentration	mg N (mg chl *a*)$^{-1}$	5	6	Hamilton et al. (2005)
UN_{max}	Max. rate of N uptake (20 ^{o}C)	mg N(mg chl *a*)$^{-1}$	3	5	Hamilton et al. (2005)
KP	Half-saturation constant for P uptake	$mg\ L^{-1}$	0.006	0.08	Robson and Hamilton (2004)
IP_{min}	Min. internal P concentration	mg P (mg chl *a*)$^{-1}$	0.25	0.19	Hamilton et al. (2005)
IP_{max}	Max. internal P concentration	mg P (mg chl *a*)$^{-1}$	2.5	3.7	Hamilton et al. (2005)
UP_{max}	Max. rate of P uptake (20 ^{o}C)	mg P mg chl *a*)$^{-1}$ day^{-1}	1	1	Hamilton and Schladow (1997)
T_{sta}	Standard growth temperature	°C	20	10	Hamilton et al. (2005)
T_{max}	Maximum growth temperature	°C	35	27	Hamilton et al. (2005)
T_{opt}	Optimal growth temperature	°C	28	18	Hamilton et al. (2005)
kr	Respiration rate coefficient	day^{-1}	0.1	0.1	Robson and Hamilton (2004)
kep	Specific attenuation coefficient for chl *a*	m^2 (mg chl *a*)$^{-1}$	0.03	0.02	
Nutrient parameters					
koN2	Denitrification rate coefficient (20 ^{o}C)	day^{-1}	0.03		Hamilton et al. (2005)
KN2	Inverted half-saturation constant for effect of oxygen on denitrification	$mg\ L^{-1}$	0.09		
vON	Temperature multiplier for denitrification	dimensionless	1.08		Robson and Hamilton (2004)
KoNH	Nitrification rate coefficient (20 ^{o}C)	day^{-1}	0.065		Hamilton et al. (2005)
Kon	Half-saturation constant for effect of oxygen on nitrification	$mg\ L^{-1}$	0.5		Hamilton et al. (2005)
vN2	Temperature multiplier for nitrification	dimensionless	1.08		Robson and Hamilton (2004)
SmpNO3	Max. release rate of NO_3 from sediment (20 ^{o}C)	$g\ m^{-2} \cdot day^{-1}$	-0.075		Hamilton et al. (2005)
KDOS-NO3	Inverted half-saturation constant for effect of DO on NO_3 release from sediment	$mg\ L^{-1}$	3		
SmpNH4	Max. release rate of NH_4 from sediment (20 ^{o}C)	$g\ m^{-2} \cdot day^{-1}$	0.105		Hamilton et al. (2005)
KDOS-NH4	Half-saturation constant for effect of DO on NH_4 release from sediment	$mg\ L^{-1}$	10		Hamilton et al. (2005)
SmpPO4	Max. release rate of PO_4 from sediment (20 ^{o}C)	$g\ m^{-2} \cdot day^{-1}$	0.03		
KDOS-PO4	Half-saturation constant for effect of DO on PO_4 release from sediment	$mg\ L^{-1}$	3		
PON1max	Rate coefficient of PONL to DONL (20	day^{-1}	0.003		Hamilton et al. (2005)
DON1max	Rate coefficient of DONL to NH_4 (20 ^{o}C)	day^{-1}	0.008		Hamilton et al. (2005)
POP1max	Rate coefficient of POPL to DOPL (20 ^{o}C)	day^{-1}	0.02		
DOP1max	Rate coefficient of DOPL to PO_4 (20 ^{o}C)	day^{-1}	0.025		
Oxygen parameters					
vsed	Temperature multiplier for sediment oxygen demand	dimensionless	1.05		Robson and Hamilton (2004)
rSOs	Sediment oxygen demand (20 ^{o}C)	$g\ m^{-2} \cdot day^{-1}$	2.15		Burger et al. (2006)
KSOs	Half saturation constant for sediment oxygen demand	$mg\ L^{-1}$	0.25		Burger et al. (2006)

3.3 Results

Analysis of the measured data corresponding to one cell in the model domain (200 m x 200 m x 3 m) showed low average coefficient of variation values (Cv) for temperature measurements, but high coefficients of variation for chlorophyll fluorescence. Table 3.2 shows the monthly averaged coefficient of variation for temperature and chlorophyll fluorescence from the Biofish where there were multiple measurements corresponding to the coordinates of individual model cells. The average, minimum and maximum values are based on C_v highlight the high variability of chlorophyll fluorescence at the model horizontal grid resolution of 200 m. This is further supported by the high standard variation of the mean. The maximum coefficient of variation for temperature within an individual model cell was 9.65% for March 2005. In general the coefficient of variation for temperature remained low, especially averaging over all cells, with a maximum average value for any month of 1.07% in February 2005. The minimum C_v of all individual model cells in each month was 0% for temperature and <0.15% for chlorophyll fluorescence. However, the maximum C_v of chlorophyll fluorescence within each month varied greatly. Highest C_v measured within one month and any model cell was in September 2004, with a value of 55.95%. The average monthly value was between 0.75 (April 2005) and 6.7% (September 2005).

Table 3.2: Monthly mean, standard deviation of mean, minimum and maximum values of the coefficient of variation of temperature ($C_{vTemperature}$) and chlorophyll *a* ($C_{vChlorophyll\ a}$). C_v was calculated for Biofish transect measurements corresponding to each model cell in Lake Rotoiti.

	$C_{vTemperature}$				$C_{vChlorophyll}$			
	Mean (%)	STD_{Mean} (%)	Min (%)	Max (%)	Mean (%)	STD_{Mean} (%)	Min (%)	Max (%)
Jun-04	0.24	0.43	0.00	3.70	1.52	2.13	0.00	18.70
Sep-04	0.45	0.68	0.00	5.84	6.70	5.09	0.15	55.95
Oct-04	0.15	0.21	0.00	1.93	6.65	3.82	0.02	23.42
Nov-04	0.71	0.84	0.00	8.52	3.50	2.68	0.01	23.72
Dec-04	0.38	0.53	0.00	3.57	2.07	1.80	0.00	10.37
Jan-05	0.66	0.66	0.00	5.56	1.14	1.11	0.00	9.43
Feb-05	1.07	1.20	0.00	7.68	0.84	1.47	0.00	24.32
Mar-05	1.05	1.65	0.00	9.65	1.07	3.01	0.00	52.71
Apr-05	0.92	1.24	0.00	6.44	0.75	0.81	0.00	6.05

3.3.1 Water temperature comparisons

Modelled and measured temperature showed good agreement. Timing of stratification and mixing was well aligned between measurements and the model in the main basin at Station 1. The onset of stratification predicted by the model around November 2004 at Station 1 was similar in timing and depth to observations in the field, but a sharper defined thermocline in the model results (Figure 3.4A I). The shallower Station 2 shows good agreement during the mixing period, but the simulations did not show evidence of stratification in December 2004. Subsequently when the water column at this station is stratified, surface modelled and measured data matched well, though temperature below the thermocline was overestimated by the model. The period of mixing simulated by the model in December 2004 at Station 2 coincided with a period of strong winds which was also evident as a deepening of the thermocline at Station 1.

The statistical output revealed that temperature was most accurately simulated at Station 1 (RMSE=0.716 °C, R=0.960) and Station 3 (RMSE=1.108 °C, R=0.982) but less so for Station 2 (RMSE=1.708 °C, R=0.947) (Table 3.3). The shallow Station 3 showed generally good agreement between modelled and measured temperature.

Table 3.3: Root–mean–square–error (RMSE) and Pearson correlation coefficient (R) values for Stations 1, 2 and 3 for comparisons of model simulations and measurements of temperature and concentrations of dissolved oxygen (DO) and chlorophyll *a*.

	RMSE			*R*		
	Station 1	Station 2	Station 3	Station 1	Station 2	Station 3
Temperature (°C)	0.716	1.708	1.108	0.960	0.947	0.982
DO (mg L^{-1})	1.004	1.756	1.280	0.969	0.796	0.576
Chlorophyll *a* (µg L^{-1})	2.482	7.338	7.975	0.781	0.363	0.536

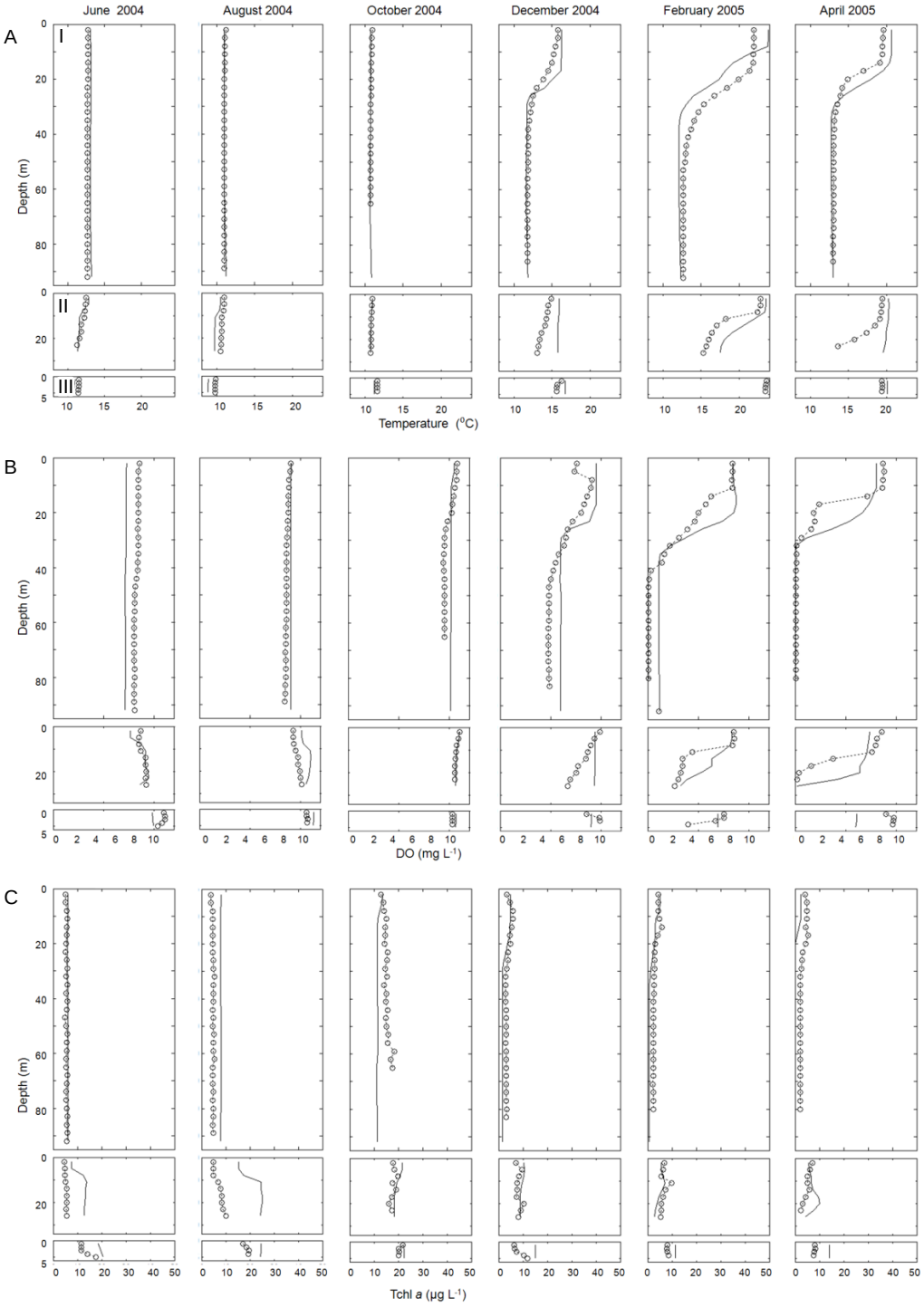

Figure 3.4: Simulated (–) and observed (○) values for (A) temperature (ºC), (B) dissolved oxygen (mg L^{-1}) and (C) total chlorophyll *a* (µg L^{-1}) at Stations 1(I), 2 (II) and 3 (III) from June 2004 to April 2005.

The thermistor chain comparison against the ELCOM model output at Station 1 over the one–year period of monitoring showed that the model accurately reproduced the observed thermal stratification in the main basin throughout the year but slightly over–estimated water temperature during the summer stratification. The unexpected weakening of the thermocline in December 2004 coincided with an unseasonally cold weather pattern; weakening of the thermal stratification was captured in the model simulations, but with a slight delay (Figure 3.5A). This was also exemplified in the difference between measured and modelled data at Station 2 (Figure 3.4) when predicted data showed a well mixed water column while measurements showed signs of stratification.

An unusual feature of the thermistor chain data was the presence of warmer water in the bottom waters (75, 80 m) than the overlying water from July 2004 to October 2004. This temperature gradient is a true density instability as concentrations of ions in the geothermal inflow do not affect water density to an extent that would compensate for the inverse temperature gradients. Similar events at the bottom of the main basin of Lake Rotoiti have been previously reported by Calhaem (1973), who examined typical temperature profiles measured in the main basin of Lake Rotoiti 1972, but no seasonal trend was observed.

The thermistor chain data from Station 2 (Figure 3.5B) confirms the overestimation of temperature during summer stratification and highlights slightly colder water predicted during winter. The onset of stratification occurred late in October 2004, approximately three weeks earlier than was predicted by the model simulations. Temperatures were generally aligned at the end of the mixing period.

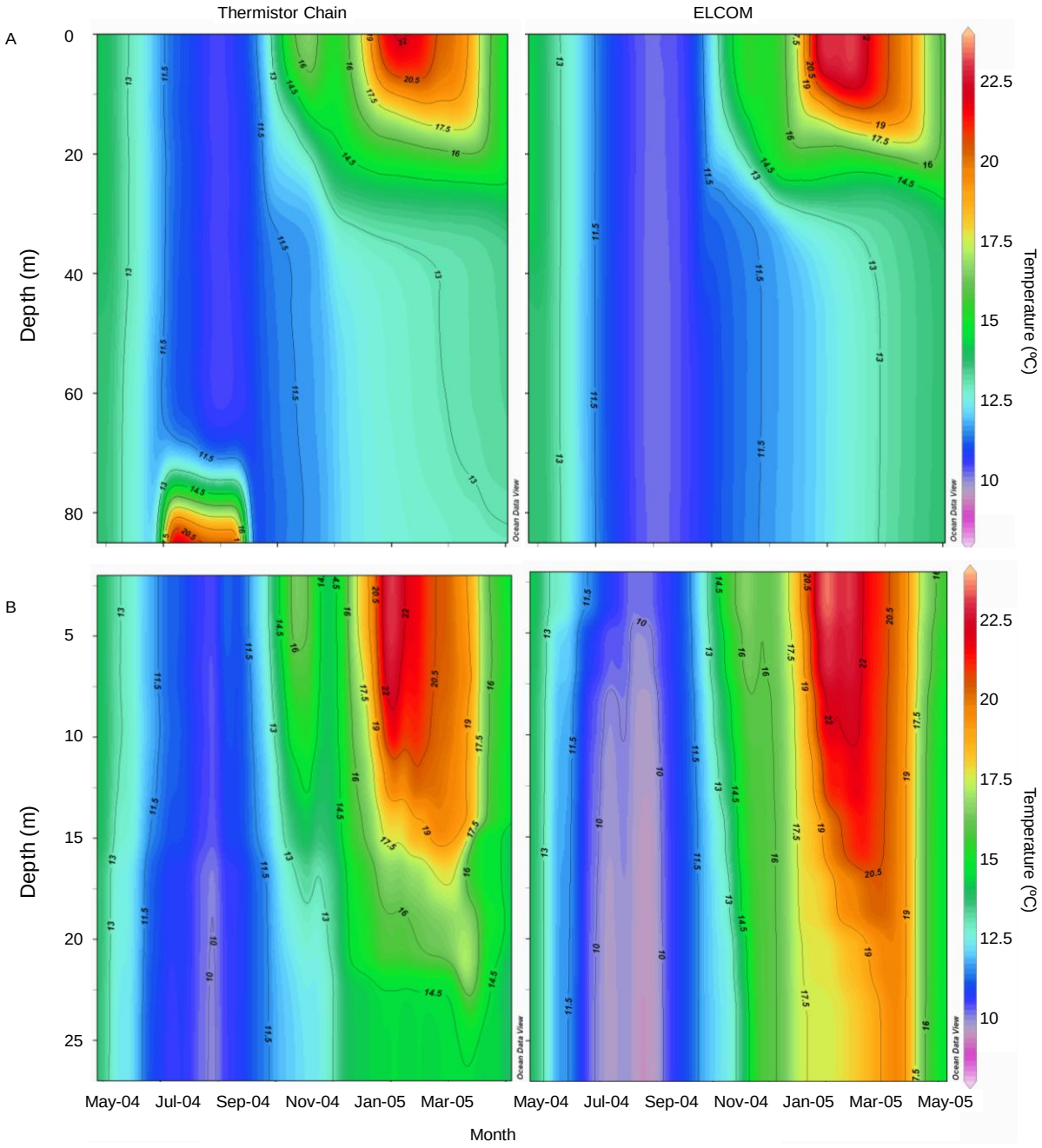

Figure 3.5: Temperature (ºC) measurements from thermistor chain at (A) Station 1 and (B) Station 2 compared with corresponding simulated ELCOM output in the main basin from 22 May 2004 to 16 May 2005.

3.3.2 Dissolved oxygen comparisons

Comparisons of simulated (ELCOM–CAEDYM output) and measured (CTD) dissolved oxygen concentrations (Figure 3.1B) yielded Pearson correlation coefficient values of 0.969, 0.796 and 0.576 and RMSE values of 1.004, 1.756 and 1.280 mg L^{-1} at Stations 1, 2 and 3, respectively (Table 3.3) representing a good fit of the modelled data to the measurements at Stations 1 and 2. At the onset of stratification dissolved oxygen concentrations were slightly over–predicted at Station 1 at the surface, while at the same time there was a delay in deoxygenation of bottom waters. Field data at Station 2 show a decrease in dissolved oxygen concentrations with depth in December 2004 while the model at that time showed little vertical variation of dissolved oxygen, which corresponded to the absence, or weaker stratification in the model simulations than in the measurements. The biggest difference between field data and model output was at shallow Station 3 in April 2005, when the modelled concentration was around 6 mg L^{-1} throughout the water column while the measured concentrations had increased to 9 mg L^{-1}.

3.3.3 Biogeochemical variable comparisons

Nurients

The model simulations for surface nutrient concentrations showed reasonable agreement with measurements at Stations 1 and 2, while Station 3 showed some discrepancies, especially towards the end of the year of simulation. At Station 1 modelled nitrate concentrations did not reach the magnitude measured during the period of water column mixing in July and August 2004, when the measured concentration was c. 0.25 mg L^{-1} and modelled values only increased to c. 0.1 mg L^{-1}. At Station 2 modelled phosphate concentrations (c. 0.02 mg L^{-1}) remained below the measured values (c. 0.04 mg L^{-1}) during winter mixing and remained in the range 0.002–0.008 mg L^{-1} during stratification, while the other nutrient species generally showed good agreement with field data. One exception was the ammonium concentration in June 2004, with a measured value (0.133 mg L^{-1}) substantially exceeding modelled levels (c. 0.03 mg L^{-1}), however throughout the rest of the year the model and field data were well aligned and both remained in

the range of 0.005 to 0.04 mg L^{-1}. A similar result occurred at Station 1 in June 2004 when there were increased ammonium levels (0.14 mg L^{-1}), however in this case the model simulations showed a similar magnitude (0.11 mg L^{-1}) two weeks prior to when measurements were made. The variation in nutrient concentrations between field data and model simulations was most evident at Station 3 in the last three months of the model run, with values of most nutrient species often more than twice those of the measured concentrations.

Nitrogen and phosphorus species for Station 1 and 2 were predicted to a level of accuracy comparable to, or better than, other studies (Trolle et al. 2008b; Gal et al. 2009) (Figure 3.6), while Station 3 generally showed higher errors. The error for dissolved nutrient concentration placed the model results at Stations 1 and 2 in the upper 30–50% compared with 153 modelling studies (Arhonditsis & Brett 2004). Calculated R values (Pearson Correlation coefficient) for predicted and measured nutrient species ranged between 0.714 (NH_4–N) and 0.938 (TP) (Table 3.4) at Station 1 and between 0.558 (TN) and 0.848 (PO_4–P) at Station 2; the latter station was in close proximity to the Ohau Channel inflow. The calibration for the shallow bay represented by Station 3 was less successful, with the maximum correlation coefficients of 0.548 (TP) across all nutrient species.

Table 3.4: Root–mean–square–error (RMSE) and Pearson correlation coefficient (R) values for Stations 1, 2 and 3 for total phosphorus (TP), phosphate (PO_4–P), total nitrogen (TN), ammonium (NH_4–N) and nitrate (NO_3–N).

	RMSE			*R*		
	Station 1	Station 2	Station 3	Station 1	Station 2	Station 3
TP (mg L^{-1})	0.007	0.008	0.022	0.938	0.793	0.548
PO_4 (mg L^{-1})	0.011	0.009	0.007	0.864	0.848	-0.057
TN (mg L^{-1})	0.091	0.093	0.320	0.882	0.558	0.252
NH_4 (mg L^{-1})	0.030	0.031	0.044	0.714	0.665	-0.026
NO_3 (mg L^{-1})	0.054	0.063	0.174	0.797	0.586	-0.193

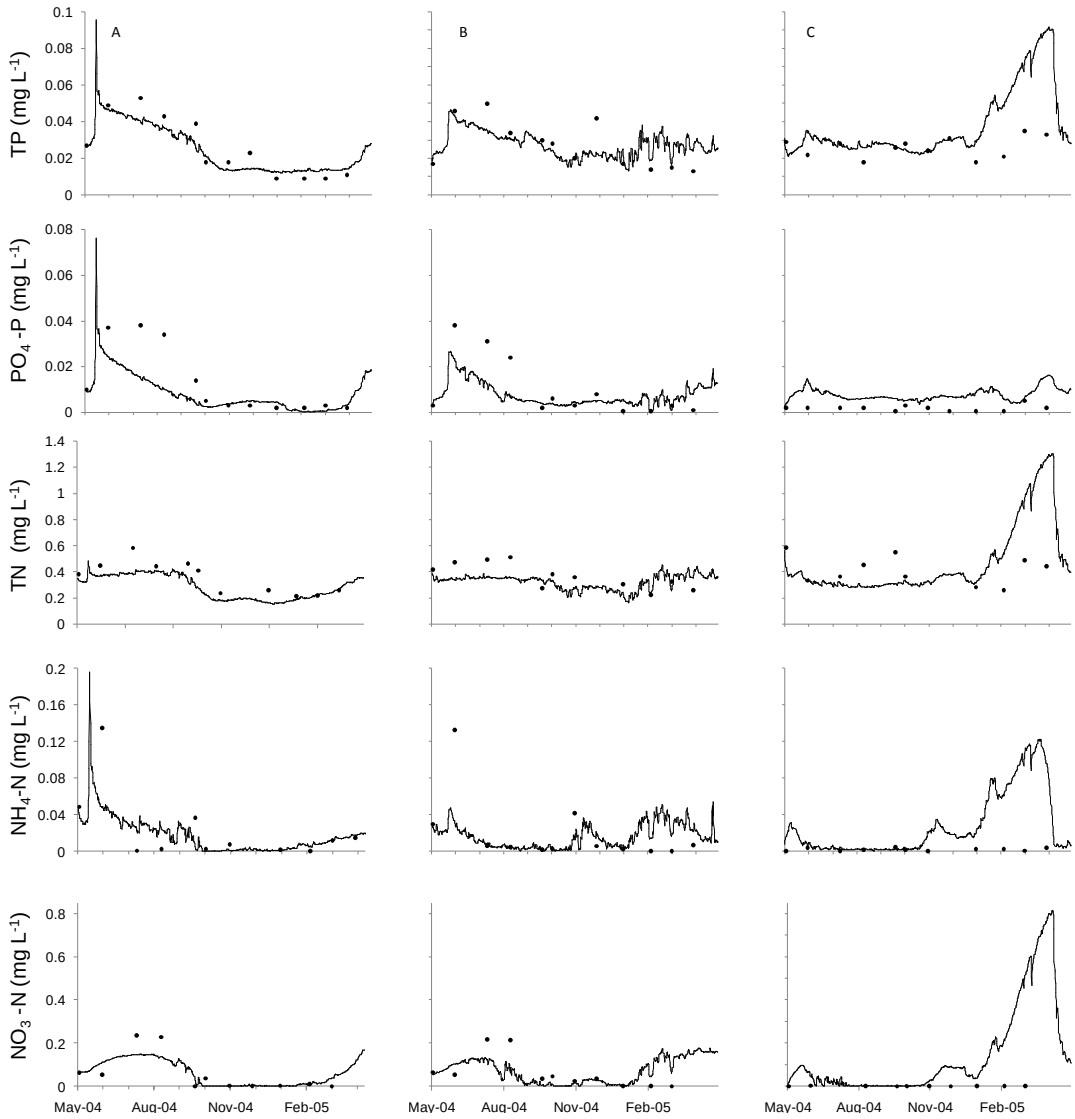

Figure 3.6: Simulated (–) and observed values (●) for nutrients TP, PO_4–P, TN, NH_4–N and NO_3–N at (A) Stations 1, (B) Station 2 and (C) Station 3 at the surface over the simulated period (May 2004 – May 2005).

Nutrient concentrations were initialised spatially based on measurements at three depths for each of three stations. Simulations of nutrient concentrations were not particularly satisfactory at Station 3, despite repeated calibration. Accumulation of nutrients at Station 3, and at a lower rate at Station 2, in the last four months of the model run proved difficult to tune down to match observations. It was locally possible to match the field nutrient data of the three stations with higher accuracy by adjusting the maximum sediment release rate of nutrients and half saturation constant values of nutrient release via dissolved oxygen. However the overall model error was increased due to model limitations which only allow the user to specify one value for each CAEDYM parameter, which applies to the entire lake.

Chlorophyll *a*

A comparison of chlorophyll *a* concentrations from the model simulations and field measurements derived from chlorophyll fluorescence from CTD casts for Stations 1, 2 and 3 gave RMSE values of 2.482, 7.338 and 7.975 μg L^{-1}, respectively, and Pearson correlation coefficient values of 0.781, 0.363 and 0.536, respectively (Table 3.3). The model comparison of Arhonditsis and Brett (2004) shows that the error at Station 1 presents itself in the top 30% (70^{th} percentile) compared with other studies. The poor statistical comparison at Station 3 is mainly generated by an overestimation of chlorophyll *a* concentration, and low R values are contributed by small number of depths grid cells. RMSE show better values than those obtained by Burger et al. (2008) using a 1D approach. The poor statistical comparison for Station 2 was accentuated during winter mixing, when the model output consistently over–estimated chlorophyll *a* concentration at this station.

3.3.4 Comparison across a fixed transect

Model outputs for temperature (Figure 3.7), dissolved oxygen (Figure 3.8) and chlorophyll *a* (Figure 3.9) for grid cells corresponding to the monthly Biofish measurements are shown based on a fixed transect along the lake. A minimum of 2200 comparisons was made for each month so that comparisons between modelled and measured variables were all highly significant ($P < 0.01$).

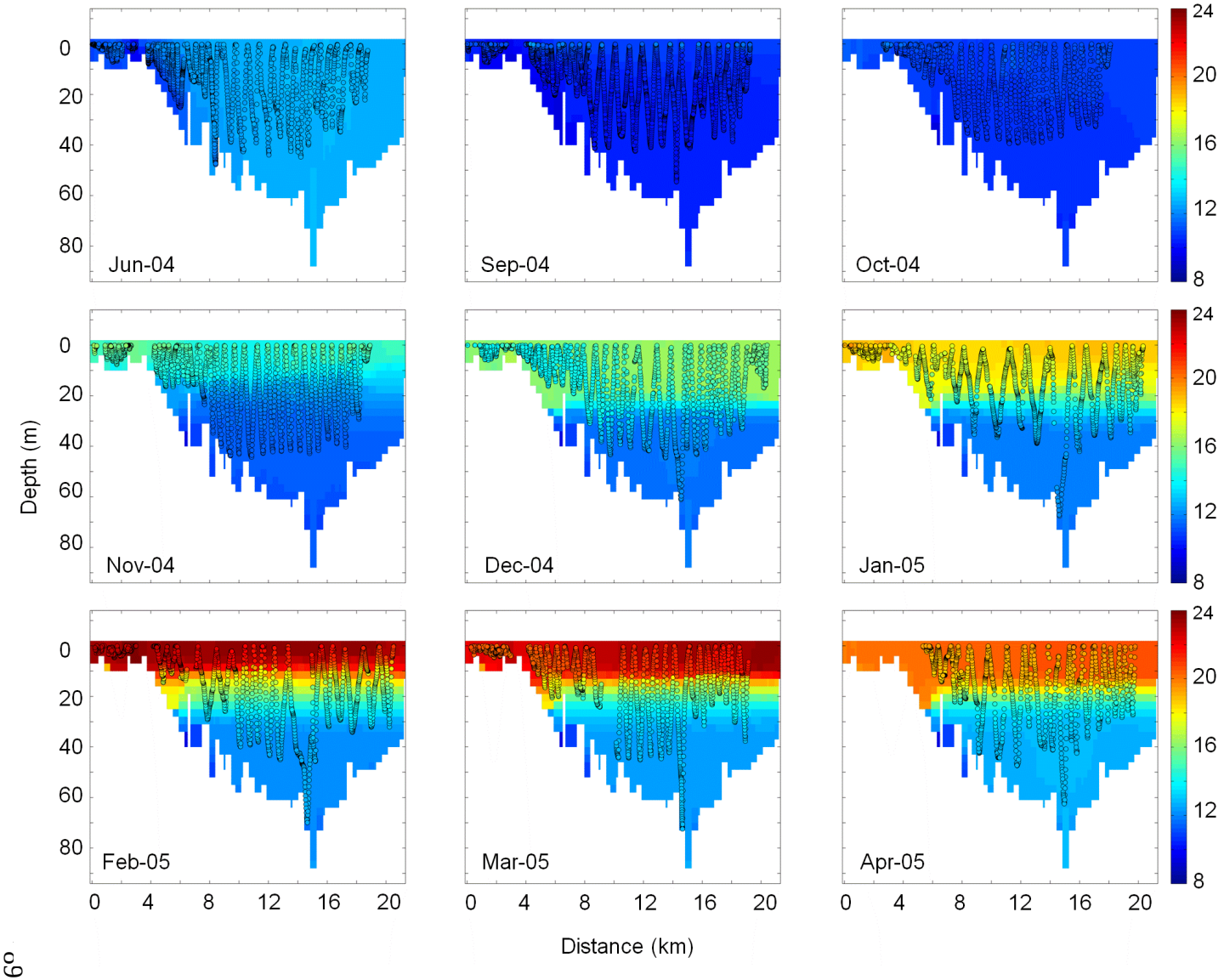

Figure 3.7: Comparison between simulated (coloured background) and measured (○) values of temperature (ºC) from June 2004 to April 2005. Measured values were derived from Biofish transect measurements, displaying every second measured value.

Temperature predictions from the model were strongly correlated with measurements over the whole year (R = 0.984), placing my results in the upper 20% (80th percentile) compared with 153 studies (Arhonditsis & Brett 2004). The annual cycle of the onset of springtime thermal stratification, thermocline formation, deepening of the thermocline in late summer, and winter mixing, were captured well in the model simulation transects. The model slightly over–predicted the surface temperature during December 2004 which confirms the observations from the calibration process when the model also over–predicted thermistor chain measurements from Station 1. Across the shallower areas of the lake (< 20 m depth) there was generally higher variability between model and field data (Figure 3.7) and the total RMSE for all Biofish measurements was 0.907 ºC (Table 3.5), slightly higher than for station 1 during model calibration.

Table 3.5: Values of Root–Mean–Square–Error (RMSE) and Pearson correlation coefficient (R) for comparison of model simulation values against corresponding Biofish measurements averaged for each model grid cell of the transect over a one year simulation period commencing 17 May 2004 compared with the model simulations of temperature (n=5250), dissolved oxygen (n=3972) and total chlorophyll *a* (n=5250).

	RMSE	*R*
Temperature (°C)	0.895	0.984
DO (mg L^{-1})	1.211	0.877
Chlorophyll *a* (µg L^{-1})	5.031	0.664

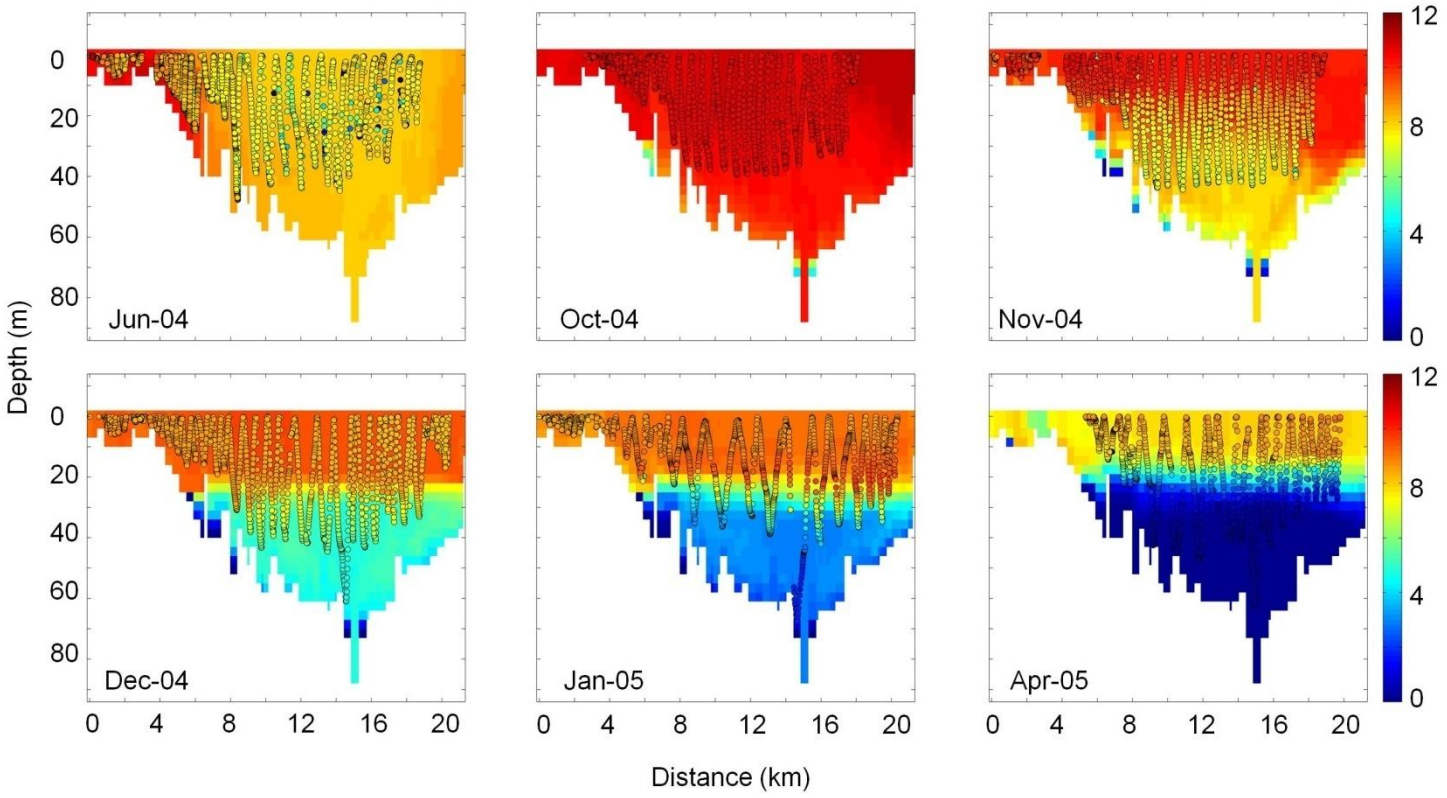

Figure 3.8: Comparison between simulated (coloured background) and measured (○) values dissolve oxygen (DO) (mg L^{-1}) from June 2004 to April 2005. Measured values were derived from Biofish transect measurements displaying every second measured value.

Biofish measurements showed that horizontal variations in dissolved oxygen were most marked in June 2004, January 2005 and April 2005 (Figure 3.8), while vertical variations were accentuated with ongoing duration of thermal stratification. The model simulations captured both the horizontal and vertical gradients observed in measurements of dissolved oxygen even though the magnitude of variation varied slightly from the field data. For example, in early winter (June 2004) measured dissolved oxygen showed little vertical variation but a trend of progressively decreasing values from west to east across the lake, with values around 9 mg L^{-1} in the western basin (corresponding to the location of Station 2) and 8 mg L^{-1} in the main basin (Station 1). The model captured this spatial variability, however it slightly over–estimated concentrations. In general the vertical changes in oxygen concentrations with stratification were captured by the model simulations but with a more strongly defined oxycline positioned around the thermocline, than was observed in the field data. The model reproduced the development of hypolimnetic anoxia during stratification, though with a slight delay (c. two weeks), but model and field data were well aligned in April 2005 when the entire hypolimnion was anoxic. Pearson correlation coefficients (R) and RMSE calculations based on model comparisons of dissolved oxygen over the whole year of monthly Biofish runs yielded r= 0.877 and RMSE = 1.211 mg L^{-1} (Table 3.5).

Chlorophyll *a* concentrations were derived from Biofish measurements by correlating them with water sample chlorophyll *a* measurements so that direct comparisons could be made with model output as total chlorophyll *a* (as the sum of the two assigned groups of phytoplankton represented by cyanobacteria and diatoms). During the time of stratification (November 2004 to April 2005) model and field data were well aligned. The model predicted spatial variability of chlorophyll *a* relating to decreasing concentrations from west to east (Figure 3.9), but with generally low chlorophyll a concentrations (< 10 μg L^{-1}). During early spring (September and October 2004) the model generally over–predicted measured chlorophyll *a* concentrations compared to the field measurements.

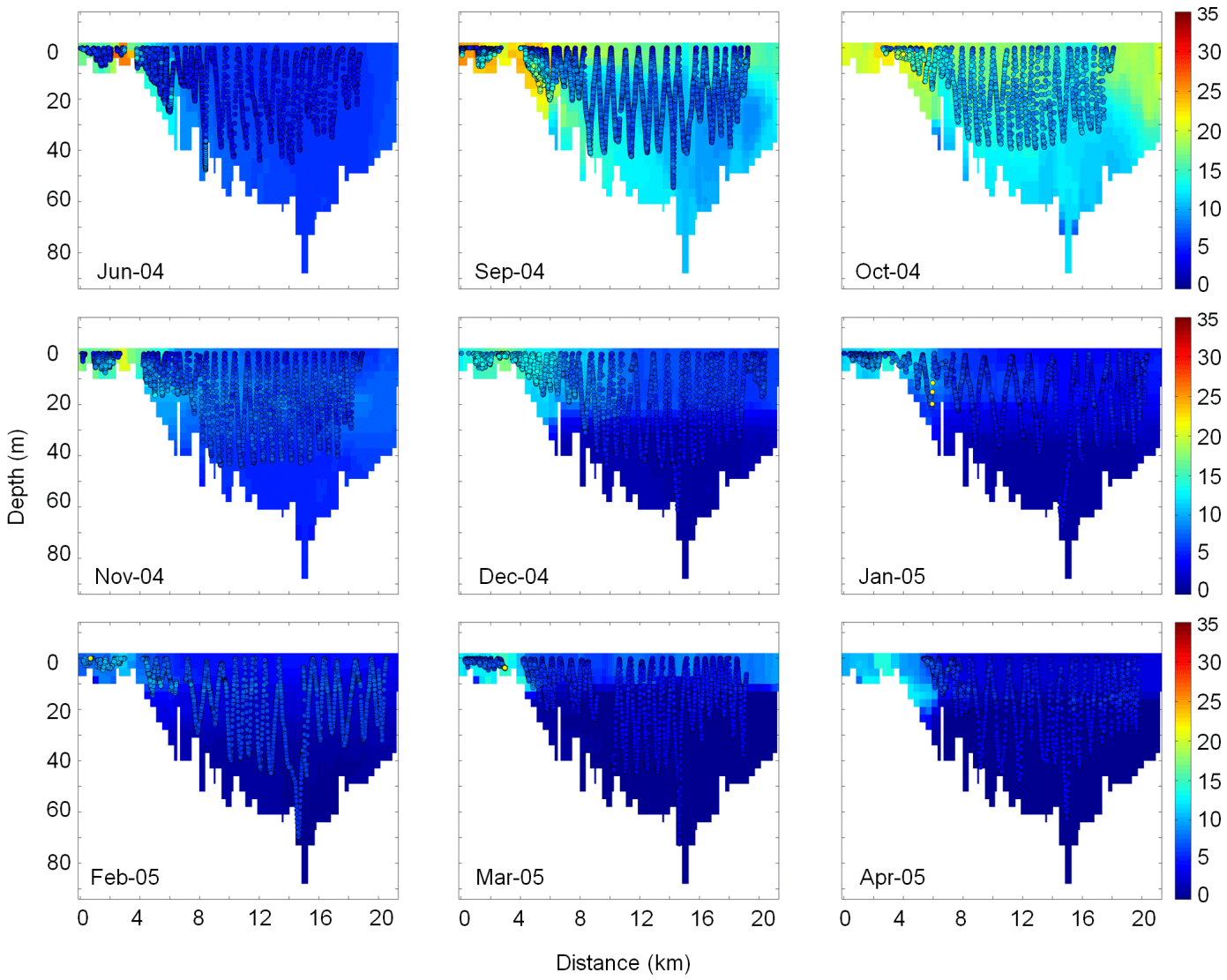

Figure 3.9: Comparison between simulated (coloured background) and measured (○) values of chlorophyll *a* (µg L^{-1}) calibrated to surface chlorophyll measurements from June 2004 to April 2005. Measured values were derived from Biofish fluorescence transect measurements displaying every second measured value.

Biofish In September 2004 the model predictions exceeded field data by 3 to 4–fold, but showed a trend of spatial variability similar to field measurements. Model and field data showed a peak in chlorophyll *a* in October 2004, when model predictions still slightly over–predict field measurements of chlorophyll *a*. In particular in June 2004 the model showed increasing concentrations in shallower areas while the Biofish measurements showed a nearly homogeneous distribution of chlorophyll *a* of c. 6 μg L^{-1} throughout the lake. Despite the general trend of alignment of model predictions and field data, the model several times over–predicted chlorophyll *a* concentration in the shallow regions compared with field measurements, without any definite seasonal trend in this anomaly.

The calculated RMSE of modelled versus measured chlorophyll *a* for the Biofish was 5.03 μg L^{-1} (Table 3.5), which is considerably better than the values achieved for Stations 2 and 3 during the discrete station comparisons (Table 3.3), but twice as high as for Station 1. The corresponding Pearson correlation coefficient value of 0.664 is better than the correlations found in the calibration with discrete station comparisons, even though the coefficients of variation of up to 6.7% within any one monthly Biofish transect and up to 56% for a single model cell (Table 3.2) was relatively high. The over–prediction of chlorophyll *a* in the western basin during July/August 2004 (Figure 3.9) coincided with a peak in chlorophyll *a* the prescribed Ohau Channel inflow boundary conditions (Figure 3.10). These boundary conditions were defined based on a measured peak of over 60 μg L^{-1} of chlorophyll *a* in the monthly measurements made in September 2004. The over–prediction in chlorophyll *a* was most accentuated at Station 2, in closest direct proximity to this inflow. The maximum simulated chlorophyll *a* concentration in the model was 34 μg L^{-1} at Station 2 in September 2004. The other two stations did not show particularly elevated values that could be correlated with the inflow data. For modelled chlorophyll results at Station 1, diatoms were dominant (in terms of chlorophyll *a*) throughout the winter (Figure 3.11A). By contrast in summer the increase in chlorophyll was mostly due to cyanobacteria. The same trend was predicted for Stations 2 and 3 (Figure 3.11B and C).

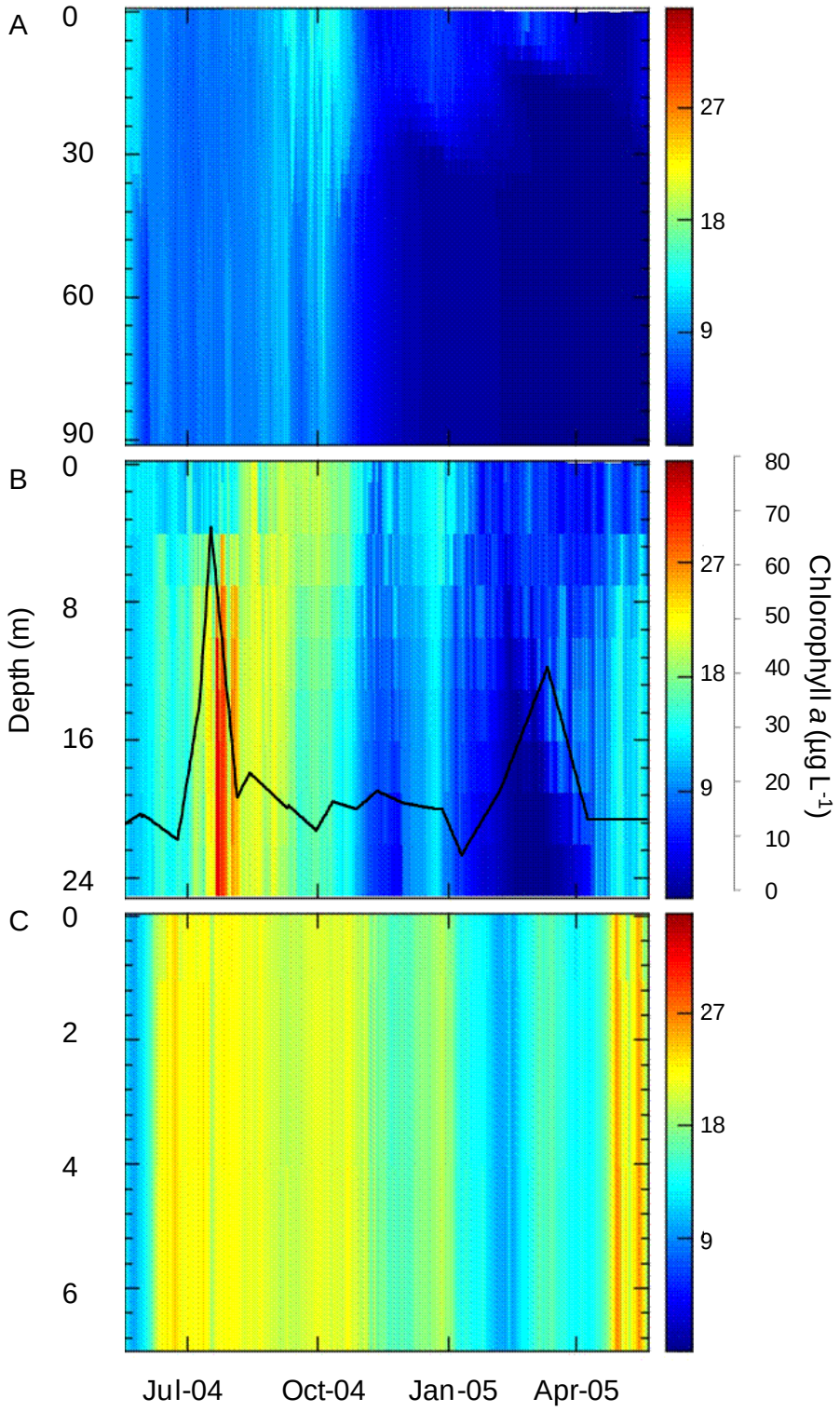

Figure 3.10: Simulated for chlorophyll *a* concentrations (µg L^{-1}) (combined value for the two groups of phytoplankton; diatoms and cyanobacteria) at (A) Station 1, (B) Station 2 and (C) Station 3. Line plot in B shows chlorophyll *a* concentration in Ohau Channel inflow.

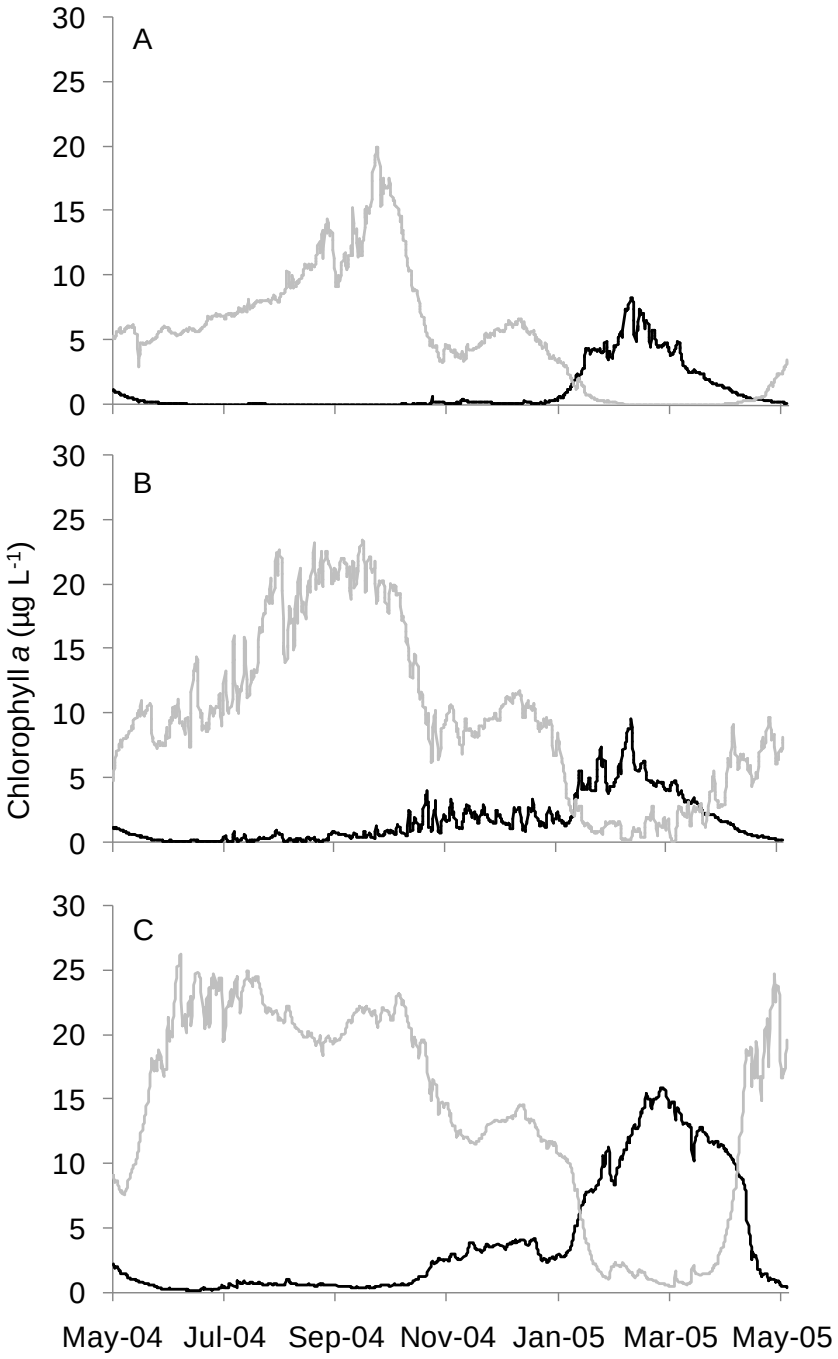

Figure 3.11: Simulated chlorophyll *a* concentration (µg L^{-1}) partitioned into the two modelled phytoplankton groups, cyanobacteria (black line) and diatoms (grey line) at (A) Station 1, (B) Station 2 and (C) Station 3 at the surface over the simulated period (May 2004– May 2005).

Ohau Channel tracer concentration

A simulated conservative tracer was introduced via the Ohau Channel with an assigned concentration value of 1 in the daily inflow forcing input. Figure 3.12 shows the change in tracer concentration on a monthly percentage basis following a lead–in period (see 3.2 Methods). The monthly change in tracer concentration at Station 1 varies between zero and 4 % at the four depths. The trend is very similar at all displayed depths during winter, coinciding with the mixed water column. The slightly higher rate of change at depths of 42 and 60 m compared with the other depths during the winter likely indicates the effects from plunging of the Ohau Channel water at or near these depths (Gibbs 1983), before the tracer fully disperses. The tracer depth distribution changes with the stratification of the water in spring, when the monthly change in tracer was higher at a depth of 21 m and at the surface. During summer stratification the change in tracer concentration at 42 and 60 m at Station 1 is near zero, likely in response to the overflow condition in the Ohau Channel, evident in increasing tracer inputs at 0 and 21 m. At Station 2 the change in tracer concentration is highly variable with values ten times higher than at Station 1, ranging between 40 and –40%. There was no significant difference in tracer concentration changes at depths of 18 and 24 m, which likely reflects the absence of variations in temperature in the thermistors at these depths at Station 2 (Figure 3.5B). In September 2004 the change in tracer concentration was –40% at 18 and 24 m, which coincides with the expected change from underflow to inter/overflow conditions (Gibbs 1983). In July 2004 there was the highest rate of increase in tracer with the exception of the surface, indicating that there was an underflow during this month, which likely continued through to August 2004 when the tracer concentration change was also near zero at the surface. During summer stratification the tracer concentration was still variable at all depths which likely indicates the variable insertion depths of the Ohau Channel. As expected, due to the well mixed nature of Station 3, the monthly change in tracer concentration did not vary with depth. Similar to Station 1, tracer concentration generally fluctuate above 0% in most months and attains values to up to 20% per month, which indicates a slightly reduced monthly exchange of the Ohau Channel at this station relative to Station 2, but with accumulating values

over time. The greatest rate of increase in tracer concentration occurred from August 2004 to September 2004, which coincides with a period when chlorophyll *a* in Ohau Channel was highest.

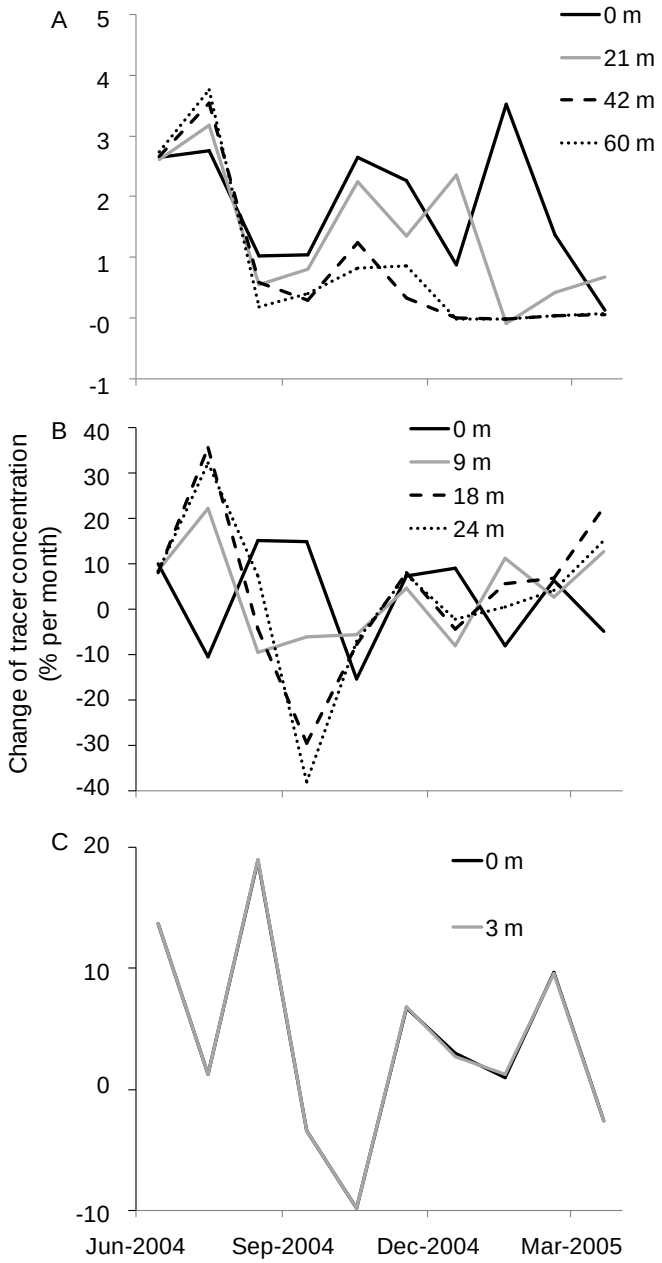

Figure 3.12: Rate of change of tracer concentration as % per month relative to the assigned tracer concentration (100%) in the Ohau Channel at (A) Station 1, (B) Station 2 and (C) Station 3.

3.4 Discussion

The highly spatially resolved field data used in this study has provided a unique opportunity to evaluate the performance of the 3D model ELCOM–CAEDYM in simulating temperature and biogeochemical variables in a large lake where it has previously been shown that there are large horizontal and vertical gradients (Vincent et al. 1991; Chapter 2). The model calibration was undertaken based on three sampling stations representative of different aspects of the complex morphometry of the lake, and validated using a fixed transect with highly resolved field measurements of temperature, dissolved oxygen and chlorophyll *a*. While these variables were simulated with error terms comparable to those that occur for field measurements within individual model cells using the Biofish, nutrient concentrations were less well replicated, most obvious at shallow Station 3. The use of discrete sampling stations for 3D model calibration has been carried out in previous studies (Missaghi & Hondzo 2010) and some studies have gone to great lengths to initialise state variables with a large number of sampling stations (e.g., León et al. 2006), but there are no studies that have validated a model with field data of similarly high spatial resolution as has been demonstrated in this study.

3.4.1 Model limitations

My study also indicated, however, that it may be difficult to use ELCOM–CAEDYM to simulate nutrient dynamics of morphologically complex lakes where a single parameterisation is applied across the whole lake. This may be a key model limitation, however increased simulated nutrient concentrations in Okawa Bay may be due to specific user-defined variables. In Okawa Bay the TN concentration increased between December 2004 and February 2005 to 1.2 mg L^{-1} compared with observed values c. 0.4 mg L^{-1}. Considering the volume of Okawa Bay and the surface area available for benthic production, a growth rate of 0.2 d^{-1} would be necessary at a density of 231 mg N m^{-2} to take up the excess nutrients in the bay. Benthic producers have not been accounted for in the model due to absence of data, however the estimated values may be realistic compared with the study of Lawniczak (2010), which provides an upper limit for N biomass in a shallow temperate lake at an advanced stage of eutrophication, when densities up

to 29720 mg N m^{-2} where reported for emerged macrophytes. In my model approach it was intended to restrict the modelled parameters to data that was available from the field to avoid increasing the possible equifinality of the model (Arhonditsis et al., 2008; Beven, 2006).

A further reason for the increase in modelled nutrients in Okawa Bay may be due to the application of the static sediment model which does not account for spatial differences in sediment nutrient concentrations. Trolle et al. (2010) analysed bottom sediment in several lakes in the Rotorua area and found that in particular in shallow lakes, the cores can vary significantly in the same basin of these lakes. Despite the capacity to adjust the nutrient transfers across the sediment–water interface according to temperature, dissolved oxygen and pH of the overlying water (Robson & Hamilton 2004; Burger et al. 2007b) the static sediment model does not provide for spatial differences due to sediment properties themselves. In large, shallow Lake Taihu (China), Trolle et al. (2009) found large horizontal variations in total carbon, nitrogen and phosphorus content of the bottom sediments, despite the relatively flat–bottomed nature of this lake. It is not unreasonable to expect even greater variations in sediment composition in a morphometrically complex lake such as Rotoiti (Håkanson 1977).

Highly different sediment release rates have been found with depth in relatively morphologically homogeneous Lake Rotorua (Burger et al. 2007b). Sediment release rates at a deep station (20 m) in this lake were significantly higher (mean 44.3 mg m^{-2} d^{-1}) than at two shallower stations (14 and 7 m) (mean of 9.3 and 7.7 mg m^{-2} d^{-1}, respectively). Similar to my simulation results for nutrient concentrations, Missaghi and Hondzo (2010) display increased nutrient concentrations from model results at a shallow station, yet did not discuss causes in detail. Model runs to calibrate sediment variables to each of the three stations improved the statistical comparisons for each station, especially Station 3. The parameter values were substantially altered (reducing nutrient release rates) in Station 3 compared with the general calibration over the whole lake, but this resulted in strongly reduced chlorophyll *a* concentrations across the model domain. This observation suggests that a dynamic sediment model may be able to

capture the horizontal differences in sediment dynamics and better adjust to the spatial variations in nutrient release rates.

No individual site–related sediment analyses were undertaken in this study, to supply the required input data for the dynamic sediment diagenesis model. Trolle (pers. comm.) found that a 1D approach with the dynamic sediment model increased the model runtime to be comparable to 3D runtimes with the static model. The complexity of Lake Rotoiti's morphometry led to a decision to use the static model to keep the runtime to an acceptable level, whilst recognising the limitations that this approach imposed with simulating nutrient concentrations.

3.4.2 Geothermal influence and temperature validation

Geothermal heat energy inputs to the ELCOM–CAEDYM model were adjusted to reproduce the observed temperature increment during stratification in the hypolimnion of Station 1, where there is a deep crater. A geothermal energy input of 165 MW into the bottom of the crater was required to accurately simulate the observed increases in water temperature in the hypolimnion over the stratified period. This heat input is about ten–fold higher than that used by Spigel (1983) in a 1D application of an earlier version of DYRESM. Spigel (1983) used a similar process to the one applied in this Chapter, of adjusting the geothermal energy to match modelled hypolimnion temperature of Lake Rotoiti to field measurements. An energy input of 10–20 MW was determined, which is also around ten–fold lower than the geothermal heat input of 140 MW estimated by Calhaem (1973). My results indicate that the geothermal heat flux in the lake is likely to be closer to that calculated by Calhaem (1973).

Nearly 60 heat conduction measurements were made in the lake bed by Calhaem (1973) from which a conductive heat flux of 10 MW was calculated. A further 130 MW due to convection was estimated using a simple heat balance calculation from the increase in hypolimnion temperature from spring to autumn. Observations, such as temperature inversions measured in the water column at the bottom (Calhaem 1973; this study Figure 3.5 A), temperature measurements in the sediment, which are hotter than predicted from conduction alone, and bubbles in

the water column that contained gas, suggest a geothermal origin of heat (Calhaem 1973). An associated convective flux was further supported by the suggestion that the steep-sided holes in the central basin would fill with sediments if there were no upwards fluid flux. Recent observations (Prof. Chris Hendy, pers. comm.) show bubbles leaving the sediment surface. The bubbles then collapse, suggesting the origin of hot fluid rather than gas, which supports previous suggestions by Calhaem (1973). Conductivity profiles of CTD casts show a progressive increase in conductivity in the hypolimnion of Lake Rotoiti over the stratification period, which further supports the presence of a convective heat flux.

Spigel (1983) calculated total rates of change in heat storage in the hypolimnion below 35 m from September 1982 to June 1982 based on temperature profiles measured at roughly weekly intervals at 12 sites in the main basin of Lake Rotoiti. Total rates of change varied from around 450 MW in spring to around 50 MW in summer. The increase in heat storage in summer and spring was explained by the combined effect of downward mixing of surface waters by strong winds in spring, thermal diffusion through the thermocline and the geothermal heating from below. Spigel (1983) simulated these processes with a daily time-step in DYRESM, which resulted in good comparison with measured hypolimnion temperatures using a boundary condition for the heat source in the range 10-20 MW. Spigel (1983) explained the difference between his and Calhaem's (1973) results as being mainly due to the downward heat flux in spring caused by strong wind-mixing events (similar to the ones observed in this study) before the stratification was fully established, that were not accounted for in the seasonal heat balance calculation and the higher rate of downward diffusion of heat at the base of the thermocline compared with estimations made by Calhaem (1973). Spigels's (1983) conclusions have been reported in Priscu et al. (1986) and Gibbs (1992), although no detailed analyses for the heat source are given in those papers.

Pasternack and Varekamp (1997) used a simple energy–mass balance box model in assessing temperature variations in, and geothermal energy inputs from, volcanic sources to Lake Ruapehu, located at the southern end of the Central Volcanic Plateau. They estimated a heat input of 385 MW in this small lake which

is substantially more geothermally active than Lake Rotoiti. Kissling and Weir (2005) developed a super–critical equation of state module to simulate thermal dispersion and transport of water in the Taupo Volcanic Zone, and used this model to calculate a total energy input of 406 MW over an area of 116 km^2. Of this they calculated an energy input of 0.39 MW km^{-2} for the area at the southern end of the Central Volcanic Plateau and 0.29 MW km^{-2} for the area around Lake Rotoiti. This leads to an estimated volcanic energy flux affecting Lake Rotoiti (34.6 km^2) of 121 MW, which is close to the estimate of Calhaem (1973). The use of a constant geothermal input of 165 MW to Lake Rotoiti appears to be within the range of conceivable values based on previous research that has sought to identify some of the geothermal energy fluxes to the Taupo Volcanic Zone. It has been shown that larger volcanic lakes have lower steady–state temperatures for a given energy input (Pasternack & Varekamp 1997), which allows these lakes to absorb more heat and maintain the same temperature. The sensitivity analysis that I carried out for geothermal inputs into Lake Rotoiti tended to reaffirm this as heat inputs of to up to 265 MW produced very little change in simulated water temperature in Lake Rotoiti. Considering the geothermal energy of 165MW represents only 3% (2% in summer) of the total heat flux entering the lake (solar flux and geothermal flux), the assumption of an energy input of 165 MW has little impact on the total heat balance of the lake and was a successful tool to adjust hypolimnion temperature, but model accuracy regarding this heat flux cannot be expected due to model and data limitations.

ELCOM is designed to downward–sweep density gradients to capture the dominant effect of mixing in stratified lakes (Hodges & Dallimore 2007). This leads to a bias in mixing direction which may not be appropriate for benthic boundary layers (Hodges 2000). The mixing model used in ELCOM is based on the mixing energy budgets developed for the 1D approach (Imberger & Patterson 1989; Hodges 2000; Hodges et al. 2000). Mixing is computed based on the turbulent kinetic energy available for mixing relative to the energy required to overcome the energy inherent in the density stratification. When mixing occurs the turbulent kinetic energy for mixing is reduced by the energy required for mixing and dissipation. Sensitivity analyses carried out when defining the model

depth grid size showed that a coarser grid in the vertical direction causes a higher dispersion of heat and a deeper thermocline. In my set–up a vertical cell size of 3 m led to best match of modelled temperatures with the field data. However the change in thermocline depth with changing vertical model grid size may possibly indicate a lower coefficient for thermal diffusity compared with in situ conditions.

It was not intended to use the model replicate the inverse temperature stratification that was observed over three months in winter at the bottom of Station 1 in the main basin of the lake. Several runs with increased geothermal fluxes to the model cells corresponding to the crater did not replicate the observed inverse stratification. The maximum depth of the model was 93 m using a horizontal grid resolution of 200 x 200 m, while maximum depth measured in Lake Rotoiti is 123 m. This confined area is the origin of the majority of the geothermal energy input into Lake Rotoiti. ELCOM uses a downward sweep method to adjust instabilities (Hodges et al. 2000). An unstable temperature gradient would be mixed through successive grid cells until the system is stable. Density differences as observed in the field are therefore not likely to be simulated with the current version of ELCOM. However the observed inverse temperature stratification appears to be a temporary anomaly in a very restricted area of the lake and does not affect the overall outcomes of the model, and was not explored further in this study. The downward–sweep method for energy dissipation may ultimately require revision for unusual density instabilities such as those demonstrated in this study. The model of Monismith and Fong (1996) to represent the case where turbulence at the bottom dominates that from the flow in a shallow estuary, used an upward sweep method to rectify density gradients and may provide the basis for further detailed research designed specifically to examine these inverse geothermal heat gradients.

3.4.1 Phytoplankton, chlorophyll *a* and zooplankton

The aim to predict the spatial variations of chlorophyll *a* concentration in Lake Rotoiti through the representation of two phytoplankton groups was achieved with higher accuracy (R=0.664, RMSE=5.031 μg L^{-1}; Table 3.5) than many comparable 1D modelling studies. The choice of calibration parameters showed

better correlations of chlorophyll *a* than studies by Burger et al. (2008) (R=0.45 and 0.29, RMSE=8.5 and 13.1 μg L^{-1}) and Trolle et al. (2008a) (R=0.140 and 0.351, RMSE=12.759 and 10.401 μg L^{-1} (calibration and validation)). However a two–compartment model of Lake Washington, representing the hypolimnion and epilimnion, with varying depths for each, validated with monthly measurements simulated chlorophyll *a* values with higher accuracy, with R^2 of 0.91 (epilimnion) and 0.69 (hypolimnion) (Arhonditsis & Brett 2005b). However considering the runtime, model dimension and complexity the results presented here demonstrate a good model fit considering that the results of a comparative study presented by Arhonditsis and Brett (2004) found a negative correlation between model complexity, length of the simulation period and spatial model dimension compared with phytoplankton predictions. Simpler approaches using a 1D (DYRESM–CAEDYM) or a two compartment model are not challenged by the highly irregular morphometry and widely differing nature of stations used for comparison of simulated and measured concentrations.

It is also been demonstrated that within a single waterbody there may be different phytoplankton species' compositions, particularly where there are shallow bays within deep lakes (Bondarenko et al. 1996). Further, it has been found that phytoplankton communities may differ greatly adjacent to a major inflow (Rueda et al. 2008). Fish and Chapman (1969) describe the western basin as acting like a separate entity within the lake boundaries. Chapter 2 also demonstrated markedly different seasonal variations in nutrient concentrations and productivity in different parts of Lake Rotoiti that could also be expected to have impacts on phytoplankton succession. The simulated chlorophyll *a* concentration of the main basin was generally representative of the measured data but was over–predicted in the shallower western area of the lake, where there was potential for confounding effects of the Ohau Channel inflow from Lake Rotorua, which has quite variable phytoplankton species composition (Burger et al. 2007a).

The effects of zooplankton grazing on phytoplankton were not simulated explicitly as the same 1D model configuration used for adjacent Lake Rotorua (Burger et al. 2007a), was also used in my study. Further to that no zooplankton

data were available for the year of interest. The contribution of zooplankton grazing on phytoplankton was included in the model through a phytoplankton loss term, however over–prediction of phytoplankton especially during the winter season indicates that model performance may be able to be improved when zooplankton grazing is taken into account.

Previous attempts to model chlorophyll *a* concentrations have not dealt with the inherent variability of measured data. There was a high coefficient of variation for chlorophyll fluorescence measurements for single model cells. Operating the model at a grid size (200 m x 200 m x 3 m) that enabled repeated simulation runs (i.e., computational times of reasonable duration) removes the expected small–scale patchiness occurring within the grid size (Hillmer et al 2008). Lake Rotoiti is dominated by two groups of phytoplankton which have been represented in the model generically as cyanobacteria and diatom groups with parameter ranges assigned accordingly. Missaghi and Hondzo (2010) modelled three stations of Lake Minnetonka using ELCOM–CAEDYM. Their study did not provide any statistical errors for chlorophyll *a* calibrations represented by one phytoplankton group, however their results point to a high degree of error in comparisons at all stations in the top 2 m. Missaghi and Hondzo (2010) reported that the failure of the model to capture measured peaks and the general difficulties in simulating chlorophyll *a* were created through their simulation of just one phytoplankton group.

3.4.2 Inflow analysis

Chlorophyll *a* concentrations simulated by the model are driven by sources and sinks due to growth and loss processes, respectively, as well as mixing and advective processes. In the latter case the Ohau Channel contributes inputs of chlorophyll *a* to adjacent model cells, which may increase or decrease concentrations for the model cells within the lake. The overestimation of chlorophyll *a* concentration in the western basin occurred over several months, without a specific seasonal pattern. This overestimation may be partly related to the monthly measured field data in the Ohau Channel inflow which was prescribed as an input to the model. The linear interpolation of the data to provide

daily inputs to the model likely generated both over– and underestimates of the values on the rising and falling limb of the interpolation, depending on the individual sampling day. It is coincidental that the highest change in tracer concentration occurred in the same months as the chlorophyll *a* peak measured in Ohau Channel and a corresponding large net increase in chlorophyll *a* occurred at Station 2 at that time, given the relatively high concentrations in the Ohau Channel inflow. The inflow data and the possible over– or underestimation of phytoplankton biomass used for model forcing does not show the same obvious impact in the main basin of the lake.

The Ohau Channel tracer accumulated to a value of around 20% at the surface of the main basin over the one–year simulation period Vincent et al. (1991) suggested that 31% of the N loading and 64% of the P loading to Lake Rotoiti occur via the Ohau Channel inflow. Most of the loading (c. 60%) occurs when there is a plunging inflow. The specific biological effects of inflows have rarely been examined in the way described in my study, however, Hillmer et al. (2008) used a conservative tracer in ELCOM to show that the Jordan River enters Lake Kinneret is diverted westwards due to a general counter–clockwise circulation within the lake in winter. They identified that nutrient inputs from this river, and the transport of these nutrients played a key role in enhancing productivity on the western side of Lake Kinneret.

My tracer implementation confirms previous findings of varying intrusion depth in the western basin (Gibbs 1983) and the inter– and underflows that intrude into the main basin of the lake at different times of year. However, contrary to previous studies (Gibbs 1983; Vincent et al. 1991), the tracer results highlight that bays in the vicinity of Ohau Channel inflow may also be greatly affected by the incoming water, potentially producing large spatial differences in phytoplankton assemblages. In Lake Taihu, China, Meiliang Bay is highly eutrophic compared with the main lake basin. Chen et al. (2003) related this spatial variation to variations in wind speed and direction. Temperature differences between constricted bays and the main lake basin can also affect water exchange due to density interflows as MacIntyre (2002) has shown in Lake Victoria. Daily

variations in temperature of Ohau Channel create density differences not only between the inflowing water and the western basin, but also the adjacent bay, which may generate variations in exchange between Ohau Channel water, the lake and the bay. Whilst the plunging inflow into the main basin of Lake Rotoiti will be largely un affected by wind direction or strength, the intrusion of Ohau Channel into adjacent Okawa Bay, which will mainly occur when there is an overflow condition, is very likely to be affected by wind velocity and water temperature variations.

3.5 Conclusions

The 3D ELCOM–CAEDYM simulations demonstrate that the model is capable of reproducing highly resolved field data of temperature, dissolved oxygen and chlorophyll *a* on a spatial basis. Whilst the hydrodynamic model (ELCOM) appeared to predict better results after geothermal heat adjustments, the water quality model (CAEDYM) clearly showed difficulties in dealing with spatial variations even though the overall model performance was satisfactory when assessed against previous studies. Spatial differences in sediment nutrient composition that are not represented in the present model resulted in increased values in the shallow embayment in particular autumn. A similar trend was found by Missaghi and Hondzo (2010) for a shallow station (10 m) in an application using ELCOM–CAEDYM for simulation of Lake Minnetonka, USA which may highlight a limitation of the model. Within the time frame of this study it was not possible to test a recently developed dynamic diagenesis module with CAEDYM, but it is recommended that future work be done to consider how to better represent the spatially varying character of bottom sediments of large, deep lakes. It would be beneficial to develop a simple sediment diagenesis model that does not significantly increase model runtimes and could dynamically simulate the lake sediments over large temporal and spatial scales.

It has been shown that the horizontal variations in Lake Rotoiti play an important role in the phytoplankton biomass and succession. The input from Lake Rotorua via the Ohau Channel is a major contributor of phytoplankton and nutrients within Lake Rotoiti, and has a direct influence on the water quality and phytoplankton

especially in the western basin. Higher frequency measurements of the composition of the Ohau Channel inflow may help to more accurately simulate its path into the lake and the eventual fate of incoming phytoplankton and nutrients. This study has highlighted that the input from the Ohau Channel not only affects the main basin and western basin, but is likely to create higher biomass in the adjacent bays. To support analysis of inflow dispersion current meter measurements in adjacent bays would be beneficial for future research.

3.6 References

Arhonditsis, G. B. and Brett, M. T. (2005a): Eutrophication model for Lake Washington (USA): Part I. Model description and sensitivity analysis. *Ecological Modelling* 187(2–3): 140–178.

Arhonditsis, G. B. and Brett, M. T. (2005b): Eutrophication model for Lake Washington (USA): Part II – model calibration and system dynamics analysis. *Ecological Modelling* 187(2–3): 179–200.

Arhonditsis, G. B. and Brett, M. T. (2004): Evaluation of the current state of mechanistic aquatic biogeochemical modeling. *Marine Ecology Progress Series* 271: 13–26.

Arhonditsis, G. B., Perhar, G., Zhang, W., Massos, E., Shi, M. And Das, A. (2008): Addressing equifinality and uncertainty in eutrophication models. *Water Resources Research* 44: W01420.

Axler, R. P. and Owen, C. J. (1994): Measuring chlorophyll and phaeophytin: Whom should you believe? *Lake and Reservoir Management* 8(2): 143–151.

Beamud, S., Diaz, M. and Pedrozo, F. (2009): Nutrient limitation of phytoplankton in a naturally acidic lake (Lake Caviahue, Argentina). *Limnology* 11(2): 103–113.

Beven, K. (2006): A manifesto for the equifinality thesis. *Journal of Hydrology* 320: 18-36.

Blumberg, A. and Mellor, G.L. (1987): A description of a three-dimensional coastal ocean circulation model. American Geophysical Union, Washington.

Bondarenko, N. A., Guselnikova, N. E., Logacheva, N. F. and Pomazkina, G. V. (1996): Spatial distribution of phytoplankton in Lake Baikal, Spring 1991. *Freshwater Biology* 35(3): 517–523.

Burger, D. F., Hamilton, D. P., Hall, J. A. and Ryan, E. F. (2007a): Phytoplankton nutrient limitation in a polymictic eutrophic lake: community versus species–specific responses. *Archiv für Hydrobiologie* 169(1): 57–68.

Burger, D. F., Hamilton, D. P. and Pilditch, C. A. (2008): Modelling the relative importance of internal and external nutrient loads on water column nutrient concentrations and phytoplankton biomass in a shallow polymictic lake. *Ecological Modelling* 211(3–4): 411–423.

Burger, D. F., Hamilton, D. P., Pilditch, C. A. and Gibbs, M. M. (2007b): Benthic nutrient fluxes in a eutrophic, polymictic lake. *Hydrobiologia* 584(1): 13–25.

Calhaem, I. M. (1973). Heat flow measurements under some lakes in North Island, New Zealand. Department of Physics., Unpublished Ph.D thesis, lodged in the Library, Victoria University of Wellington.: 1–191.

Casulli, V. and Cheng, R. T. (1992): Semi–implicit finite difference methods for three–dimensional shallow water flow *International Journal for Numerical Methods in Fluids* 15(6): 629–648.

Chen, Y., Fan, C., Teubner, K. and Dokulil, M. (2003): Changes of nutrients and phytoplankton chlorophyll–*a* in a large shallow lake, Taihu, China: an 8–year investigation. *Hydrobiologia* 506–509: 273–279.

Cody, A. D. (2007): Geodiversity of geothermal fields in the Taupo Volcanic Zone. DOC Research & Development Series, Department of Conservation.

Eder, M., Rinke, K., Kempke, S., Huber, A. and Wolf, T. (2008): Seeweite Bodensee–Messkampagne 2007 als Test fuer Bodensee Online. *Wasser Wirtschaft* 98(10): 34–38 (In German).

Fish, G. R. and Chapman, A. (1969): Synoptic surveys of Lakes Rotorua and Rotoiti. *New Zealand Journal of Marine and Freshwater Research* 3: 571–584.

Gal, G., Hipsey, M. R., Parparov, A., Wagner, U., Makler, V. and Zohary, T. (2009): Implementation of ecological modeling as an effective management and investigation tool: Lake Kinneret as a case study. *Ecological Modelling* 220(13–14): 1697–1718.

Gibbs, M. M. (1983): Penetration of Ohau Channel water into Lake Rotoiti. Taupo Research Laboratory, Department of Scientific and Industrial Research. File report 63. 9 pp.

Gibbs, M. M. (1992): Influence of hypolimnetic stirring and underflow on the limnology of Lake Rotoiti, New Zealand. *New Zealand Journal of Marine and Freshwater Research* 26: 453–463.

Håkanson, L. (1977): The influence of wind, fetch, and water depth on the distribution of sediments in Lake Vänern, Sweden. *Canadian Journal of Earth Sciences* 14(3): 397–412.

Hamilton, D. P. (2004). An historical and contemporary review of water quality in the Rotorua Lakes. In Miller, N. (Ed.): Proceedings Rotorua Lakes Symposium 2003. Rotorua, New Zealand. Pp 3–15.

Hamilton, D. P., McBride, C. and Uraoka, T. (2005): Lake Rotoiti fieldwork and modelling to support considerations of Ohau Channel diversion from Lake Rotoiti. *Centre for Biodiversity and Ecology Research* Department of Biological Science, School of Science and Engineering, University of Waikato, Hamilton.

Hamilton, D. P. and Mitchell, S. F. (1996): An empirical model for sediment resuspension in shallow lakes. *Hydrobiologia* 317(3): 209–220.

Hamilton, D. P., O'Brien, K. R., Burford, M. A., Brookes, J. D. and McBride, C. G. (2010): Vertical distributions of chlorophyll in deep, warm 3 monomictic lakes. *Aquatic Sciences* 72(3): 295–307.

Hillmer, I., van Reenen, P., Imberger, J. and Zohary, T. (2008): Phytoplankton patchiness and their role in the modelled productivity of a large, seasonally stratified lake. *Ecological Modelling* 218(1–2): 49–59.

Hipsey, M.R., Antenucci, J.P., Romero, J.R. and Hamilton, D. (2007): Computational Aquatic Ecosystem Dynamics Model: CAEDYM v3. Science Manual. Centre for Water Research, the University of Western Asutralia. Retrieved July 2008, from http://www.cwr.uwa.edu.au.

Hodges, B. (2000): Numerical techniques in CWR–ELCOM. Report. WP 1422–BH. Centre for Water Research, University of Western Australia.

Hodges, B. and Dallimore, C. (2007): Estuary Lake and Computer Model: ELCOM Science Manual Code v2.2. Centre for Water Research, University of Western Australia.

Hodges, B., Imberger, J., Saggio, A. and Winters, K. B. (2000): Modelling basin scale waves in a stratified lake. *Limnology and Oceanography* 45(7): 1603–1620.

Huang, G. H. and Xia, J. (2001): Barriers to sustainable water–quality management. *Journal of Environmental Management* 61(1): 1–23.

Hurst, A. W., Bibby, H. M., Scott, B. J. and McGuinness, M. J. (1991): The heat source of Ruapehu crater lake; deductions from the energy and mass balances. *Journal of Volcanology and Geothermal Research* 46(1–2): 1–20.

Imberger, J. and Patterson, J. C. (1989). Physical Limnology. *Advances in Applied Mechanics* 27**:** 303–475.

Jolly, V. H. (1959). A Limnological Study of some New Zealand lakes. Ph.D thesis lodged in the Library: Dunedin, University of New Zealand.: 1–95.

Jørgensen, S.E. (2010): A review of recent developments in lake modelling. Ecological Modelling, 221:689-692.

Jørgensen, S. E., Ray, S., Berec, L., Straskraba M. (2002): Improved calibration of a eutrophication model by use of the size variation due to succession. *Ecological Modelling*, 153(3): 269–277.

Jørgensen, S.E., Fath, B.D., Grant, W.E., Legovic, T. and Nielsen, S.N. (2008): New initiative for thematic issues: An invitation. *Ecological Modelling*, 215:273-275.

Kamarainen, A. M., Yuan, H., Wu, C. H. and Carpenter, S. R. (2009): Estimates of phosphorus entrainment in Lake Mendota: a comparison of one–dimensional and three–dimensional approaches. *Limnology and Oceanography: Methods* 7: 553–567.

Kissling, W. M. and Weir, G. J. (2005): The spatial distribution of the geothermal fields in the Taupo Volcanic Zone, New Zealand. *Journal of Volcanology and Geothermal Research* 145: 136–150.

Koçyigit, M. B. and Falconer, R. A. (2004): Three-dimensional numerical modelling of wind-driven circulation in a homogeneous lake. *Advances in Water Resources* 27: 1167-1178.

Laval, B., Imberger, J., Hodges, B.R. and Stocker, R. (2003): Modeling Circulation in Lakes: Spatial and Temporal Variations. *Limnology and Oceanography* 48(3): pp. 983–994.

Lawniczak, A. E. (2010): The role of emerged macrophytes in nutrient cycling in Lake Niepruszewskie (western Poland). *International Journal of Oceanography and Hydrobiology* 39: 75-83.

León, L. F., Lam, D. C. L., Schertzer, W. M., Swayne, D. A. and Imberger, J. (2005): Modeling as a tool for nutrient management in Lake Erie: a hydrodynamics study. *Journal Great Lakes Research* 31: 309–318.

León, L. F., Smith, R. E. H., Romero, J. R. and Hecky, R. E. (2006): Lake Erie hypoxia simulations with ELCOM–CAEDYM. *3rd Biennial meeting of the International Environmental Modelling and Software Society*: 6 pp.

MacIntyre, S., Romero, J. R. and Kling, G. W. (2002): Spatial–temporal variability in surface layer deepening and lateral advection in an embayment of Lake Victoria, East Africa. *Limnology and Oceanography* 47(656–671).

Mao, J., Chen, Q. and Chen, Y. (2008): Three–dimensional eutrophication model and application to Taihu Lake, China. *Journal of Environmental Sciences* 20(3): 278–284.

Mazumder, A. and Taylor, W. D. (1994): Thermal Structure of Lakes Varying in Size and Water Clarity. *Limnology and Oceanography* 39(4): 968–976.

Missaghi, S. and Hondzo, M. (2010): Evaluation and application of a three–dimensional water quality model in a shallow lake with complex morphometry. *Ecological Modelling* 221(11): 1512–1525.

Mooij, W., Trolle, D., Jeppesen, E., Arhonditsis, G., Belolipetsky, P., Chitamwebwa, D., Degermendzhy, A., DeAngelis, D., De Senerpont Domis, L., Downing, A., Elliott, J., Fragoso, C., Gaedke, U., Genova, S., Gulati, R., Håkanson, L., Hamilton, D., Hipsey, M., ‘t Hoen, J., Hülsmann, S., Los, F., Makler-Pick, V., Petzoldt, T., Prokopkin, I., Rinke, K., Schep, S., Tominaga, K., Van Dam, A., Van Nes, E., Wells, S. and Janse, J. (2010): Challenges and opportunities for integrating lake ecosystem modelling approaches. Aquatic Ecology, 44:633-667.

Monismith, S. G. and Fong, D. A. (1996): A simple model of mixing in stratified tidal flows. *Journal of Geophysical Research* 101: 28583 – 28595.

National Institute of Water and Atmospheric Research Ltd. (NIWA). (2005): CliFlo: NIWA's National Climate Database on the Web. Retrieved 12 July 2005, from http://cliflo.niwa.co.nz.

Nixdorf, B. and Deneke, R. (1997): Why 'very shallow' lakes are more successful opposing reduced nutrient loads. *Hydrobiologia* 342/343: 269–284.

Pasternack, G. B. and Varekamp, J. C. (1997): Volcanic lake systematics I. Physical constraints. *Bulletin of Volcanology* 58: 528–538.

Pedrozo, F. L., Temporetti, P. F., Beamud, G. and Diaz, M. M. (2008): Volcanic nutrient inputs and trophic state of Lake Caviahue, Patagonia, Argentina. *Journal of Volcanology and Geothermal Research* 178(2): 205–212.

Penny, J., Brian, M. and Geoffrey, P. (1996): The determination of total nitrogen and total phosphorus concentrations in freshwaters from land use, stock headage and population data: testing of a model for use in conservation and water quality management. *Freshwater Biology* 36(2): 451–473.

Priscu, J. C., Spigel, R. H., Gibbs, M. M. and Downes, M. T. (1986): A numerical analysis of hypolimnetic nitrogen and phosphorus transformations in Lake Rotoiti, New Zealand: a geothermally influenced lake. *Limnology and Oceanography*. 31: 812–831.

Robertson, D. M. and Ragotzkie, R. A. (1990): Changes in the thermal structure of moderate to large sized lakes in response to changes in air temperature. *Aquatic Sciences – Research Across Boundaries* 52(4): 360–380.

Robson, B. J. and Hamilton, D. P. (2004): Three–dimensional modelling of a Microcystis bloom event in the Swan River estuary, Western Australia. *Ecological Modelling* 174(1–2): 203–222.

Romero, J. R., Antenucci, J. P. and Imberger, J. (2004): One– and three–dimensional biogeochemical simulations of two differing reservoirs. *Ecological Modelling* 174: 143–160.

Rueda, F. J., Schladow, S. G. and Clark, J. F. (2008): Mechanisms of contaminant transport in a multi–basin lake. *Ecological Applications* 18(8): 72–87.

Saygi–Babug, Y. (2004): Primary production in shallow eutrophic Yenicaga Lake (Bolu, Turkey). *Fresenius Environmental Bulletin* 13: 98–104.

Schladow, S. G. and Hamilton, D. P. (1997): Prediction on water quality in lakes and reservoirs: Part II – Model calibration, sensitivity analysis and application. *Ecological Modelling* 96: 111–123.

Schwab, D.J. and Bedford, K.W. (1994): Initial Implementation of the Great Lakes Forecasting System: A Real-Time System for Predicting Lake Circulation and Thermal Structure. *Water Pollution Research Journal of Canada*, 29:203-220.

Søndergaard, M., Jensen, J. P. and Jeppesen, P. (2005): Seasonal response of nutrients to reduced phosphorus loading in 12 Danish lakes. *Freshwater Biology* 50: 1605–1615.

Song, Y., Semazzi, F.H.M., Xie, L. and Ogallo, L.J. (2004): A coupled regional climate model for the Lake Victoria basin of East Africa. International Journal of Climatology, 24:57-75.

Spigel, R. H. (1983): Outline for reasons for a revised geothermal heat flux estimate for Lake Rotoiti, Department of Civil Engineering, University of Canterbury (unpublished report in reference to: Spigel, R. H. and Timperley, M. (1983): Geothermal influences on the limnology of Lake Rotoiti – Preliminary conclusions from the 1982 field data. Taupo Research Labrotory File report 27/T/58.

Spillman, C. M., Imberger, J., Hamilton, D. P., Hipsey, M. R. and Romero, J. R. (2007): Modelling the effects of Po River discharge, internal nutrient cycling and hydrodynamics on biogeochemistry of the Northern Adriatic Sea. *Journal of Marine Systems* 68(1–2): 167–200.

Taran, Y. and Rouwet, D. (2008): Estimating thermal inflow to El Chichón crater lake using the energy–budget, chemical and isotope balance approaches. *Journal of Volcanology and Geothermal Research* 175(4): 472–481.

Thoma, M., Grosfeld, K., Filina, I. and Mayer, C. (2009): Modelling flow and accreted ice in subglacial Lake Concordia, Antarctica. *Earth and Planetary Science Letters* 286(1–2): 278–284.

Thoma, M., Grosfeld, K. and Mayer, C. (2007): Modelling mixing and circulation in subglacial Lake Vostok, Antarctica. *Ocean Dynamics* 57(6): 531–540.

Tilzer, M. M. (1990). Large Lakes: Ecological Structure and Function, Springer. Pp. 339–367.

Trolle, D., Jørgensen, T. B. and Jeppesen, E. (2008a): Predicting the effects of reduced external nitrogen loading on the nitrogen dynamics and ecological state of deep Lake Ravn, Denmark, using the DYRESM–CAEDYM model. *Limnologica* 38: 220–232.

Trolle, D., Skovgaard, H. and Jeppesen, E. (2008b): The Water Framework Directive: Setting the phosphorus loading target for a deep lake in Denmark using the 1D lake ecosystem model DYRESM–CAEDYM. *Ecological Modelling* 219(1–2): 138–152.

Trolle, D., Zhu, G., Hamilton, D. P., Luo, L., McBride, C. and Zhang, L. (2009): The influence of sediment nutrient dynamics on the response of lake ecosystems to restoration and climate change. *Hydrobiologia* 627: 31–44.

Vincent, W. F. (1983): Phytoplankton production and winter mixing: Contrasting effects in two oligotrophic lakes. *Journal of Ecology* 71: 1–20.

Vincent, W. F., Gibbs, M. M. and Dryden, S. J. (1984): Accelerated eutrophication in a New Zealand lake: Lake Rotoiti, Central North Island. *New Zealand Journal of Marine and Freshwater Research* 18: 431–440.

Vincent, W. F., Gibbs, M. M. and Spigel, R. H. (1991): Eutrophication processes regulated by a plunging river inflow. *Hydrobiologia* 226: 51–63.

Vincent, W. F., Spigel, R. H., Gibbs, M. M., Payne, G. W., Dryden, S. J., May, L. M., Woods, P., Pickmere, S., Davies, J. and Shakespeare, B. (1986): The impact of Ohau Channel outflow from Lake Rotorua on Lake Rotoiti. Taupo Research Laboratory, Division of Marine and Freshwater Science, DSIR 46.

Viner, A. B. and White, E. (1987). Phytoplankton growth. Inland Waters of New Zealand. A. B. Viner, DSIR Science Information Publishing Centre: Pp. 191–223.

Chapter 4

Modelling the impact of the Ohau Channel diversion wall on water quality of Lake Rotoiti, New Zealand

Abstract

Lake Rotoiti is a large, warm monomictic, eutrophic lake in North Island, New Zealand. Ohau Channel is the major inflow into Lake Rotoiti, arising from eutrophic Lake Rotorua. The construction of a 1275 m diversion wall along the western shoreline of Lake Rotoiti was completed at the end of July 2008. It was designed to improve the water quality of Lake Rotoiti by reducing the intrusion of the inflow into the lake, instead diverting it towards the major outflow, Kaituna River. In this study I investigated how the diversion of the Ohau Channel inflow to Lake Rotoiti affected the thermal structure and water quality of Lake Rotoiti on a spatial–temporal basis. A three dimensional model was used to analyse the water quality of Lake Rotoiti during a one year period commencing upon the completion of the diversion wall. The performance of a 3D water quality model, ELCOM–CAEDYM, was evaluated statistically and showed that temperature, dissolved oxygen and chlorophyll *a* predictions were simulated adequately, but difficulties arose with comparison of nutrient concentrations. This study highlights some of the limitations of highly spatially resolved numerical modelling methods of simulating lake water quality, and demonstrates their strengths and weaknesses in contributing to future lake management decisions.

4.1 Introduction

Urbanisation and human modifications of the landscape have resulted in increases in sediment and nutrient runoff, producing deterioration of water quality in many freshwater lakes around the world (Carpenter et al. 1998). Considerable effort and investment have recently been made to improve water quality using an array of lake restoration methods to either reduce external loads or to artificially manipulate the physical, chemical or biological conditions within a lake (Cooke et al. 2005; Jeppesen et al. 2005). While reductions in catchment nutrient loads may take many years to have effect, in response to changes in land use or management practices, diversion of nutrient–rich inflows has the potential to effect relatively rapid improvements in lake water quality (Moss et al. 1990). Indirectly, this method has a long history of application, as wastewater was commonly diverted from many lakes, as early as 1930s, when the first alteration to divert sewage from Lake Washington was undertaken (Edmondson & Lehman 1981). However many projects were implemented to reduce excessive nutrient loading (Ahlgren 1972; Carvalho et al. 1995), and as recently as the 1990s for some iconic lakes in New Zealand (Burger et al. 2008). However, lake water quality has not always responded as expected and in some cases phosphorus and chlorophyll concentrations have not changed significantly following removal of wastewater point sources (Welch et al. 1986; Burger et al. 2008).

As noted by Moss et al. (1990), not all diversions of inflows have been successful. Perrow at al. (1994) found in Alderfen Broad that an inflow diversion brought about an initial reduction of total phosphorus concentrations and phytoplankton biomass, but this was followed by a period of high internal phosphorus loading which ultimately led to anoxic conditions and fish kills. The diversion of freshwater streams from Mono Lake provides another example of adverse effects related to increased salinity and reductions in the size of this lake (Jellison et al. 1998). Moss et al. (2005) present results for two diverse lakes in the same catchment area in Cheshire, North West England, after diversion of two sewage treatment works in 1991. Over the following period of 12 years, both lakes

showed phosphorus reduction, however neither of the lakes showed significant changes in chlorophyll *a* concentration.

In Lake Rotorua water quality initially improved following diversion of treated wastewater to a land–based polishing system in 1991 (Rutherford et al. 1996), but since the late 1990s there has been a clear trend of increasing nutrient concentrations, higher algal biomass and frequent blooms of cyanobacteria (Burger et al. 2008). Water from Lake Rotorua provides the inflow to Lake Rotoiti and was considered by several authors (Vincent et al. 1986, 1991; Gibbs 1992; Burger et al. 2008) to be the main factor contributing to deterioration of water quality in Lake Rotoiti. In 2007 construction commenced on a steel–sheeting wall supported by piles driven vertically into the sediments of Lake Rotoiti, to divert the existing Ohau Channel inflow to Lake Rotoiti, into a side–arm leading to the lake outflow. The wall was completed in July 2008 at a cost of c. NZ $10M.

Numerical models are used widely to analyse lake water quality impacts following inflow diversions and to consider management decisions for water quality improvement (Jellison & Melack 1993). When plunging inflows are diverted from a waterbody there is potential to change oxygen dynamics by removing the oxygenation effect of the inflow for hypolimnetic waters (Gibbs 1992), potentially increasing rates of deoxygenation, which could be expected to lead to increased rates of nutrient release from the lake bed. While a relatively simple box or one–dimensional modelling approach has been adopted to provide long–term indications of the effect of an inflow diversion, there have been few applications undertaken where either 1) the inflow diversion has actually taken place and model performance has been validated, or 2) the spatial dynamics of the inflow have been examined using a model of higher dimension (i.e., a three dimensional (3D) model).

To attempt to satisfy the demanding requirements to validate 3D model applications, remote sensing has sometimes been used for spatial predictions of temperature or chlorophyll *a* concentration (Hedger et al. 2002; Spillman et al.

2007) while high frequency field measurements (e.g., thermistor chains) have sometimes provided temporal matches similar to model output frequency (León et al. 2005). There are few applications, however, involving combinations of highly resolved spatial and temporal data for model validation purposes, especially in the presence of a major lake management perturbation. Full validation of a model, with a major perturbation equivalent to that provided by the Ohau Channel diversion wall has not been undertaken using the prescription advocated by Jørgensen et al. (2008).

In this study I investigated how diversion of the Ohau Channel inflow to Lake Rotoiti affected the thermal structure and water quality of Lake Rotoiti on a spatial–temporal basis. The model that had previously been calibrated and validated for Lake Rotoiti (Chapter 3) before the construction of the diversion wall was used to simulate changes in the lake thermal structure and water quality based on the morphology of the present diversion wall configuration. I used a fixed parameter approach, without further calibration of model parameters from those used in Chapter 3. A model based on fixed parameters without calibration, based on literature values has previously been simulated successfully by Gal et al. (2009), when ELCOM–CAEDYM was used to simulate 5 phytoplankton groups in Lake Kinneret, but this approach did not address changes of water quality after an inflow diversion.

The main objective of my study was to document the effect of the inflow diversion using comparisons of in situ data against model simulation output, and to use the model simulations to understand how the diversion wall affected the transport of water from the Ohau Channel into the lake. A further objective was to test the performance of the 3D water quality model using parameters calibrated on the basis of data for a year prior to the diversion wall construction. This study demonstrates how 3D models can be used to simulate highly resolved spatial–temporal distributions of water quality variables, and how their application can then be used to determine human induced perturbations to lake ecosystems.

4.2 Study Site

Lake Rotoiti (main basin located at 38º 02’ 39.5 S, 176º 25’ 30.0 E) is a deep (max. depth 124 m), warm monomictic, meso–eutrophic lake in North Island, New Zealand. It has a surface area of 34.6 km^2. The lake is relatively long and narrow but with two distinct basins; a deep eastern basin and a shallow western basin, separated by a narrow constriction (Figure 4.1) The diversion wall completed in August 2008 is connected to the shoreline immediately south of the Ohau Channel inflow and has a length of 1275 m, running north into the Okere Arm and towards the Kaituna outflow, roughly parallel to the shore (Figure 4.1 and Figure 4.2), diverting water from eutrophic Lake Rotorua (Burger et al. 2007) directly towards the outflow.

The Ohau Channel inflow was previously found to intrude into Lake Rotoiti as an underflow, interflow or overflow, dependent on the temperature of the Ohau Channel outflow from Lake Rotorua relative to the thermal structure of Lake Rotoiti (Vincent et al. 1986 and Chapter 3). Inflows from Lake Rotorua into the main basin of Lake Rotoiti are greatest in winter when the water intrudes into the lake as an underflow and follows the deepest lake contour into the main lake basin. At other times of the year when interflows or overflows occur, the inflow is more likely to be short–circuited into a proximal sidearm where the Kaituna River outflow is located. While the inflow is recognised as a major cause of deterioration in water quality of Lake Rotoiti (Vincent et al. 1984, 1986, 1991; Gibbs 1992), it may have also had beneficial effects by oxygenating bottom water when it intrudes into the stratified lake as an underflow (Gibbs 1992).

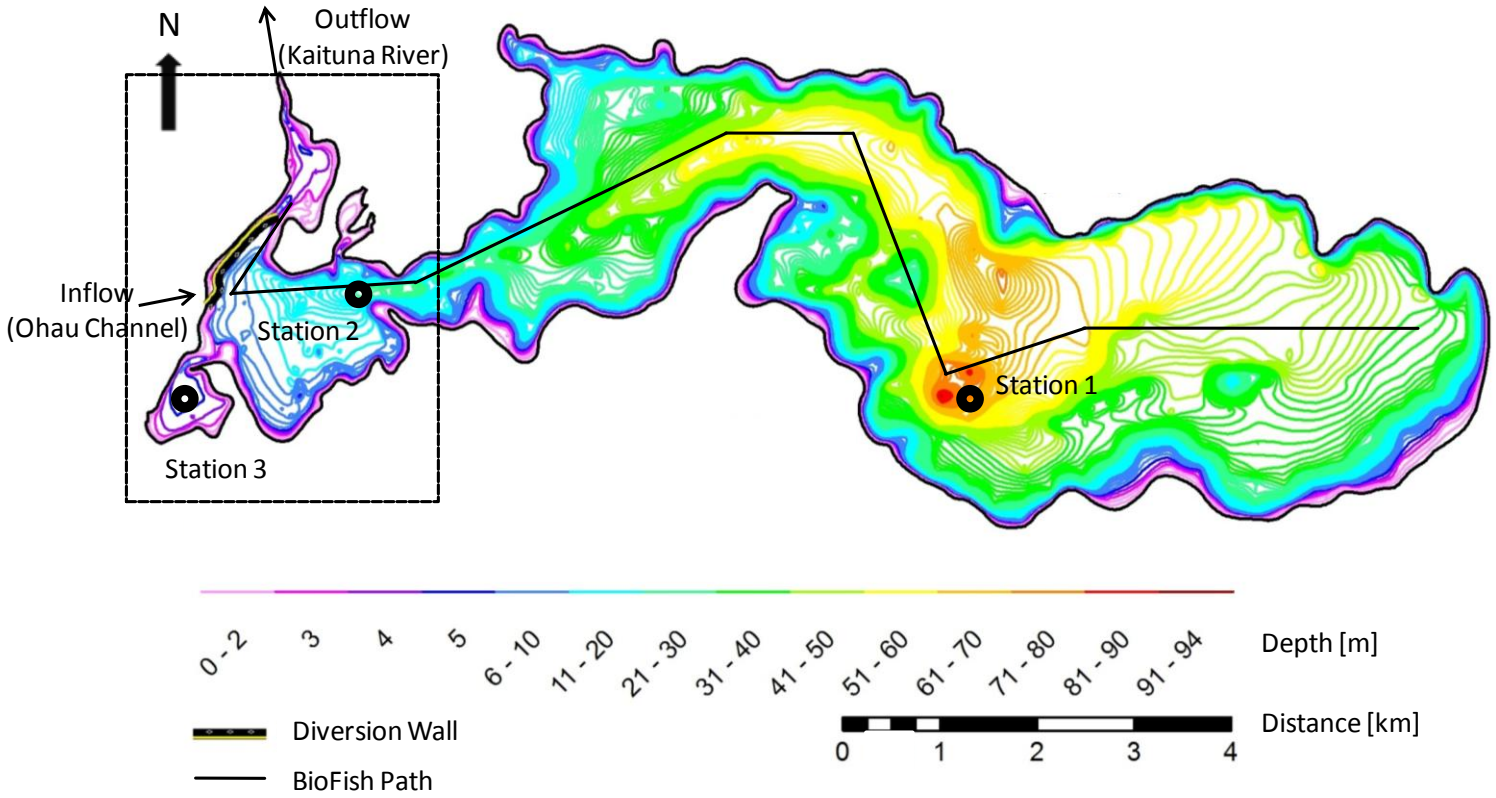

Figure 4.1: Bathymetric map of Lake Rotoiti. Monthly Biofish transect (black line) for sampling August 2008 – July 2009. The area within the dashed line is shown in greater detail in Figure 4.2.

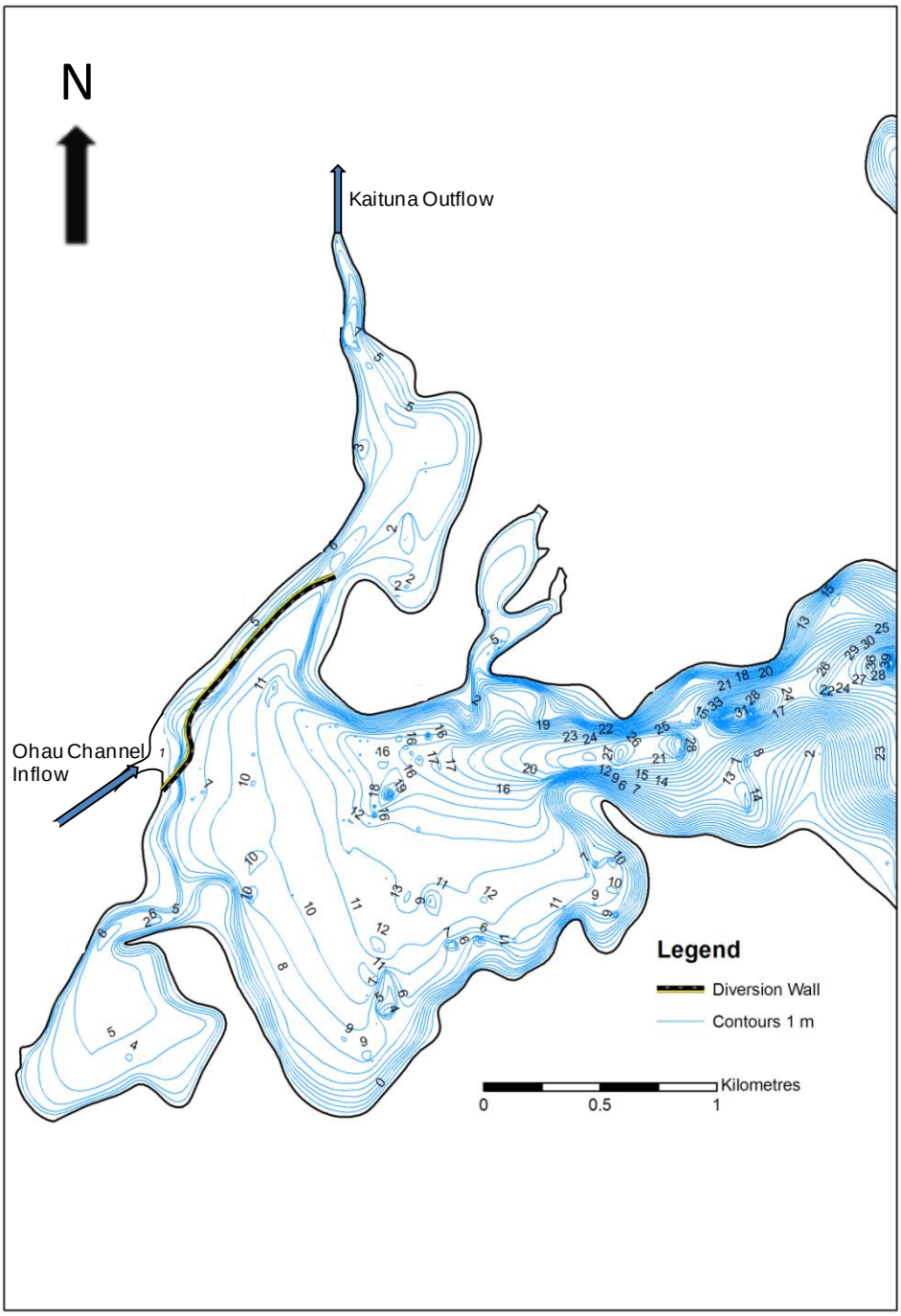

Figure 4.2: Bathymetric map of the western basin of Lake Rotoiti. Ohau Channel diversion wall is represented by the bold black line.

4.3 Materials and methods

The Estuary, Lake and Coastal Ocean Computer Model (ELCOM) is a three–dimensional (3D) hydrodynamic model that simulates water temperature and salinity spatially and temporally (Hodges et al. 2000; Hodges & Dallimore 2007); driven by external forcings of wind stress, surface heating/cooling and inflows/outflows. ELCOM has been coupled to the Computational Aquatic Ecosystem Dynamic Model (CAEDYM), to simulate interactions between hydrodynamics generated by ELCOM and biological, physical and chemical processes generated by CAEDYM (Hipsey et al. 2007). The ELCOM model is based on the unsteady Reynolds–averaged, Boussinesq, scalar transport and Navier–Stokes equation for incompressible flow using the hydrostatic assumption for pressure (Hodges et al. 2000). An Euler–Lagrange method is used to simulate advection of momentum (Casulli & Cheng 1992) with a conjugate–gradient solution used for the free–surface height. CAEDYM consists of process based differential equations that simulate concentrations of biogeochemical variables dynamically. The general categories of these biogeochemical variables of relevance to this study include phytoplankton, particulate and dissolved organic matter and dissolved inorganic nutrients. Conservative tracers were used in this study to track the fate, firstly, of water entering Lake Rotoiti via the Ohau Channel inflow, described as leakage of the diversion wall, and secondly, the exchange of water from Okawa Bay with the western basin and the main lake. Ohau Channel tracer was introduced with a nominal daily constant concentration of 1 and Okawa Bay water was labelled with a second tracer of value 1 at the beginning of the simulation. The tracers are not subject to any of the decay or generation processes of the other biogeochemical variables within ELCOM–CAEDYM.

The ELCOM–CAEDYM model bathymetry for Lake Rotoiti was configured to have a constant 3 m vertical resolution and horizontal dimensions of 200 m x 200 m in the same configuration as used in the bathymetry for Chapter 3. The inflow boundary conditions for the model consisted of one major inflow (Ohau Channel) that enters Lake Rotoiti in the western basin, twelve smaller inflows at different locations around the lake and two additional underwater geothermal springs which

intrude into the deepest part of the lake, and one main outflow located at the northern end of the western basin, as described in Chapter 3. The geothermal inflows located in the main basin of the lake remained unchanged to the model set–up for the period of May 2004 to May 2005 (Chapter 3). A constant geothermal energy of 165 MW was used in the bottom of the main basin to simulate the geothermal heat source originating in the main basin where lake depths exceed 70 m (Calhaem 1973). Two areas of geothermal inflow were specified near Station 1, one of which was with a constant temperature of 120 ºC at a flow rate of 0.25 $m^3 s^{-1}$ for a region located around the deepest part of the lake (the crater) and a second one which was assigned a temperature of 35 ºC at a discharge rate of 0.58 $m^3 s^{-1}$ for an area north–east of the crater. The areas of geothermal heat sources conform to their locations according to Calhaem (1973).

Some changes were made to the model configuration used in Chapter 3. The first was the implementation of a levee in the model bathymetric input file, which was used for the simulations that included the Ohau Channel diversion wall (Figure 4.2). The levee placed a solid boundary between two adjacent ELCOM cells using a ghost cell so that adjacent wet cells had no interconnection. Initial conditions for starting the simulation with defined concentrations of dissolved nutrient concentrations, dissolved oxygen, temperature and chlorophyll *a* were based on field measurements at three stations on 19 August 2008. The model was run for 350 days.

Ohau Channel inflow input data to the model was based on monthly field measurements taken over the 350 days of the simulation. Monthly inorganic and total nutrient concentrations and phytoplankton biomass (separated in the simulation into the dominant groups of diatoms and cyanobacteria) were interpolated to daily values for model forcing. The Ohau Channel had an average discharge of 16.94 $m^3 s^{-1}$ over the simulation period, and was entered as input to the model as daily average values based on continuous measurements. The smaller inflows, which are mostly spring–fed, were kept constant over the simulation period based on the data retrieved for the simulation period May 2004–May 2005 (see Chapter 3). Meteorological forcing included daily averages of air temperature, solar radiation, atmospheric pressure, relative humidity, wind speed,

cloud cover, to estimate long wave radiation (Hodges & Dallimore 2007) and daily rainfall. Meteorological data for input to the model were from measurements at Rotorua airport meteorological station, 7 km from Lake Rotoiti. These data were obtained from the CLIFLO database (National Institute of Water and Atmospheric Research 2008).

No further calibration of the model was undertaken from the calibrated version for the period May 2004 – May 2005, which is described in Chapter 3.

Between August 2008 and June 2009 monthly depth–undulating transects were taken periodically with a Biofish (ADM–Elektronik, Germany). Measurements were made with the Biofish of temperature (ADM–Elektronik, Germany), dissolved oxygen (AMT Analysenmeβtechnik GmbH) and chlorophyll fluorescence (Dr. Haardt Optik Mikroelektronik miniBackScat I) at 4 Hz frequency, together with a Global Positioning System reference and water depth (Garmin GPSMAP 168 Sounding). An average of 2650 data points was measured each month following the 18 km long path shown in Figure 4.1. Stored Biofish data were processed with Matlab software, filtered to every second measurement and projected onto model output of the Biofish depth–length transect.

For statistical analysis the Biofish readings of temperature, dissolved oxygen, and chlorophyll fluorescence were averaged for measurements collected within a region corresponding to each cell of the model domain. Chlorophyll fluorescence was calibrated to chlorophyll *a* concentration and chlorophyll *a*, temperature and dissolved oxygen were compared to model output of the corresponding variable using Root–Mean–Square–Error (RMSE) and Pearson correlation coefficient (R) values.

Concentrations of ammonium (NH_4–N), nitrate (NO_3–N), soluble reactive phosphorus (SRP), total nitrogen (TN) and total phosphorus (TP) from surface waters for all three stations were obtained from a monthly sampling program conducted by the regional monitoring authority, Environment Bay of Plenty. Nutrient concentrations were compared to the model output at the corresponding

location and time of measurement, and RMSE and Pearson correlation coefficients values were calculated for the comparison.

The tracer simulations were analysed by plotting a monthly fractional change in Ohau Channel tracer concentration at the three stations after allowing a 14–day 'spin–up' period. This period was found to be 10 days following the intrusion time of the Ohau Channel tracer into the main basin at Station 1 (Chapter 3) before the inflow diversion. Monthly changes in Okawa Bay tracer concentration at Station 1 and 2 was calculated for the current model as well as the pre–diversion wall scenario (May 2004– May 2005) (Chapter 3) for direct comparison.

4.4 Results

4.4.1 Water temperature simulations

There was a high correspondence between the simulated temperature and the temperature from field measurements averaged for the corresponding model cells for the period August 2008 to June 2009. The model simulation captured the seasonal interplay of mixing and stratification (Figure 4.3), and comparison with measurements yielded R = 0.982 and RMSE = 0.894 ºC (Table 4.1). Temperature tended to be slightly over–predicted throughout the water column during the latter phase of stratification (January to April 2009) and at the same time horizontal temperature gradients occurred, mostly in the first 1–2 km of the transect away from the diversion wall (Figure 4.1). In the western basin, where Station 2 was located, there was little variation in temperature in both the model simulations as well as the Biofish measurements. The errors of the present model simulation are similar to the calibrated model for the one–year simulation period commencing May 2004 (R = 0.984, RMSE = 0.895; see Chapter 3).

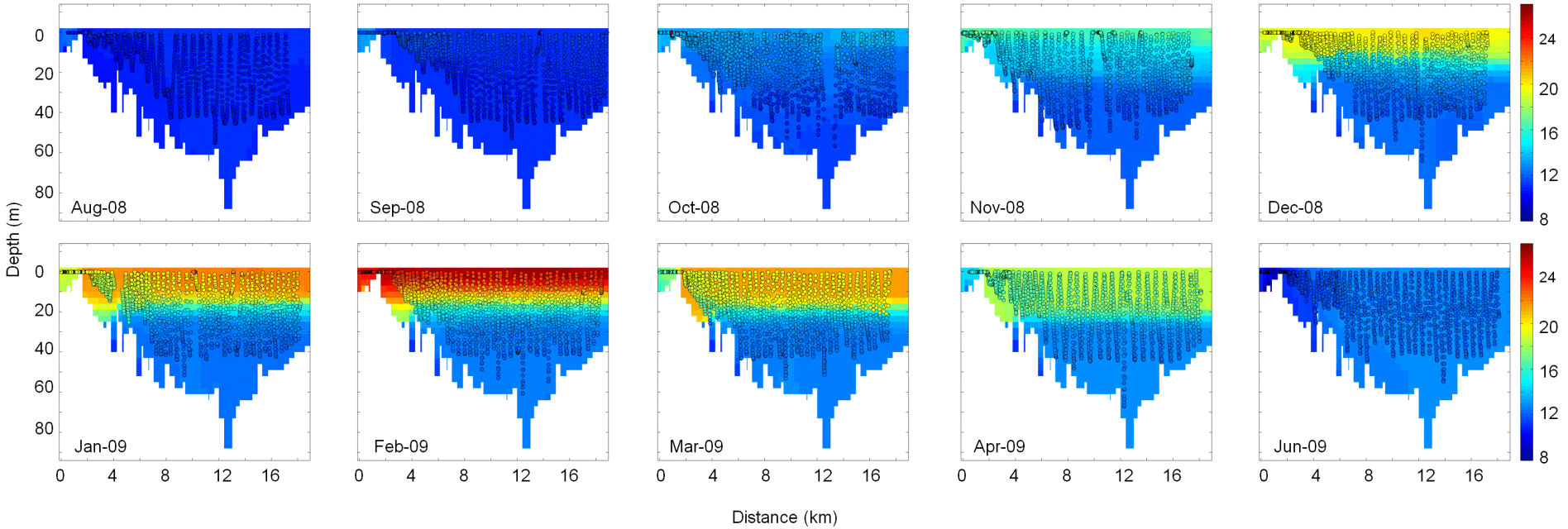

Figure 4.3: Comparison of simulated water temperature (coloured background, ºC) and measurements (○) taken at monthly intervals fr om August 2008 to June 2009.

Table 4.1: Values of Root–Mean–Square–Error (RMSE) and Pearson correlation coefficient (R) for comparison of model simulation values against corresponding Biofish measurements averaged for each model grid cell of the transect over a one year simulation period commencing 19 August 2008 compared with the model simulations of temperature (n=8527), dissolved oxygen (n=6986) and total chlorophyll *a* (n=8527).

	RMSE	*R*
Temperature (°C)	0.894	0.982
DO (mg L^{-1})	1.655	0.760
Chlorophyll *a* (µg L^{-1})	3.886	0.456

4.4.2 Dissolved oxygen simulations

Dissolved oxygen concentrations in Lake Rotoiti were slightly over–predicted over the annual cycle, most notably during the period of stratification. Figure 4.4 shows the relationship between the average dissolved oxygen field data from the Biofish transect for each model cell and the corresponding model output. The Pearson correlation coefficient for the comparison is 0.760 and the RMSE value is 1.655 mg L^{-1} (Table 4.1).

Oxygen depletion from bottom waters commenced with the onset of thermal stratification around September 2008 (Figure 4.4) but the decline in oxygen tended to be slightly slower in the simulations. For example, in December 2008 the measured oxygen concentration in the hypolimnion was around 1.5 mg L^{-1} lower than the simulated concentration, but in February 2009 measured and modelled levels of oxygen in the hypolimnion were well aligned. During June 2009 when the water column was well mixed, both the model simulation and the measured data showed horizontal gradients, with values around 7 mg L^{-1} in the main basin gradually increasing to 9 mg L^{-1} in the shallower western basin.

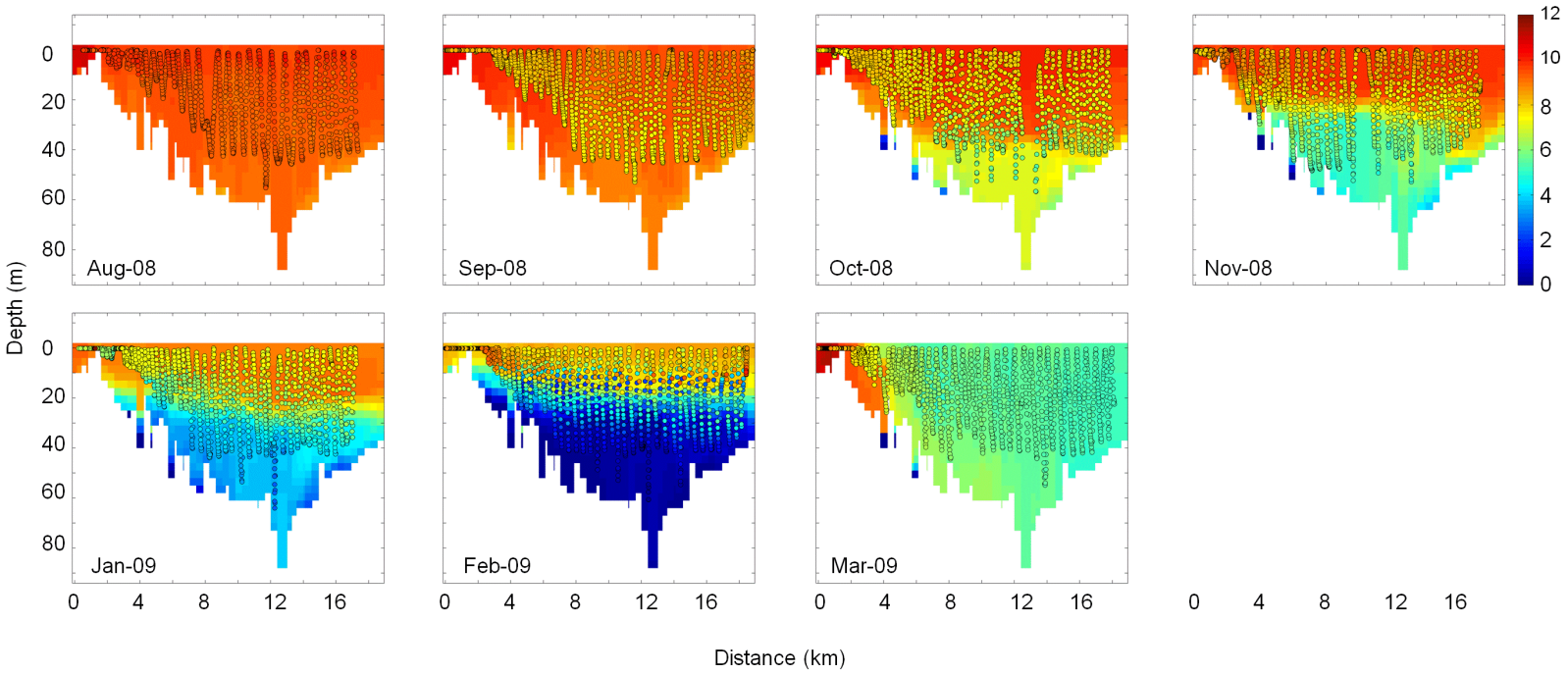

Figure 4.4: Comparison of simulated dissolved oxygen (coloured background, mg L^{-1}) and measurements (○) taken at monthly intervals from August 2008 to June 2009.

4.4.3 Chlorophyll *a* simulations

Compared with the field measurements and model results from 2004–2005, measured and modelled chlorophyll *a* values were generally lower in the post–wall period from August 2008 to June 2009. Chlorophyll *a* concentrations were overestimated in the model simulations in the months of August and September 2008. Following this period, from October 2008 to December 2008, field data were predicted well by the model, which captured the trend of higher values in the western basin with a gradual decline towards the main basin (Figure 4.5). In October and November 2008 elevated chlorophyll concentrations occurred, around 30 m and 20 m depth respectively, in the western end of the main basin. Surface concentrations of chlorophyll *a* were slightly over–predicted during this time, however this was restricted mostly to the western basin.

In February 2009 there was little horizontal variation in measured chlorophyll but there was elevated chlorophyll at 15 m depth in contrast to the model simulations which indicated a surface bloom (cyanobacterial chlorophyll concentrations up to 14 μg L^{-1}) in the top 5 m. In the western basin in March 2009 there was an increase in measured chlorophyll concentrations, with values up to 13 μg L^{-1} which exceeded corresponding chlorophyll values in the simulated data (Figure 4.5).

When the model predicted an increased contribution of diatoms to chlorophyll in April to June 2009 the modelled chlorophyll concentration was mainly increased in the western basin. Values up to 16 μg L^{-1} gradually declining towards the main basin to 10 μg L^{-1} in the most western part of the main basin and 6 μg L^{-1} in the main basin were predicted, contrary to field measurements that remained around 10 μg L^{-1}. Despite the underestimation of chlorophyll *a* concentration in the western basin during March 2009, the model generally showed a trend in over–estimate chlorophyll *a* concentrations in this area. Over the whole simulation period, the Pearson correlation coefficient value was 0.456 and the RMSE was 3.89 μg L^{-1} for the comparison of model simulations with measurements (Table 1).

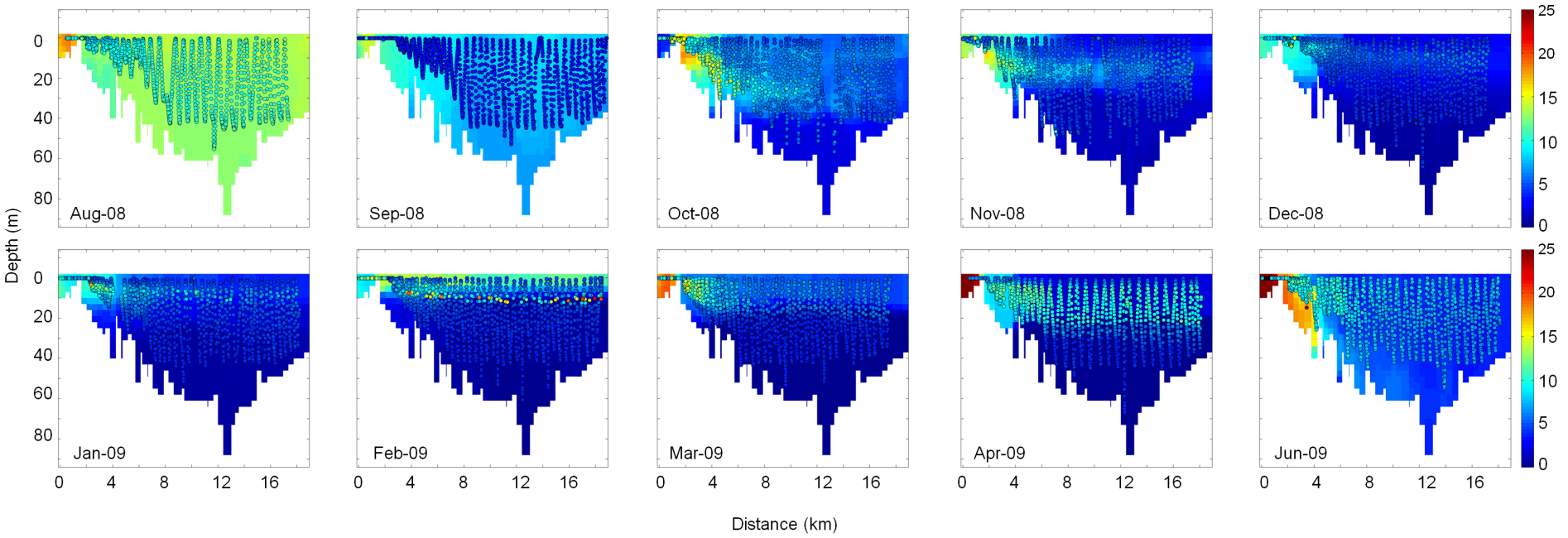

Figure 4.5: Comparison of simulated chlorophyll *a* (coloured background, µg L^{-1}) and measurements (○) taken at monthly intervals from August 2008 to June 2009.

The fit of the simulation to measured chlorophyll *a* concentrations is within the range of other modelling studies which have used DYRESM–CAEDYM, with Pearson correlation coefficient (R) and RMSE values for chlorophyll *a* of 0.29 and 13.1 µg L^{-1} (Burger et al. 2008) and 0.35 and 10.40 µg L^{-1} (Trolle et al. 2008a). An application of ELCOM–CAEDYM involving simulation of five phytoplankton groups in Lake Kinneret yielded R^2 values between 0.03 and 0.5 for different phytoplankton groups while a Spearman correlation analysis of this simulation resulted in values between 0.21 and 0.82 for the different phytoplankton groups (Gal et al. 2009). Further modelling study with DYRESM–CAEDYM applied to Lake Kinneret by Bruce et al. (2006), showed that the normalized mean absolute error for the phytoplankton groups simulated fall close to the normalized mean standard deviation of the field data indicating a good model fit.

4.4.4 Nutrient simulations

The general trend of modelled surface nutrient concentrations at Stations 1 and 2 was for low values over spring and summer stratification but with increasing concentrations at the end of stratification when the surface mixed layer started to deepen (Figure 4.6). This general trend was not apparent at shallow Station 3. Contrary to the other two stations, at Station 3 simulated nutrient concentrations started to increase in the middle of summer (January 2008) towards a maximum in late March 2008 followed by a decrease over the subsequent two months. The only exception to this trend was the phosphate concentration, which remained low throughout the modelled period at Station 3, with a maximum concentration of 0.03 mg L^{-1} in June 2009. Compared with measured data, there was up to a 6–fold increase in the simulated nutrient concentrations of PO_4–P and NH_4–N at Station 1 in May and June 2009 and a marked increase of simulated NO_3–N to up to 0.29 mg L^{-1}, while field measurements remained below 0.005 mg L^{-1} in the month of May and June 2009. The same trend occurred at Station 2 even though the fractional increase was slightly lower than that simulated for Station 1.

Table 4.2: Root–mean–square–error (RMSE) and Pearson correlation coefficient (R) values for Stations 1, 2 and 3 for total phosphorus (TP), phosphate (PO_4–P), total nitrogen (TN), ammonium (NH_4–N) and nitrate (NO_3–N).

	RMSE			*R*		
	Station 1	Station 2	Station 3	Station 1	Station 2	Station 3
TP (mg L^{-1})	0.026	0.023	0.026	0.497	0.208	0.436
PO_4 (mg L^{-1})	0.024	0.020	0.007	0.778	0.805	-0.171
TN (mg L^{-1})	0.162	0.166	0.398	-0.194	-0.205	0.287
NH_4 (mg L^{-1})	0.023	0.023	0.047	0.891	0.748	-0.244
NO_3 (mg L^{-1})	0.123	0.140	0.312	0.251	0.345	-0.153

Pearson correlation coefficients for nutrient species varied between –0.205 (Station 2, TN) and 0.891 (Station 1, NH_4–N) at Stations 1 and 2 (Table 4.2) but were not a lot different from values derived from DYRESM–CAEDYM applications by Burger et al. (2008), who reported Pearson correlation values between –0.01 (NH_4–N) and 0.41 (TN) and RMSE between 0.007 mg L^{-1} (PO_4–P) and 0.232 mg L^{-1} (TN) and the summary data for a large number of studies, that is presented by Arhonditsis and Brett (2004). A comparison of the latter summary data against my simulation results puts the results for NH_4–N at Station 1 and 2 in the upper 20% and for PO_4–P in the upper 40%. Values of RMSE are generally highest at Station 3 with the exception of PO_4–P (Table 4.2). It was expected that there would be low correlations at Station 3 as the calibration in Chapter 3 had already been shown to have some deficiencies for the period May 2004 to May 2005. In summary, values of the Pearson correlation coefficient at Stations 1 were as high as 0.891 (Station 1, NH_4–N) but even yielded negative values (–0.194, Station 1) in the case of TN and were between 0.805 (PO_4–P) and –0.205 (TN) at Station 2, while Station 3 generally showed low or negative correlation coefficient values between simulated and measured surface concentrations of all nutrient species.

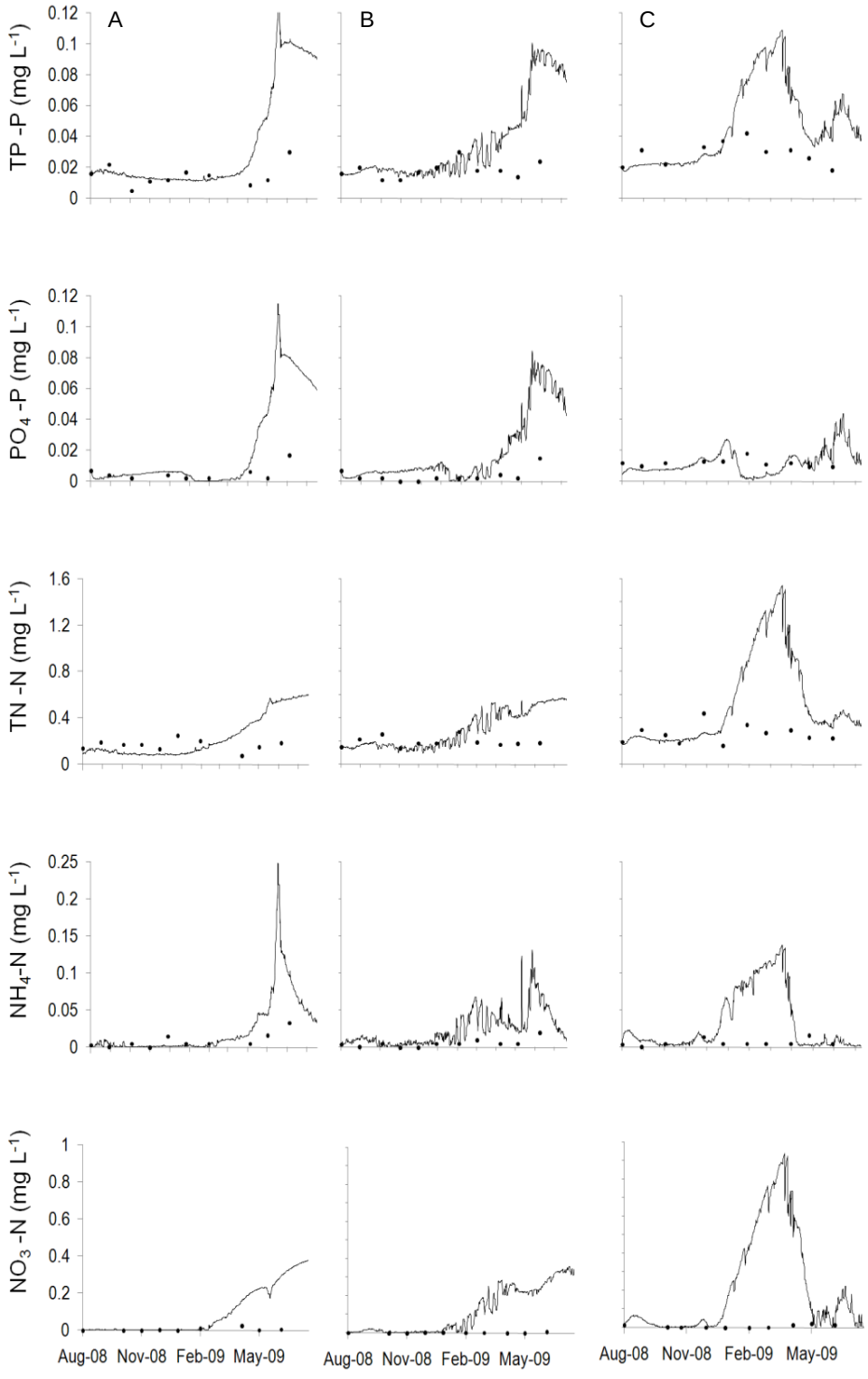

Figure 4.6: Simulated (line) and observed (○) values for total nutrients TP and TN and dissolved inorganic nutrients PO_4–P, NH_4–N and NO_3–N at (A) Station 1, (B) Station 2 and (C) Station 3 at the surface over the simulated period of August 2008 until August 2009.

4.4.5 Ohau Channel and Okawa Bay tracer

The monthly change in Ohau Channel tracer concentration at 0, 21, 42 and 60 m for Station 1, at 0, 9 18 and 24 m for Station 2 and at 0 and 3 m for Station 3 (Figure 4.7), showed a marked decrease compared with the simulations from June 2004 to May 2005 (Chapter 3).

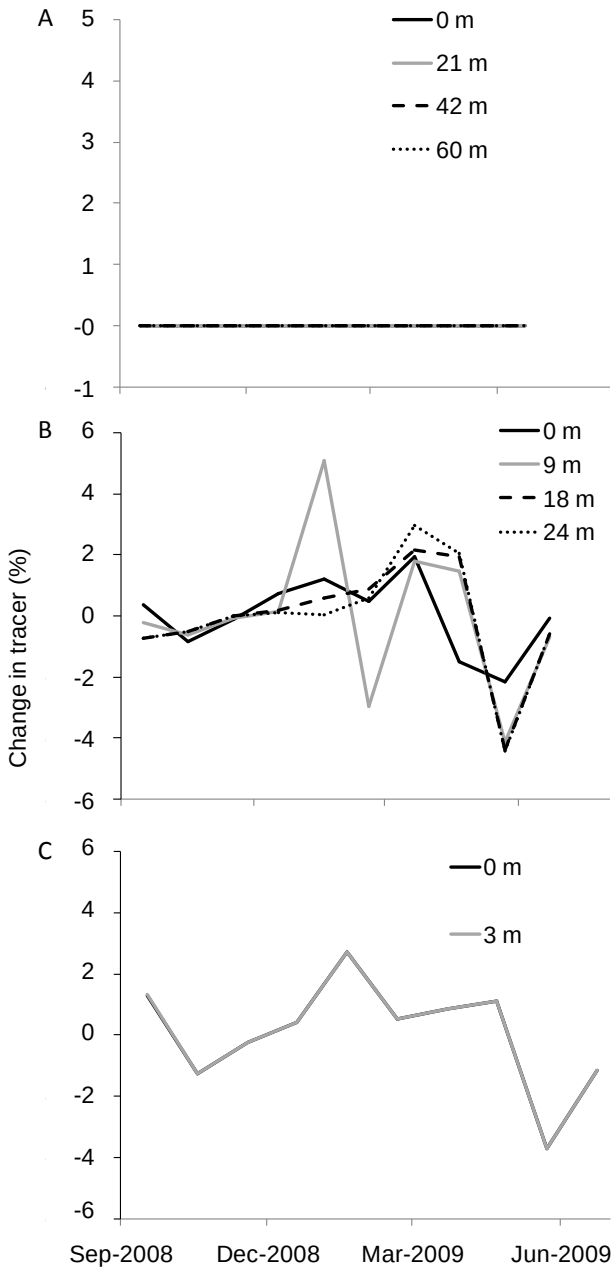

Figure 4.7: Rate of change of tracer concentration as % per month relative to the assigned tracer concentration (100%) in the Ohau Channel at (A) Station 1, (B) Station 2 and (C) Station 3.

The Ohau Channel tracer was at no time predicted to penetrate into the main basin (Station 1, Figure 4.7A) indicating reduced inflow of Ohau Channel water compared with the pre–diversion simulation in Chapter 3, when the maximum change in Ohau Channel tracer was 4% (Figure 4.8A and Chapter 3). In the western basin (Station 2) the monthly change in tracer concentration was between 4 and 5% after the inflow diversion. The four displayed depths for this station show a similar general trend of slightly increased rates of tracer input from August 2008 to March 2009, after which time there is a decrease and a switch to –4% in the month of June 2009 at all simulated depths. This switch to negative tracer concentration coincided with the end of the stratification period. The only significant vertical difference in the general trend at Station 2 was at 9 m depth where the tracer increased by 5% in January 2009 compared with the previous month. In Okawa Bay (Station 3) the value changed between –3 and 4% (Figure 4.7C) at both depths, indicating a reduced input of Ohau Channel into Okawa Bay compared with the pre–diversion case values that were between –10 and 20% (Chapter 3, Figure 3.12). In Okawa Bay tracer concentrations tended to be slightly positive during the earlier period of the simulation followed by a sudden decrease to the minimum value of –4% by June 2009.

The tracer of Okawa Bay water, which was based on water in the bay assigned a value of 100% at the beginning of the simulation, showed a monthly change of only between 0 to 1 % pre– and post–diversion wall in the main basin (Figure 4.8A). The maximum monthly change in the Okawa Bay tracer in the main basin of 1.5% for 42 and 60 m depth (Figure 4.9A) coincided with the end of the stratification period for the post–diversion wall case, while prior to the inflow diversion maximum change of Okawa Bay tracer in the main basin (Station 1) was simulated during summer. Before the inflow diversion the maximum rate of change of Okawa Bay tracer in the western basin (Station 2) was simulated to occur during summer, while there was a sudden switch to a negative value at Station 2 at the end of the stratification period (June 2009) (Figure 4.8B), similar to Ohau Channel tracer during this time at the same location. The Okawa Bay tracer dispersion was predicted to be more variable in the western basin throughout the year compared with the main basin. A comparison of pre– and

post–diversion cases in the western basin revealed a change in Okawa Bay tracer concentration from –5 to 5% pre–diversion and–3 to 7% post–diversion.

Consideration was made of whether the rate of exchange between Okawa Bay and the western basin may have been affected by wind direction and wind speed. The daily mean wind speed at Rotorua Airport, which was used as forcing input for the model, tended to be higher from August 2008 to August 2009 compared with May 2004 to May 2005 (Figure 4.9). In 2008–2009 (Figure 4.9B) the dominant daily wind direction was west to south–west, while in 2004–2005 it had a strong southerly component but with a fairly even spread of westerly and easterly components. Wind forcing in 2008–2009 is mostly aligned with the direction of the pathway from Okawa Bay to the western basin (Figure 4.9C).

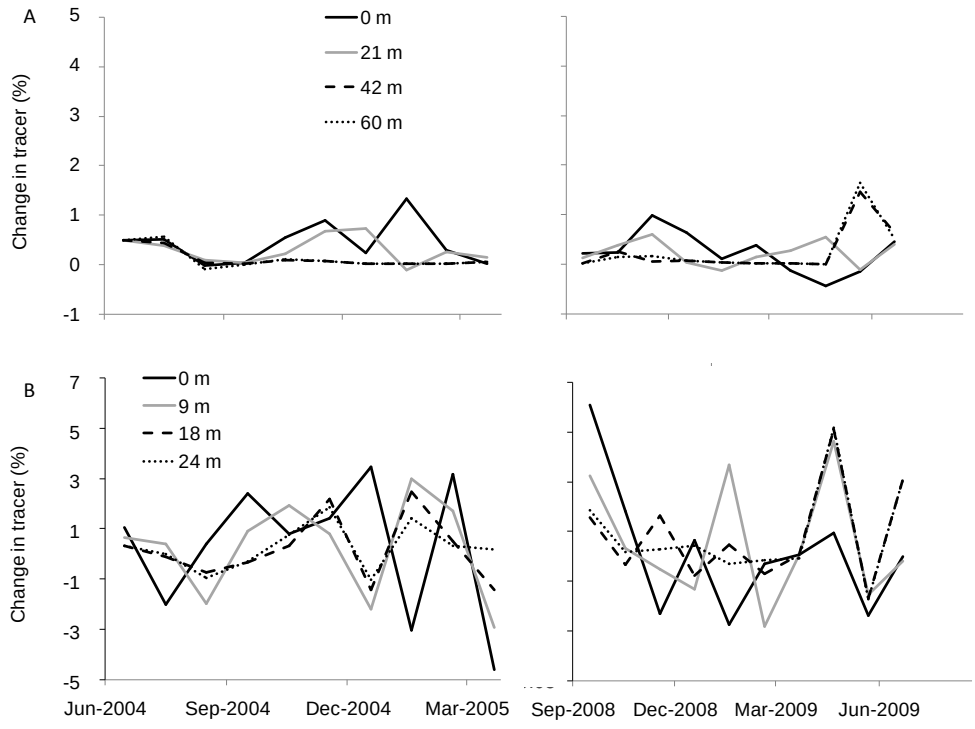

Figure 4.8: Rate of change of Okawa Bay tracer concentration as % per month relative to the assigned tracer concentration (100%) in the Okawa Bay at (A) Station 1 and (B) Station 2 pre– (left) and post–diversion wall (right).

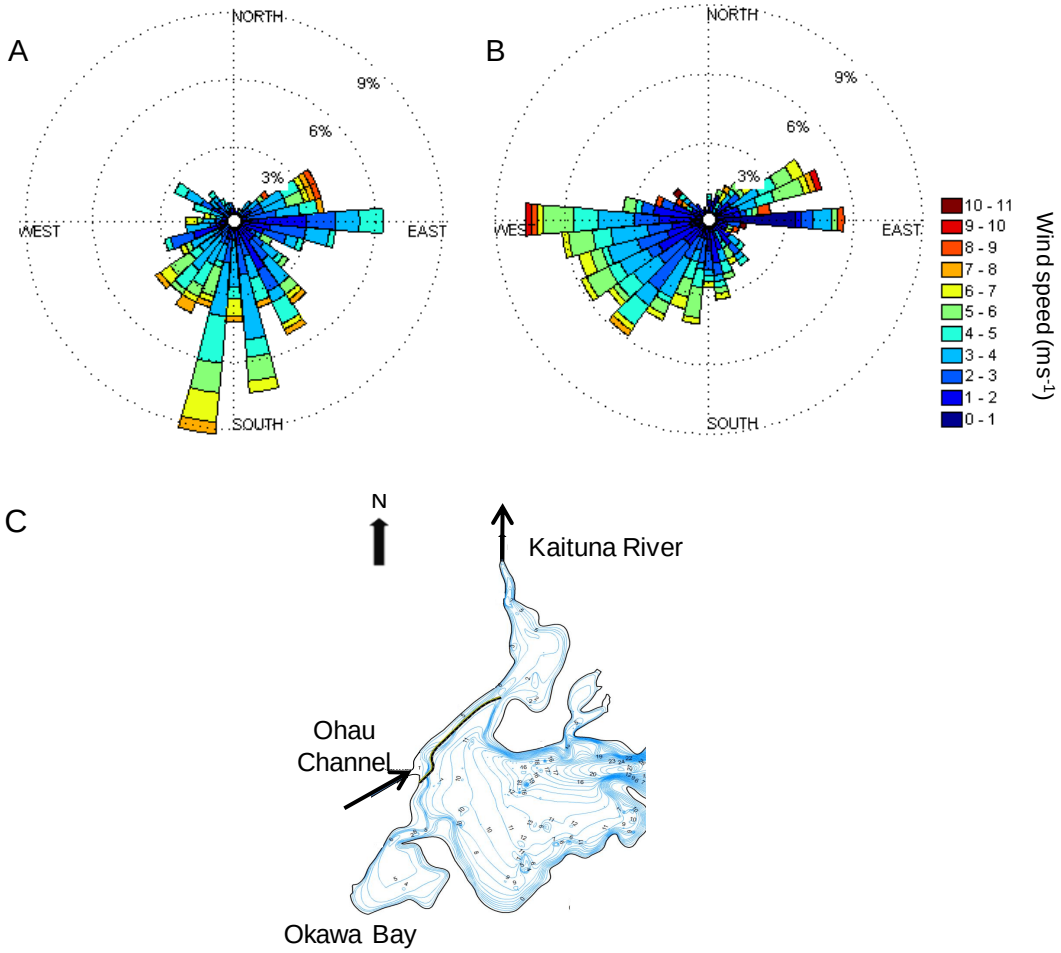

Figure 4.9: Wind rose of speed and direction for the period of the model simulations from (A) May 2004 to May 2005 and (B) August 2008 to August 2009; (C) western basin of Lake Rotoiti and Okawa Bay.

4.5 Discussion

4.5.1 Water quality in Lake Rotoiti after the inflow diversion

The work presented in this chapter indicates that the diversion of Ohau Channel inflow appears to have had a beneficial effect in reducing chlorophyll a concentrations in Lake Rotoiti. Field measurements showed a chlorophyll maximum at a depth of approximately 15 m in February 2009. Deep chlorophyll maxima are generally an indication of high water clarity that allows the chlorophyll layer to persist below the surface mixed layer in large lakes (Pérez et al. 2002; Hamilton et al. 2010). Deep chlorophyll maxima have been commonly

observed in three oligotrophic lakes (Taupo, Tarawera and Rotoma), but the relatively high light attenuation in Lake Rotoiti, driven by high levels of chlorophyll in surface waters, was considered to prevent the formation of a deep chlorophyll maximum in this lake (Hamilton et al. 2010) before the implementation of the diversion wall.

Even though field data and model results indicated a rapid, beneficial effect of the diversion wall, it is not certain how the lake will change as it adjusts towards a new equilibrium state in response to the wall. Inflow diversions may cause immediate reductions in external loading, but lake trophic state response can be widely different. Jeppesen et al. (2005) tracked the effect of nutrient load reductions in 35 lakes and found that a new equilibrium for TP was generally reached after 10–15 years and that this response time was only marginally influenced by the hydraulic residence time. The time on which an ecosystem responds until the new steady state equilibrium is reached, even in small lakes with a high flushing rate, can take several years. For example despite a residence time of a few weeks, the net retention of TP was still negative 13 years after reduced sewage loading to shallow hypertrophic Lake Søbygård, while TN decreased proportionately with the loading reduction (Jeppesen et al. 1998). The high and persistently negative P retention was attributed to a high P pool in the sediment, amounting to 240 g P m–2 in the upper 23 cm of sediment. The complexity of response times, with apparent lag and 'memory' effects in response to nutrient load reductions, brings into question whether even the most complex mechanistic model descriptions of lake ecosystems are capable of reproducing these dynamics.

The assessment of the success of the inflow diversion is difficult to determine after only one year of data for Lake Rotoiti. The proposed long recovery period of lake ecosystems (Jeppesen et al. 2005) and the diversity of long–term responses to changes in inflow composition make it difficult to undertake a direct comparison. For example, even though the phosphorus load to Lake Sammamish was reduced by one–third after a sewage diversion, chlorophyll a and phosphorous concentrations did not change significantly over several subsequent years (Welch

et al. 1986). A management plan to short circuit inflows through Lake Delavan to reduce phosphorus loads resulted in only minor reductions compared with an alum treatment of the lake (Robertson et al. 2000). Efforts to dilute inflowing water and diverting sewage effluent from Lake Moses were reported to have successfully decreased in–lake phosphorus and chlorophyll a concentrations by over 70% when the lake approached a steady state condition 2–4 years later (Welch et al. 1992). In Lake Rotorua, despite sewage diversion from the lake in 1991, trophic status has changed little (Burger et al. 2008).

4.5.2 Change in tracer post diversion

The results of the tracer implementation indicate that the influence of Ohau Channel inflow on the three selected stations has been greatly reduced. There was very little change in the exchange of Okawa Bay water with the western basin of the lake between the pre– and post–diversion cases. Temperature differences between shallow constricted bays can generate significant water exchange due to density interflows (MacIntyre et al. 2002) but there was little variation in water temperature for the two cases. The predominant wind direction of west to south–west winds is most likely to promote transport of surface water from Okawa Bay into the western basin. This exchange is further supported when surface stratification promotes horizontal dispersion due to less friction and the inhibition of vertical mixing (Rueda et al. 2008). During the modelling period 2008–2009 the wind directions were clearly aligned to promote water exchange between Okawa Bay and the western basin, while the results of the tracer indicated a similar exchange to the simulation period 2004–2005. This indicates that the exchange rate between these areas possibly decreased post–inflow diversion, but the magnitude of this change can only be determined by applying the same weather forcing conditions to both scenarios. It may be useful to determine the change in water exchange following an inflow diversion as bays could potentially act as a generator for algal biomass (Chapter 2) and in long term predictions; this may counteract the improvement achieved by the inflow diversion.

4.5.3 Model comparison and performance

Comparisons of the performance of ecosystem models in an objective and a quantitative way is often not straightforward. Differences in model complexity, simulation run time and spatial dimensions make direct comparisons amongst models difficult, and the user defined output variables often differ between models. Even though a complex model may provide for higher degrees of freedom in the selection of parameters, it does not necessarily predict the field data with greater accuracy and it may even be characterized by very low predictive ability (Friedrichs at al. 2006). Three–dimensional modelling studies are rare for large lakes with complex morphometry where there are complementary field data that allow for comprehensive horizontal and vertical testing of model simulation output against measured data. In my study there were significant variations in model performance between stations in different lake basins where there were wide variations in water depth. Rarely have there been horizontally resolved data to allow for this type of model performance testing.

No model simulations have been undertaken to allow more detailed testing of the time scales and scenarios associated with pre– and post inflow diversions in lakes. Arhonditsis and Brett (2005) simulated eutrophication in Lake Washington after a sewage diversion in 1963. They tested the performance of a simple 2–compartment vertical model calibrated for the period of 1995–2006 in simulating scenarios with the pre–diversion nutrient loadings. They report accurate predictions of phytoplankton community response, even though the model consistently under–estimated nitrate and over–estimated summer ammonium levels. The predictive capability of the model in terms of the inflow diversion was not tested. The long run time of the model for Lake Rotoiti and the complex morphometry of this lake, with two distinct basins and a large shallow embayment as well as geothermal inflows, contribute to a level of modelling complexity that has rarely been applied in 3D modelling approaches. The simulation of a very large inflow diversion within this complex domain has not previously been undertaken. In Lake Rotoiti, the measured data and the model simulations indicate an initial response after one year, of reduced trophic status following inflow

diversion, but there is a need for stable 3D models with reasonable run time to determine long term changes on which the final outcome of the diversion may be better predicted.

Arhonditis and Brett (2004) found that increases in model complexity, model dimension and run–time were generally negatively correlated with model performance (i.e. statistical fit between model simulations and measured data), with phosphorus the only exception, amongst the state variables. The results presented in this chapter can be placed in the upper 30% for comparisons of temperature amongst other models, but in the lower 30% for chlorophyll a. Direct comparisons with other 3D models cannot readily be made as most other model comparisons are of a visual nature for phytoplankton (e.g. Robson and Hamilton 2004; Spillman et al. 2007). Missaghi and Hondzo (2010) calculated a low R2 of between 0.17 and 0.35 for chlorophyll a concentrations at three stations in a shallow lake over a period of six months using a 3D model. Remote sensing data may offer future opportunities to validate the surface–resolved output of 3D modelling studies. Approaches have been made to integrate remotely sensed data with a computational fluid dynamics model to predict surface distributions of chlorophyll a concentration and temperature (Alvarez et al. 2007), but only a limited number of case studies have been undertaken to date where remote sensing data has been compared with a complex ecological model (e.g. Spillman et al. 2007) and none of these has extended to statistical comparisons.

Model uncertainties and limitations

Ecosystem models are limited by the structural set-up and the user-defined variables. Recent publications criticise the simplistic representation of sediment models (Mooji et al 2010) and the limitation of data available to improve the representation of sediment dynamics in existing models (Trolle et al. 2010). To undertake long term predictions of water quality it may be essential to integrate a dynamic sediment model. The model does not simulate regeneration of the pools of phosphorus and nitrogen within the sediments. Sediment nutrient release rates are controlled by user–defined maximum release rates as well as temperature, dissolved oxygen concentrations and pH in the overlying water layer. Internal

nutrient loading is expected to change under a regime of reduced external loading, until a new equilibrium is reached (Trolle et al. 2008b). Only a dynamic sediment model is able to adjust release rates to these new loadings from the water column. The fixed parameter approach, which attempted to simulate the results presented here with no further calibration from the pre–diversion case, is likely to have caused the rapid increase in surface nutrient concentrations which is associated with sediment nutrient releases.

In Chapter 3 it was shown for the pre–diversion case that nutrient levels in the model simulations rose rapidly in the latter phase of the one–year simulation period, in particular at shallow station 3, whilst measured data remained consistently lower. Calculations indicate that this excess level in nitrogen could theoretically have been taken up by benthic producers, but sensitivity analysis indicates that the error was mainly attributed to the static sediment model, which appeared to be unable to reproduce spatial differences in the sediment composition of a complex lake with one assigned parameter set for the whole domain; in common with some of the outcomes of Chapter 3. For spatial and temporal accuracy in sediment release rates, and consequently water column nutrient concentrations, a simplified sediment diagenesis model which provides a dynamic solution for sediment changes within a reasonable run time, would provide for the extended model simulation duration necessary to properly evaluate future scenarios. The model therefore is not only restricted by the simplicity of the sediment algorithms, but also by the user defined variables. In the model presented here paucity of data in terms of benthic production and sediment composition led to model uncertainties. There is a requirement that in the future more dynamic mechanisms be included in ecosystem models related to benthic producers and sediment releases.

Model predictions of chlorophyll a concentrations may be further improved by the addition of zooplankton grazers; during the months of August 2008 and September 2008, the model simulation over–predicted the measurements in the field. Bruce et al. (2006) simulated three zooplankton and three phytoplankton groups for Lake Kinneret over the period of 1997–1998. The results of their 1D

DYRESM–CAEDYM model application showed a good fit between modelled and measured data, represented by the normalised–mean–absolute–error, which was considered acceptable when the simulated error fell within or close to one standard deviation of the observed monthly average field data. Arhonditsis and Brett (2004) showed that a negative correlation exists between modelled zooplankton predictions and the three factors of simulation period, spatial dimension and model complexity. Considering the model presented here is at the higher end of all three of these factors it might be notable if the inclusion of zooplankton grazers could actually improve model performance. As with many other applications, however, no zooplankton data were available over either of the two simulation years.

Geothermal heat source

The geothermal energy input used in the model simulation was found to be 165 MW based on results generated in Chapter 3, prior to the inflow diversion, to match the increases in hypolimnion temperature over the period of stratification. It is likely that the geothermal effects on water temperature would be more sensitive after the implementation of the inflow diversion, due to less dilution of the geothermal inflow corresponding to times when there was an underflow of Ohau Channel water. The exact magnitude and nature of the geothermal source remains uncertain, however, and there is some evidence based on temperature variations within the deepest part of the lake (see Chapter 3) that this heat source may be variable. There are multiple interacting processes that affect nutrient concentrations such as increased decomposition of organic matter due to the increased temperature from geothermal heating, as well as a higher rate in oxidation of organic matter, which is kept in suspension due to the hypolimnetic stirring (Priscu et al. 1986). These processes should be represented within the model due to the temperature dependence of biogeochemical rates and the incorporation of sedimentation of organic matter within the framework of a complex hydrodynamic model.

Gibbs (1992) suggested that hypolimnetic stirring may reduce hypolimnetic oxygen depletion in spring. He also suggested that the Ohau Channel underflow

delays anoxia until autumn, and that the diversion of this inflow could promote earlier deoxygenation within the stratified period. Both the measured data and the model simulations showed the initiation of deoxygenation in the hypolimnion in October 2008, which has historically been the period of onset of deoxygenation. Anoxia (considered to be DO < 0.5 mg L–1) of the hypolimnion occurred in mid–February 2009, which was when it occurred prior to the implementation of the inflow diversion (Chapter 3). No significant change could be confirmed in the annual oxygen cycle, but it may be that the increased effect of hypolimnetic stirring, due to reduction of the underflow, counteracted the early deoxygenation that was hypothesised by Gibbs (1992).

Model calibration process

Automated calibration of complex deterministic water quality models with many parameters has two advantages. It can reduce the time–consuming iterative judgement of model fit and can provide for a more objective parameter set. The advantages of an automated calibration process for complex ecological models have been discussed in the literature by Gupta et al. (1999). Automated calibration has been used for river (e.g. Rode et al 2007) and watershed models (e.g. Lin and Radcliffe 2006). Madsen (2000) formulated an automatic calibration strategy for a rainfall–runoff model, when the model calibration focussed on optimising four main objectives. Madsen (2000) suggests that no single parameter set is capable of optimising all objectives simultaneously and uses a balanced aggregated objective function to weight the different objectives, which has been shown to provide an efficient compromise solution. However an automated calibration procedure is only under development for CAEDYM (Hipsey et al. 2006) with the main focus on the coupling with the 1D model DYRESM. The current runtime of 3D models that attempt simulations within complex domains and ideally simulate over durations of several years, would require access to several parallel computers or a supercomputer to be able to undertake a high number of calibration runs. The model used in this study had several sensitive parameters. If the user were to restrict a sensitivity analysis or auto–calibration procedure to a selection to 10 parameter and three potential values for each parameter a sum of nearly 60000

model parameterisation simulations would be generated. This is hardly feasible and it therefore remains uncertain if the pre–defined and selected parameter values provide for the best model fit. Under these circumstances the value of manual calibration and trial–and–error fit of model parameters based on user knowledge, should not be under–estimated. Manual calibration of complex ecosystem models appears to be more efficient as the experienced user can limit the number of calibration runs, however with increasing computer capacity and access to super–computers, auto–calibration may be considered more viable in future.

Sensitivity analysis was undertaken for modelling parameters that were identified through initial trial–and–error calibration, to strongly influence the model result. Due to the higher sensitivity of the parameter for the initial productivity–irradiance curve (Ik) in Chapter 3, several model runs were undertaken to test for sensitivity in this scenario. The intensive sensitivity analysis for this parameter served two purposes. Firstly it was used to identify if this parameter should be focussed on in future studies and secondly it was used to analyse if this parameter could readily affect the balance between light and nutrient limitation in a specific phytoplankton group (i.e., cyanobacteria). The expected change in the error for chlorophyll a, judged by RMSE and Pearson correlation coefficient values, did not change significantly when Ik was changed between 100 and the upper value used in this study of 370 µmol m–2 s –1. This parameter has been reported in the literature to have a range of 72–920 µmol m–2 s –1 (van Rijn and Cohen 1983). Robson and Hamilton (2004) reported a value of 500 µmol m–2 s –1 for cyanobacteria in the Swan River Estuary. The sensitivity analysis illustrated that parameter limits may be wide. The parameter Ik showed high sensitivity in the pre–wall scenario presented in Chapter 3, but not post–wall in Chapter 4 which indicates that parameter sensitivity may be specific to particular conditions. It may be beneficial for future research to investigate the constraints this parameter places on phytoplankton growth.

4.6 Conclusions

The implementation of the diversion wall in Lake Rotoiti interrupted the flow from Ohau Channel into Lake Rotoiti. Roughly 70% of the nutrient loads in Lake Rotoiti were estimated to origin from adjacent Lake Rotorua via the channel. The implementation of the diversion wall resulted in overall water quality gains for Lake Rotoiti and the previously predicted deterioration of water quality associated with greater deoxygenation of the hypolimnetic waters of the lake did not occur with the successful attempt to make rapid improvements in the water quality of Lake Rotoiti.

The geothermal heat inputs into the hypolimnion continue to influence Lake Rotoiti's seasonal stratification cycle in a similar way to the pre–diversion case. Field measurements and model simulations showed that the wall was likely to have reduced chlorophyll concentrations in Lake Rotoiti relatively rapidly after its completion despite the relatively long residence time of water in the lake post–diversion (c. 5 yr) compared with pre–diversion (1.5 yr). ELCOM–CAEDYM simulations captured the evolution of the effects on chlorophyll of the diversion wall, based on parameter inputs that were fixed from the pre–wall calibration. However simulations of nutrient concentrations post–wall were less satisfactory and it is suggested that localised effects due to variations in sediment nutrient concentrations across the lake may have been responsible for anomalies in simulated nutrient concentrations. The fixed parameter approach used in this study did not appear to have the flexibility to capture the wide extent of spatial variations in water column nutrient concentrations in different parts of the lake. To have an acceptable run time of the model for the purpose of repeated calibration and refinement of parameter values, a simplified sediment diagenesis model could be implemented to simulate different bottom sediment features (e.g. nutrient levels) and releases related to the different morphological areas.

The diversion wall in Lake Rotioiti has successfully prevented Ohau Channel water from entering Lake Rotoiti in substantial quantities and, despite some model uncertainties, a model has been set up to be able to capture the magnitude of

changes in biomass after the inflow diversion. The research presented here provides a sound basis for further research in ecosystem modelling in geothermally influenced lakes and has provided an extreme test of the capabilities of the ELCOM–CAEDYM in simulating the interactions of benthic geothermal springs with sediment and nutrient recycling and primary production in geothermal systems.

4.7 References

Ahlgren, I. (1972): Changes in Lake Norrviken after sewage diversion. *Verhandlungen internationale Vereinigung Limnologie* 18: 355–361.

Alvarez, G. A., Salinas, R. A. and Malthus, T. J. (2007): Integrating CFD modelling, neural networks and remote sensing: controlled prediction of chlorophyll–*a* concentration in the Mejillones of South Bay. *IET computer vision* 1(2): 55–65.

Arhonditsis, G. B. and Brett, M. T. (2004): Evaluation of the current state of mechanistic aquatic biogeochemical modeling. *Marine Ecology Progress Series* 271: 13–26.

Arhonditsis, G. B. and Brett, M. T. (2005): Eutrophication model for Lake Washington (USA): Part II - model calibration and system dynamics analysis. *Ecological Modelling* 187(2-3): 179-200.

Bruce, L. C., Hamilton, D., Imberger, J., Gal, G., Gophend, M., Zohary, T., Hambright, K. D. (2006): A numerical simulation of the role of zooplankton in C, N and P cycling in Lake Kinneret, Israel. *Ecological Modelling* 119: 412–436.

Burger, D. F., Hamilton, D. P., Hall, J. A. and Ryan, E. F. (2007): Phytoplankton nutrient limitation in a polymictic eutrophic lake: community versus species–specific responses. *Archiv für Hydrobiologie* 169(1): 57–68.

Burger, D. F., Hamilton, D. P. and Pilditch, C. A. (2008): Modelling the relative importance of internal and external nutrient loads on water column nutrient concentrations and phytoplankton biomass in a shallow polymictic lake. *Ecological Modelling* 211(3–4): 411–423.

Calhaem, I. M. (1973): Heat flow measurements under some lakes in North Island, New Zealand. Ph.D thesis. Department of Physics. Victoria University of Wellington**:** 191 pp.

Carpenter, S. R., Caraco, N. F., Correll, D. L., Howarth, R. W., Sharpley, A. N. and Smith, V. H. (1998): Nonpoint pollution of surface waters with phosphorus and nitrogen *Ecological Applications* 8: 559–568.

Carvalho, L., Beklioglu, M. and Moss, B. (1995): Changes in a deep lake following sewage diversion – a challenge to the orthodoxy of external phosphorus control as a restoration strategy? *Freshwater Biology* 34: 399–410.

Casulli, V. and Cheng, R. T. (1992): Semi–implicit finite difference methods for three–dimensional shallow water flow. *International Journal for Numerical Methods in Fluids* 15(6): 629–648.

Cooke, G. D., Welch, E. B., Peterson, S. A. and Nichols, S. A. (2005): Restoration and Management of Lakes and Reservoirs, Taylor & Francis Group: 591 pp.

Edmondson, W. T. and Lehman, J. T. (1981): The effect of changes in the nutrient income on the condition of Lake Washington. *Limnology and Oceanography* 26(1): 1–29.

Friedrichs, M. A. M., Hoodc, R. R., Wiggert, J. D. (2006): Ecosystem model complexity versus physical forcing: Quantification of their relative impact with assimilated Arabian Sea data. *Deep–Sea Research* 53: 576–600.

Gal, G., Hipsey, M. R., Parparov, A., Wagner, U., Makler, V. and Zohary, T. (2009): Implementation of ecological modeling as an effective management and investigation tool: Lake Kinneret as a case study. *Ecological Modelling* 220(13–14): 1697–1718.

Gibbs, M. M. (1992): Influence of hypolimnetic stirring and underflow on the limnology of Lake Rotoiti, New Zealand. *New Zealand Journal of Marine and Freshwater Research.* 26: 453–463.

Gupta, H.V., Sorooshian, S. and Yapo P.O. (1999): Status of automated calibration for hydrologic models: comparison with multilevel expert calibration. *Journal of Hydrologic Engineering* 4(2):135–143.

Hamilton, D. P., O'Brien, K. R., Burford, M. A.,Brookes, J. D. and McBride, C. G. (2010): Vertical distributions of chlorophyll in deep, warm monomictic lakes. *Acquatic Sciences* 72(3): 295–307.

Hedger, R. D., Olsen, N. R. B., Malthus, T. J. and Atkinson, P. M. (2002): Coupling remote sensing with computational fluid dynamics modelling to estimate lake chlorophyll–*a* concentration. *Remote Sensing of Environment* 79(1): 116–122.

Hipsey, M. R., Antenucci, J.P., Romero, J.R and Hamilton, D. P. (2007): Computational Aquatic Ecosystem Dynamics Model: CAEDYM v3 Science Manual. Centre for Water Research University of Western Australia.

Hipsey, M. R., Gal, G., Antenucci, J. P., Zohary, T., Makler, V., Imberger, J. (2006): Lake Kinneret water quality management system. Proceedings of the Seventh International Conference on Hydroscience and Engineering, Philadelphia, PA, September 2006. 37 pp.

Hodges, B. and Dallimore, C. (2007): Estuary Lake and Computer Model: ELCOM Science Manual Code v2.2. Centre for Water Research, University of Western Australia.

Hodges, B., Imberger, J., Saggio, A. and Winters, K. B. (2000): Modelling basin scale waves in a stratified lake. *Limnology and Oceanography* 45(7): 1603–1620.

Jellison, R. and Melack, J. M. (1993): Meromixis in hypersaline Mono Lake, California. 1. Stratification and Vertical Mixing During the Onset, Persistence, and Breakdown of Meromixis. *Limnology and Oceanography* 38(5): 1008–1019.

Jellison, R., Romero, J. and Melack, J. M. (1998): The onset of meromixis during restoration of Mono Lake, California: Unintended Consequences of Reducing Water Diversions. *Limnology and Oceanography* 43(4): 706–711.

Jeppesen, E., Søndergaard, M., Jensen, J. P., Havens, K. E., Anneville, O., Carvalho, L., Coveney, M. F., Deneke, R., Dokulil, M. T., Foy, B., Gerdeaux, D., Hampton, S., Hilt, S., Kangur, K., Köhler, J., Lammens, E. H. H. R., Lauridsen, T. L., Manca, M., Miracle, M. R., Moss, B., Nõges, P., Persson, G., Phillips, G., Portielje, R., Romo, S., Schleske, C. L., Straille, D., Tatrai, I., Willén, E. and Winder, M. (2005): Lake response to reduced nutrient loading – an analysis of contemporary long–term data from 35 case studies. *Freshwater Biology* 50: 1747–1771.

Jeppesen, E., Søndergaard, M., Jensen, J. P., Mortensen, E., Hansen, A.–M. and Jørgensen, T. (1998): Cascading trophic interactions from fish to bacteria and nutrients after reduced sewage loading: An 18–year study of a shallow hypertrophic lake. *Ecosystems* 1: 250–267.

Jørgensen, S. E., Fath, B. D., Grant, W. E., Legovic, T. and Nielsen, S. N. (2008): New initiative for thematic issues: An invitation. *Ecological Modelling* 215(4): 273–275.

León, L. F., Lam, D. C. L., Schertzer, W. M., Swayne, D. A. and Imberger, J. (2005): Modeling as a tool for nutrient management in Lake Erie: a hydrodynamics study. *Journal Great Lakes Research* 31: 309–318.

Lin, L. and Radcliffe, D. E. (2006): Automatic calibration and predictive uncertainty analysis of a semidistributed watershed model. *Vadose Zone Journal* 5:248–260.

MacIntyre, S., Romero, J. R. and Kling, G. W. (2002): Spatial–temporal variability in surface layer deepening and lateral advection in an embayment of Lake Victoria, East Africa. *Limnology and Oceanography* 47: 656–671.

Madsen, H. (2000): Automatic calibration of a conceptual rainfall–runoff model using multiple objectives. *Journal of Hydrology* 235:276–288.

Mitra, A. (2009): Are closure terms appropriate or necessary descriptors of zooplankton loss in nutrient-phytoplankton-zooplankton type models? *Ecological Modelling* 220: 611-620.

Mitra, A. and Davis, C. (2010): Defining the "to" in end-to-end models. *Progress in Oceanography* 84: 39-42.

Missaghi, S. and Hondzo, M. (2010): Evaluation and application of a three–dimensional water quality model in a shallow lake with complex morphometry. *Ecological Modelling* 221(11): 1512–1525.

Mooij, W., Trolle, D., Jeppesen, E., Arhonditsis, G., Belolipetsky, P., Chitamwebwa, D., Degermendzhy, A., DeAngelis, D., De Senerpont Domis, L., Downing, A., Elliott, J., Fragoso, C., Gaedke, U., Genova, S., Gulati, R., Håkanson, L., Hamilton, D., Hipsey, M., ‘t Hoen, J., Hülsmann, S., Los, F., Makler-Pick, V., Petzoldt, T., Prokopkin, I., Rinke, K., Schep, S., Tominaga, K., Van Dam, A., Van Nes, E., Wells, S. and Janse, J. (2010): Challenges and opportunities for integrating lake ecosystem modelling approaches. *Aquatic Ecology* 44: 633-667.

Moss, B., Barker, T., Stephen, D., Williams, A. E., Balayla, D. J., Beklioglu, M. and Carvalho, L. (2005): Consequences of reduced nutrient loading on a lake system in a lowland catchment: deviations from the norm? *Freshwater Biology* 50(10): 1687–1705.

Moss, B., Stansfield, J. and Irvine, K. (1990): Problems in the restoration of a hypertrophic lake by diversion of a nutrient rich inflow. *Internationale*

Verhandlungen für theoretische und angewandte Limnologie 24(1): 568–572.

National Institute of Water and Atmospheric Research Ltd (NIWA) (2008): CliFlo: NIWA's National Climate Database on the Web. Retrieved 15 July 2008, from http://cliflo.niwa.co.nz.

Pérez, G. L., Queimaliños, C. P. and Modenutti, B. E. (2002): Light climate and plankton in the deep chlorophyll maxima in North Patagonian Andean lakes *Journal of Plankton Research* 24(6): 591–599.

Perrow, M. R., Moss, B. and Stansfield, J. (1994): Tropic interactions in a shallow lake following a reduction on nutrient loading: a long–term study. *Hydrobiologia* 275/276: 43–52.

Priscu, J. C., Spigel, R. H., Gibbs, M. M. and Downes, M. T. (1986): A numerical analysis of hypolimnetic nitrogen and phosphorus transformations in Lake Rotoiti, New Zealand: a geothermally influenced lake. *Limnology and Oceanography*. 31: 812–831.

van Rijn, J. and Cohen, Y. (1983): Ecophysiology of the Cyanobacterium *Dactylococcopsis salina*: Effect of light intensity, sulphide and temperature. *Journal of General Microbiology* 129: 1849–1856.

Robertson, D. M., Goddard, G. L., Helsel, D. R. and MacKinnon, K. L. (2000): Rehabilitation of Delavan Lake, Wisconsin. *Lake and Reservoir Management* 16(3): 155–176.

Robson, B. J. and Hamilton, D. P. (2004): Three–dimensional modelling of a Microcystis bloom event in the Swan River estuary, Western Australia *Ecological Modelling* 174(1–2): 203–222.

Rode, M., Suhr, U. and Wriedt, G. (2007): Multi-objective calibration of a river water quality model--Information content of calibration data. *Ecological Modelling* 204(1-2): 129-142.

Rueda, F. J., Schladow, S. G. and Clark, J. F. (2008): Mechanisms of contaminant transport in a multi–basin lake. *Ecological Applications* 18(8): 72–87.

Rutherford, J. C., Dumnov, S. M. and Ross, A. H. (1996): Predictions of phosphorus in Lake Rotorua following load reductions. *New Zealand Journal of Marine and Freshwater Research.* 30: 383–396.

Spillman, C. M., Imberger, J., Hamilton, D. P., Hipsey, M. R. and Romero, J. R. (2007): Modelling the effects of Po River discharge, internal nutrient cycling and hydrodynamics on biogeochemistry of the Northern Adriatic Sea. *Journal of Marine Systems* 68(1–2): 167–200.

Trolle, D., Jørgensen, T. B. and Jeppesen, E. (2008a): Predicting the effects of reduced external nitrogen loading on the nitrogen dynamics and ecological state of deep Lake Ravn, Denmark, using the DYRESM–CAEDYM model. *Limnologica* 38: 220–232.

Trolle, D., Skovgaard, H. and Jeppesen, E. (2008b): The Water Framework Directive: Setting the phosphorus loading target for a deep lake in Denmark using the 1D lake ecosystem model DYRESM–CAEDYM. *Ecological Modelling* 219(1–2): 138–152.

Vincent, W. F., Gibbs, M. M. and Dryden, S. J. (1984): Accelerated eutrophication in a New Zealand lake: Lake Rotoiti, Central North Island. *New Zealand Journal of Marine and Freshwater Research.* 18: 431–440.

Vincent, W. F., Gibbs, M. M. and Spigel, R. H. (1991): Eutrophication processes regulated by a plunging river inflow. *Hydrobiologia.* 226: 51–63.

Vincent, W. F., Spigel, R. H., Gibbs, M. M., Payne, G. W., Dryden, S. J., May, L. M., Woods, P., Pickmere, S., Davies, J. and Shakespeare, B. (1986): The impact of Ohau Channel outflow from Lake Rotorua on Lake Rotoiti. Taupo Research Laboratory, Division of Marine and Freshwater Science, DSIR 46.

Welch, E. B., Barbiero, R. P., Bouchard, D. and Jones, C. A. (1992): Lake trophic state change and constant algal composition following dilution and diversion. *Ecological Engineering* 1(3): 173–197.

Welch, E. B., Spyridakis, D. E., Shuster, J. I. and Horner, R. R. (1986): Declining lake sediment phosphorus release and oxygen deficit following waste water diversion. *Journal Water Pollution Control federation* 58(1): 92–96.

Chapter 5

General Conclusions

5.1 Research summary

Understanding and predicting of phytoplankton distributions and dynamics are essential in the management of aquatic ecosystems. It is not a question of whether lakes are spatially variable, but how much this spatial variability influences water quality at a whole system scale. Complex three–dimensional models, such as ELCOM–CAEDYM, can be used to greatly enhance the capability to understand the spatial variability in lakes and to analyse the relevant driving factors such as morphometry and external forcing factors such as inflows, outflows and meteorology. The spatial variability of temperature and water quality variables of Lake Rotoiti was simulated satisfactorily using the three–dimensional model ELCOM–CAEDYM. The version of the model used in this application applied an assumption of a fixed sediment composition (static sediment model). Application of the model to a major change in the inflow dynamics brought about by a diversion of the Ohau Channel, highlighted that the static sediment model applied in ELCOM–CAEDYM may be too simplistic and that a more complex sediment diagenesis model may better simulate the changes in nutrient concentrations that occur under a major regime change brought about by the inflow diversion.

The aim of Chapter 2 was to quantify the relative importance of spatial and seasonal variations in phytoplankton productivity in surface waters in a morphologically complex, deep lake. The shallow embayment showed significantly higher productivity in most months of the year compared with the

surface of the other two stations, but there were no significant differences from September–December 2004. No relationships were observed between measured environmental variables and primary productivity or specific production. The dissolved inorganic nutrient concentrations at deeper stations showed a typical pattern for monomictic lakes of higher levels during winter mixing and declining concentrations during thermal stratification, but surface concentrations were low throughout the whole year at the shallow station. The high variability between sites indicates that it is important to account for local differences in productivity in morphologically diverse lakes, and that in such cases whole lake productivity estimates may vary greatly depending on the location and depth of productivity measurements.

In Chapter 3 the primary objective was to model the spatial and temporal variability of water quality and temperature in geothermally–influenced Lake Rotoiti. Whilst Arhonditsis and Brett (2004) have previously shown that increased model complexity does not improve model performance and that phytoplankton predictive capacity is negatively correlated with the spatial model dimension, it was shown in Chapter 3 that the performance of the ELCOM–CAEDYM model in simulating chlorophyll *a* was at least comparable to other modelling approaches. ELCOM–CAEDYM also proved to be a useful tool in reproducing the highly spatially resolved field data of temperature, dissolved oxygen and chlorophyll *a* collected in monthly transects of the lake. Chapter 3 shows that ELCOM–CAEDYM is capable of managing a geothermal heat flux at the bottom of the lake via a sub–surface inflow. The temperature was determined by stepwise change of the heat flux until model simulations matched the hypolimnion temperature. The input of 165 MW provided for simulations with a good model fit to hydrodynamics. Correlations showed low sensitivity to the change in geothermal energy within a wide range (165–265MW), reaffirming the robustness of the model for water quality analysis. Errors of modelled surface nutrient concentrations indicate a lack of spatial model accuracy regarding sediment nutrient release rates and compositions and the lack of benthic producers, which could possibly account for excess nutrient concentrations in the shallow embayment.

The model calibration from Chapter 3 provided a basis for evaluating the three–dimensional model in terms of a major management decision. Specifically, the Ohau Channel inflow to Lake Rotoiti, which arises from Lake Rototi, was diverted towards the outlet of Lake Rotoiti with a wall completed in August 2008. One of the objectives addressed in Chapter 4 was to test the performance of the model that had been calibrated and validated for Lake Rotoiti (Chapter 3) before the implementation of the inflow diversion, and its performance in simulating water quality in the lake post–diversion wall. A second objective was to evaluate the effectiveness wall itself, in diverting water out of the main basin of Lake Rotoiti, and the expected improvements in lake water quality. The simulated chlorophyll *a* concentrations were reasonably well aligned with field data. The analysis of a tracer input in the Ohau Channel inflow with the model configured to represent the diversion wall in Lake Rotoiti showed that the wall was successfully diverting almost all water directly to the outflow of Kaituna River. Concerns that an inflow diversion may promote the early onset of deoxygenation and prolongue anoxic conditions in Lake Rotoiti (Gibbs 1992) could not be confirmed.

This chapter further supports a dynamic representation of the complex process of sediment diagenesis to be able to capture the temporal and horizontal variation in sediment nutrient concentrations, and the resulting way in which the sediments then contribute to horizontal variations in the water column constituents. However the manual calibration process of the CAEDYM model leaves uncertainties regarding the assigned parameters. Automated calibration processes are not always suitable for complex economical models, but may supply a basis for the manual calibration process. The development of automated processes of calibration may improve model fit and account for a more objective calibration process and model result, providing sufficient computing capacity is available.

5.2 Future work

In this study high–frequency field measurements were used to provide a rigorous of test the performance of a three–dimensional coupled hydrodynamic–water quality model for prediction of spatial and temporal distributions of temperature,

and concentrations of chlorophyll *a* and dissolved oxygen. The results represented some improvement over similar studies to simulate chlorophyll concentrations using a one–dimensional model approach, while providing insights into the fate and transport of phytoplankton and nutrients within the lake, both vertically and horizontally. The results highlighted the difficulties in the capability of the model to accurately simulate nutrient concentrations on a spatial basis and to adjust for a different set of conditions to those used for the initial calibration of the model. Individually adjusting sediment nutrient release rates to specific sites produced improvements in matching nutrient concentrations observed in the field. However, these adjustments compromised the good correlation between measured and modeled chlorophyll *a* concentrations. The implementation of a dynamic sediment diagenesis module in ELCOM–CAEDYM may be one way to improve the prediction of nutrient concentrations in this morphologically variable lake system but would significantly increase the simulation runtime. A simplified dynamic sediment model with an intermediate level of complexity could provide for a reasonable runtime and sufficient accuracy to capture the apparently variable sediment composition in Lake Rotoiti.

The implementation of a dynamic sediment model that represents the sediment diagenesis process is likely to require additional sediment parameters that may need to be determined theoretically as my study focused on changes in water column variables. Ideally, for calibration of the sediment diagenesis model monthly data would be required to capture the redox–driven nutrient transformations that follow those associated with changes in levels of dissolved oxygen and deposition of particulates within the water column (Trolle et al. 2008b).

Consideration could also be given to measurements of water column nutrient concentrations at higher spatial and temporal resolution than those used in my study, in addition to the measurements of sediment nutrient concentrations required for implementation of the sediment diagenesis model. Pearson correlation coefficient and RMSE values between modeled and measured data showed that, for inorganic nutrients in particular, a considerable part of variability

in the lake could not be explained by the model simulations. As demonstrated in Chapter 4 the performance of ELCOM–CAEDYM was satisfactory for temperature, dissolved oxygen and chlorophyll *a* concentrations but there was a need for more resolved temporal and spatial data on nutrient concentrations in order to better understand the processes driving these variables.

The approach chosen in this study to calibrate the model based on three sampling stations to be able to predict water quality variables based on low cost and low time intensive field sampling leaves the question open if model calibration may be improved by using highly spatially resolved field data as used for output comparison in this study. Progress in sampling techniques such high frequency nutrient analysis and monitoring buoys for continuous measurements will provide sampling at a high resolution. While the frequency of remote sensing techniques is currently not satisfactory, it may provides high resolution field data for model initialisation or comparison. This may in future give more accurate measurements at possibly higher frequency for the model calibration process.

The change from a manual model calibration process to an automated or semi–automated calibration process may improve the model accuracy. The development of automated calibration techniques to be able to determine and assign seasonal changing parameters as suggested by Jørgensen (2008) may further improve model fit and should be further examined.

The low sensitivity if the modelled geothermal energy via the sub–surface inflow in the main basin shows that the model may have some limitations when the exact geothermal energy needs to be determined. This is further indicated by the lower determined geothermal energy of 10–20 MW when a similar approach was used to adjust hyplimnion temperatures using the 1D approach DYRSEM (Spigel 1983). However the model is capable of reproducing accurately the thermocline and provide a good fit with hydrodynamic measurements to be able to analyse water quality parameters.

It may be required to determine the exact geothermal energy, in particular for smaller lakes when, e.g. different water level scenarios are simulated. In cases

when higher accuracy is required regarding the geothermal energy specific geothermal model as, e.g. the energy mass balance model used by Paternack and Varekamp (1997) may be more useful, which may also provide for simulation of the anomalies of geothermal lakes.

This thesis demonstrated the successful simulation of temperature and water quality in Lake Rotoiti both with and without inflow diversion. Lake recovery may be a long process, with an array of different responses to load reductions (Jeppesen et al. 2005). The response may not only vary amongst lakes, but there may also be high spatial variability within a lake. One important motivation for this study was to support decisions to restore and sustain the water quality of Lake Rotoiti. Due to the unknown length of recovery and the diversity of possible responses to inflow diversions (e.g. Welch et al. 1992; Robertson et al. 2000) future work could extend to simulations with models using several different time and space scales in order to better understand the evolution of responses and time required to reach a steady state in response to a given set of conditions. This work could include scenarios such as global warming or changes in water level in Lake Rotoiti, and this type of assessment could consequently provide a valuable tool for comprehensive assessments of lake water quality and the support of future management decisions.

5.3 References

Arhonditsis, G. B. and Brett, M. T. (2004): Evaluation of the current state of mechanistic aquatic biogeochemical modeling. *Marine Ecology Progress Series* 271: 13–26.

Jeppesen, E., Søndergaard, M., Jensen, J. P., Havens, K. E., Anneville, O., Carvalho, L., Coveney, M. F., Deneke, R., Dokulil, M. T., Foy, B., Gerdeaux, D., Hampton, S., Hilt, S., Kangur, K., Köhler, J., Lammens, E. H. H. R., Lauridsen, T. L., Manca, M., Miracle, M. R., Moss, B., Nõges, P., Persson, G., Phillips, G., Portielje, R., Romo, S., Schleske, C. L., Straille, D., Tatrai, I., Willén, E. and Winder, M. (2005): Lake response to reduced nutrient loading – an analysis of contemporary long–term data from 35 case studies. *Freshwater Biology* 50: 1747–1771.

Jørgensen, S. E., Fath, B. D., Grant, W. E., Legovic, T. and Nielsen, S. N. (2008): New initiative for thematic issues: An invitation. *Ecological Modelling* 215(4): 273–275.

Monismith, S. G. and Fong, D. A. (1996): A simple model of mixing in stratified tidal flows. *Journal of Geophysical Research* 101: 28583 – 28595.

Pasternack, G. B. and Varekamp, J. C. (1997): Volcanic lake systematics I. Physical constraints. *Bulletin of Volcanology* 58: 528–538.

Robertson, D. M., Goddard, G. L., Helsel, D. R. and MacKinnon, K. L. (2000): Rehabilitation of Delavan Lake, Wisconsin *Lake and Reservoir Management* 16(3): 155–176.

Spigel, R. H. (1983): Outline for reasons for a revised geothermal heat flux estimate for Lake Rotoiti, Department of Civil Engineering, University of Canterbury (unpublished report in reference to: Spigel, R. H. and Timperley, M. (1983): Geothermal influences on the limnology of Lake Rotoiti – Preliminary conclusions from the 1982 field data. Taupo Research Labrotory File report 27/T/58.

Trolle, D., Jørgensen, T. B. and Jeppesen, E. (2008): Predicting the effects of reduced external nitrogen loading on the nitrogen dynamics and ecological state of deep Lake Ravn, Denmark, using the DYRESM–CAEDYM model. *Limnologica* 38: 220–232.

Vincent, W. F., Gibbs, M. M. and Dryden, S. J. (1984): Accelerated eutrophication in a New Zealand lake: Lake Rotoiti, Central North Island. *New Zealand Journal of Marine and Freshwater Research.* 18: 431–440.

Welch, E. B., Barbiero, R. P., Bouchard, D. and Jones, C. A. (1992): Lake trophic state change and constant algal composition following dilution and diversion. *Ecological Engineering* 1(3): 173–197.